DEPARTMENT OF THE NAVY
NAVAL SHIP RESEARCH AND DEVELOPMENT CENTER
WASHINGTON, D. C. 20007

UNSTEADY PROPELLER LOADING–MEASUREMENT, CORRELATION WITH THEORY, AND PARAMETRIC STUDY

by

Robert J. Boswell
and
Marlin L. Miller

October 1968 Report 2625

TABLE OF CONTENTS

LIST OF FIGURES

LIST OF TABLES

NOTATION

$A_L{}^n(r)$	Fourier cosine coefficients of longitudinal wake velocity
a	Ω/V_A inverse pitch of helicoidal surface
$B_L{}^n(r)$	Fourier sine coefficients of longitudinal wake velocity
$c(r)$	Chord length
D	Propeller diameter
EAR	Expanded area ratio, expanded blade area divided by disk area
$\tilde{F}_H$	Amplitude of harmonic of horizontal side force
$\tilde{F}_V$	Amplitude of harmonic of vertical side force
$\tilde{F}_1$	Amplitude of harmonic of lagging component of side force rotating with propeller
$\tilde{F}_2$	Amplitude of harmonic of leading component of side force rotating with propeller
J	V_A/nD advance coefficient
J_m	Bessel function of the first kind of order m
$\tilde{K}_F$	$\tilde{F}/\rho n^2 D^4$ force coefficient based upon amplitude of harmonic of force
$\tilde{K}_M$	$\tilde{M}/\rho n^2 D^5$ moment coefficient based upon amplitude of harmonic of moment
K_m	Modified Bessel function of the second kind of order m
$\bar{K}_Q$	$\bar{Q}/\rho n^2 D^5$ torque coefficient based upon steady component of torque
$\tilde{K}_Q$	$\tilde{Q}/\rho n^2 D^5$ torque coefficient based upon amplitude of harmonic of torque
$\bar{K}_T$	$\bar{T}/\rho n^2 D^4$ thrust coefficient based upon steady component of thrust
$\tilde{K}_T$	$\tilde{T}/\rho n^2 D^4$ thrust coefficient based upon amplitude of harmonic of thrust
k	$\frac{\omega c}{2U_r}$ reduced frequency

k	Order of blade harmonic
$\tilde{L}(r)$	Unsteady lift on a blade element
$L_{QS}(r)$	Quasi-steady lift on a blade element
$\tilde{M}_H$	Amplitude of harmonic of horizontal bending moment
$\tilde{M}_V$	Amplitude of harmonic of vertical bending moment
$\tilde{M}_1$	Amplitude of harmonic of leading component of bending moment rotating with propeller
$\tilde{M}_2$	Amplitude of harmonic of lagging component of bending moment rotating with propeller
n	Order of shaft harmonic
n	$2\pi\Omega$ revolutions per second
$\vec{n}$	Normal to helicoidal surface at loading point
$\vec{n}'$	Normal to helicoidal surface at control point
P	Propeller pitch
p	Perturbation pressure
$\bar{Q}$	Steady component of torque
$\tilde{Q}$	Harmonic amplitude of torque
R	Radius of propeller
R	Descartes distance
$Re[]$	Real part of [ ]
R_n	$c(0.7R) \cdot \bar{U}_r(0.7R)/\nu$ Reynolds number of propeller
r	Radial coordinate of control point
r_h	Radius of hub
S	Lifting surface
$S(\rho, \theta_a)$	Blade-loading distribution
$\bar{T}$	Steady component of thrust

$\tilde{T}$	Amplitude of harmonic of thrust
t	Time
$\bar{U}_r(r)$	Mean resultant inflow velocity
$V(r, \phi)$	Local inflow velocity to propeller plane
V_A	Speed of advance
$V_L(r, \phi)$	Local longitudinal inflow velocity to propeller plane
$V_N^n(r)$	Fourier coefficients of wake velocity normal to the blade
$V_L^n(r)$	Fourier coefficients of longitudinal wake velocity
$V_T^n(r)$	Fourier coefficients of tangential wake velocity
V_{VM}	Volume mean velocity into propeller disk
x	Longitudinal coordinate of control point
x, r, ϕ	Cylindrical coordinate system of control points
Z	Number of blades
β	Advance angle of a propeller blade section
$\Gamma^B(\rho)$	Total bound vorticity of blade section
γ_r^B	Bound radial vorticity
γ_s	Shed vorticity (see Figure 1)
γ_t	Trailing vorticity (see Figure 1)
η_0	Efficiency of propeller in open water
θ	Angular coordinate of loading point
θ_α	Angular chordwise location of loading point
θ_b	Projected section semichord length in radians
θ_p	Propeller angular position relative to position where $M_1 = M_V$
θ_0	Initial angular position of loading point in propeller plane
$\bar{\theta}_m$	$\frac{2\pi}{Z}(m-1)$, $m = 1, 2 \ldots Z$

λ	Wavelength of sinusoidal gust velocity
ν	Kinematic viscosity of the fluid
ξ, ρ, θ	Cylindrical coordinate system of loading points
ρ	Radial coordinate of loading point
ρ	Mass density of fluid
$\sigma(r)$	Angular measure of blade skew
σ_T	Angular skew at blade tip
r'	Variable of integration
ϕ	Angular coordinate of control point
$\phi(k)$	Sears function
$\phi_w{}^n$	$\tan^{-1}[A_L{}^n(r)/B_L{}^n(r)]$ phase angle of nth harmonic of wake
ϕ	Angular chordwise location of control point
ϕ_0	Angular position of control point in propeller plane
χ	Linear chordwise coordinate
ψ	$2\pi/Z$ angular spacing between blades
Ω	Angular velocity of propeller in radians per second
ω	Angular frequency of loading

ABSTRACT

Objectives of the present study are to measure the unsteady forces and moments on a series of marine propellers due to circumferentially nonuniform inflow; to correlate the measured unsteady thrust and torque with calculated values, based on various proposed theories; and to investigate variation of unsteady thrust and torque over a range of pertinent parameters, using the method determined from those described to be the best available for calculating unsteady loading.

All six components of unsteady loading were measured on a series of four three-bladed propellers, consisting of three unskewed propellers of varying blade widths and one with extreme skew in both 3- and 4-cycle flow fields. The experimental results indicate that all components of blade-frequency loading increase to some maximum value then decrease with increasing expanded area ratio. The extreme skew resulted in a reduction in blade-frequency thrust and torque to about 10 percent of the unskewed value and a reduction in side forces and bending moments to about 50 percent of the unskewed value.

Experimental blade-frequency thrust and torque were compared with values calculated by the following techniques: quasi-steady, two-dimensional unsteady, combination quasi-steady two-dimensional unsteady, and three-dimensional unsteady. The three-dimensional unsteady theory yields the best correlation with experiment; however, the numerical techniques employed breakdown for narrow-bladed propellers and for propellers with blade overlap.

The parametric study reveals that for a given number of blades, blade frequency thrust and torque can be reduced effectively by considerably skewing the blades.

ADMINISTRATIVE INFORMATION

This report incorporates a Master of Science Thesis by Robert J. Boswell entitled "Measurement, Correlation with Theory, and Parametric Investigation of Unsteady Propeller Forces and Moments," submitted to the Department of Aerospace Engineering of the Pennsylvania State University in August 1967, with additional data not presented in the thesis. The work was initiated at the Naval Ship Research and Development Center under authorization of Naval Ship Systems Command Subproject S-F013 01 03, Task 10441, NSRDC Problem 526-111 and was completed under Naval Ship Systems Command Subproject S-F113 11 09, Task 3801, NSRDC Problem 526-150.

INTRODUCTION

The problem under consideration concerns the unsteady loading produced on a propeller operating in a circumferentially nonuniform velocity field. An understanding of this problem and its satisfactory solution are of particular importance in the field of marine propulsion in which propellers operate in the wake of the propelled body. Similar problems arise in rotating propulsors of various types such as pumps, compressors, turbines, and fans. The circumferential nonuniformity of the inflow causes the blade elements to experience periodic variations in inflow velocity and angle of attack, resulting in undesirable fluctuations in local loading. This unsteady loading produces unsteady forces and moments which are transmitted through the propeller shafting and bearings and often produce severe vibration and noise. Forces of this type are commonly called wake-bearing forces.

However, reaction to circumferentially nonuniform inflow is not the only mechanism by which the propeller may produce unsteady loading on the vessel. As a consequence of the loading and finite thickness of the propeller blades, a pressure field is created around the propeller. This pressure field creates a time-dependent pressure fluctuation at a fixed point on the body in the proximity of the propulsor. Unsteady forces transmitted to the body in this manner are commonly known as pressure forces.

The unsteady loading on the body produces a reaction at the propeller causing unsteady loading on the propeller blades. The resultant unsteady forces and moments on the propeller are transmitted back to the vessel through the propeller shafting and bearings. Hence these forces produced by interaction with the solid boundary are called interference-bearing forces. These pressure forces and interference-bearing forces may occur regardless of whether the flow into the propeller plane (in the absence of the propeller) is uniform or nonuniform. This report pertains to only the wake-bearing forces.

IMPORTANCE OF STUDY

Many calculation schemes, based on theories of various degrees of sophistication, have been proposed for predicting the wake-bearing forces. These theories may be generally classified as follows: quasi-steady, utilizing steady-state propeller tests; quasi-steady, utilizing steady-state lifting-line techniques; two-dimensional along a strip, using unsteady airfoil theory; combination techniques, using both unsteady two-dimensional corrections and quasi-steady three-dimensional corrections; and three-dimensional unsteady techniques.

The range of validity of these various theories has not been established because of the lack of systematic reliable experimental data. Available experimental data have been, in the past, either of questionable accuracy, not systematic, or not sufficiently extensive; or they may have included contributions from extraneous influences such as pressure forces and interference bearing-forces not considered in the theories.

Thus, there is a clear need for accurate fundamental experimental measurements of unsteady loading solely attributable to the circumferential nonuniform inflow. These measurements should be accurate and should systematically cover a wide range of the most important parameters. Blade width is especially important since, to a great extent, it determines the effective reduced frequency, blade aspect-ratio, and the amount of blade interaction. The two-dimensional unsteady theory and several of the three-dimensional unsteady theories assume large aspect ratios; hence, it is of interest to establish the limit of aspect ratio for which these theories might yield reasonable predictions. The quasi-steady techniques assume zero reduced frequency; thus, it is important to establish the limit of reduced frequency to which these may be applied. The two-dimensional theory completely neglects interaction between the blades, and several of the three-dimensional techniques consider interaction effects very approximately; hence, this might limit the application of these techniques to relatively narrow blades.

Another important parameter is blade skew. With skew, the blade sections at the various radii will enter the high-wake region at different times. Intuitively, this will produce a phase variation of loading with radius and thus reduce the amplitude of the net fluctuating loading. However, the magnitude of the reduction in loading with skew, and how closely this can be calculated, is not yet established.

Since there are a large number of parameters, and such experiments are very expensive and difficult, it is not feasible to conduct experiments for a complete range of conditions. Such a parametric study must be conducted theoretically. However, to establish confidence in any theory, sufficient comparable experimental data must be available to determine the accuracy and range of validity of the particular theory.

Once confidence in a particular calculation scheme is established, then a theoretical parametric study would be of great importance in establishing the variation of unsteady loading with various parameters. Such information is essential for a rational approach to the design of propulsors that can keep vibratory forces and moments at a minimum.

STATEMENT OF PROBLEM

Keeping the previously described considerations in mind, the present study has been planned with the following objectives:

1. To obtain a fundamental set of accurate experimental measurements of the unsteady forces and moments produced on marine propellers by circumferentially nonuniform inflow. These experiments duplicated the important basic assumptions of the mathematical models: a known velocity field and an absence of nearby boundaries. The propellers and velocity fields were carefully selected to permit isolating the effect of important parameters and determining the range of applicability of the various theories. In particular, quantitative data were obtained on the dependence of the components of unsteady loading upon blade width and skew.

2. To determine the range of validity of the various calculation techniques by comparing experimental blade-frequency harmonics of thrust and torque for a range of blade widths with calculated values based upon the following approaches: quasi-steady, using uniform flow tests; quasi-steady, using steady-state lifting-line theory; two-dimensional unsteady; combination quasi-steady and two-dimensional unsteady; and three-dimensional unsteady.

3. To undertake a parametric investigation utilizing the thus determined best available method for predicting unsteady thrust and torque to obtain an understanding of the effect of various propeller parameters on unsteady loading. The variation of fluctuating thrust and torque with pitch, blade width, and skew and the relative thrust and torque response with number of blades and blade harmonic were investigated.

Previous experimental studies related to the present work as well as the various theoretical treatments previously described are reviewed in the next two sections.

REVIEW OF PREVIOUS EXPERIMENTAL STUDIES

The first measurements were made by Lewis[1] in 1935. He measured the total (bearing plus pressure) force on the stern of a twin-screw commercial ship model, setting the desired direction of the force by adjusting the relative angular position of the two propellers. He measured the surface forces alone by driving the propellers from a following model so that there was no connection between the propellers and the forward model upon which the forces were measured. He then found the bearing forces by vector subtraction of the measured surface forces from the measured total forces.

Lewis and Tachmindji[2] later extended this technique to single-screw merchant ships. Here the direction of the force cannot be controlled; thus, both vertical and horizontal forces act upon the model simultaneously. Interaction problems due to the nonsymmetric elastic properties of the models produced considerable difficulty.

Later investigators measured the unsteady bearing forces directly. Resonance and interaction problems limited the earlier investigations to low frequencies and either thrust and torque or transverse forces and bending moments. Wereldsma[3] was the first to measure all six components of force and moment simultaneously.

Several investigators have conducted extensive measurements of the various components of bearing force and moment behind realistic single-screw hull configurations. The primary objective of these measurements was to obtain information regarding the dependence of the various components of force and moment on the geometry of the stern and propeller (particularly the number of blades). Van Manen and Kamps[4] measured the effects of radical variation in ship afterbody shape and propeller geometry on the unsteady thrust and torque. For two tanker stern configurations, Van Manen and Wereldsma[5] measured the dependence of the

---

[1] References are listed on page 76.

fluctuating thrust, torque, and bending moments on the number of blades, blade-outlined shape type of rudder, and the draft of the vessel. Kumai et al.[6] measured the dependence of all six components of propeller loading on the number of blades for two different tanker stern configurations. Both Van Manen and Kamps and Van Manen and Wereldsma measured only the axial component of wake (no harmonic analysis was performed), and Kumai presented no wake data. The primary conclusion from these studies is that for a single-screw commercial ship, a propeller with an even number of blades produces large blade-frequency thrust and torque and small transverse forces and bending moments, whereas an odd number of blades produces small blade-frequency thrust and torque but large transverse forces and bending moments.

Extensive measurements of the dependence on blade-area ratio of the thrust and torque variations with four-bladed propellers as well as transverse force and bending moment variations with five-bladed propellers were conducted by Krohn[7,8] behind a single-screw commercial ship model. In each series, the blade-area ratio varied from 0.35 to 0.75 while all other parameters were held invariant. The measured unsteady thrust and torque were compared with calculated values, based on a combination quasi-steady two-dimensional unsteady theory developed in the report and the combination theory of Ritger and Breslin.[9] The transverse forces and bending moments were compared with the former theory only. The measurements and both theories indicated that all forces and moments increased with blade width. The theories agreed with the measured thrust and torque within 100 percent and with transverse forces and bending moments within 10 percent.

Hadler et al.[10] measured the alternating thrust on two different submerged submarines, both the model and the full scale. The full-scale measurements were plagued by hull and shaft resonances. The measurements were compared with calculated values based upon the quasi-steady techniques developed at the Center by McCarthy,[11] Yeh,[12] and Haskins and elsewhere by the combination technique of Ritger and Breslin.[9]

In 1963, Lewis[13] adapted the techniques he developed in 1935 to measuring the interaction and wake-bearing forces in a water tunnel. He measured the force on a strut in close proximity to the propeller, with and without the propeller shaft connected to the strut, both in a uniform flow and in a circumferentially nonuniform flow produced by screens. The interaction-bearing force was then the vector difference of the forces measured on the strut in uniform flow with and without the propeller shaft connected to the strut. The wake-bearing force was the difference between the total force, measured with the propeller shaft connected to the strut and the propeller operating in the wake and the corresponding force measured in uniform flow. In these experiments, Lewis determined only the transverse components of propeller-bearing forces (i.e., fluctuating thrust and torque was not determined).

An important result of the Lewis experiments is that the interaction of a body with the propeller can produce sizeable fluctuating-bearing forces. Hence in any attempted correlation with theories which predict the fluctuating-bearing forces due to circumferentially nonuniform inflow, it is imperative that the experiment not contain fluctuating loading due to interactions

with solid boundaries. Lewis compared his measurements of wake-bearing forces for one propeller with predictions based on the two-dimensional sinusoidal gust theory of Sears[14] and obtained agreement within 10 percent.

For evaluating methods of calculating unsteady propeller loading due to circumferentially nonuniform inflow, measurements made behind realistic bodies have many shortcomings:

1. As shown by Lewis[13] the presence of a solid boundary in the proximity of the propeller may produce unsteady propeller loading of the same magnitude as that produced by the nonuniform inflow. The theories to be evaluated herein do not consider these potential flow interaction effects (image effects). There is presently no method of calculating these interaction effects for the complex geometries of realistic propelled bodies.

2. There are also interaction effects due to viscosity. The action of the propeller may produce a reduction in the adverse pressure gradient on the after portion of the propelled body. This will alter the boundary layer profile and delay separation (if separation exists). This, in turn, may considerably alter the harmonic content of the velocity field from that measured in the absence of the propeller. This interaction effect is expected to become more important as the afterbody becomes fuller or closer to the propeller. Burstein[15] found a considerable variation in harmonic content of the wake of a body of revolution with fins, depending on whether or not the propeller was operating.

3. The magnitude of the measured quantities is generally small, thus causing reduced accuracy in the measurements. This inaccuracy applies to the measured forces and moments as well as to the wake data upon which the calculated forces and moments depend.

In attempting to obtain a better understanding of the mechanism of the wake-bearing forces, several investigators have conducted experiments in which one or more of the aforementioned effects are eliminated.

Tachmindji and Dickerson[16] measured fluctuating thrust in a water tunnel on one propeller operating in wakes, produced by an upstream strut at various angles of attack. However, they did not define the inflow velocity fields in sufficient detail to allow rotational comparison with theory. Also, the low natural frequency of the shafting system causes some doubt concerning the validity of these results.

In an attempt to provide systematic experimental data to check theoretical calculations, Wereldsma[17,18] conducted two series of experiments. All six components of unsteady loading were measured on a series of propellers operating in wakes produced by upstream flat plates parallel to the flow and intersecting the propeller axis. The propellers were powered by a vessel situated downstream and towed with the plate configuration.

In the first series of tests, Wereldsma[17] measured all six components of loading on a series of three-, four-, and five-bladed propellers operating in two different "simple" wake patterns, produced by single plates. One plate extended from the propeller axis beyond the propeller diameter in one direction and the other extended beyond the propeller diameter in both directions. Only one plate was used in a given test. The propeller series was designed

so that the effect of blade-area ratio, skew, blade gap, and the applicability of the principle of superposition could be studied.

The wakes generated by the single flat plates did not exhibit large amplitudes in the harmonics which produced loading on the propellers tested. This resulted in reduced accuracy of the measurements. Also, the amplitudes and phases varied with harmonic number. Since propellers with different numbers of blades are sensitive to different harmonic components, it is difficult to draw conclusions from direct comparisons of the results for propellers with different numbers of blades. Thus definite conclusions on the effect of blade gap and the applicability of the principle of superposition could not be drawn.

To remedy the problem of weak signals, Wereldsma[18] modified the geometry of the wake-producing plates. He replaced the single plates by a radial fan of equally spaced plates equal in number to the number of propeller blades, thus developing strong blade-frequency harmonics in the wake. Only unsteady thrust and torque were measured on a series of three- and five-bladed propellers of varying blade widths, including one propeller with skew. The downstream vessel was close to the propeller and thus produced nonsymmetrical inflow disturbances in the plane of the propeller. Hence, the wake displayed relatively large first- and second-shaft harmonics.

The nonuniform inflow field, measured in the propeller plane in the absence of the propeller, is the result of the viscous wakes of the flat plates. Thus, the possibility still exists, although less than if the wake-producing body were blunt, that action of the propeller alters the harmonic content of the incoming flow. Also, the solid boundary of the downstream vessel can cause unsteady loading on the propeller due to potential flow interaction (image effects).

Wereldsma made no detailed comparison with theory. However, he showed that for the two-dimensional sinusoidal gust problem, the lift increased when the chord length increased for a fixed gust frequency. Thus he concluded that the two-dimensional strip approach predicted a monotonically increasing lift with increasing blade width. This is not necessarily true since reduced frequency is a function of radius, producing a variation of the phase of lift (thrust) with radius.

Brown[19] measured the blade-frequency thrust and torque in a water tunnel in a nonuniform inflow field generated by upstream nozzles. The velocity field was adjusted so that the blade-frequency harmonic dominated, thus producing strong blade-frequency thrust and torque signals. Unfortunately, Brown tested only one propeller in one wake pattern and could not draw conclusions regarding the effect of propeller and wake geometry on the unsteady loading. Brown compared his measurements with two-dimensional unsteady strip theory and with his own three-dimensional theory. The strip theory was about 20 percent high, whereas the three-dimensional theory was about 30 percent low.

Measurements have recently been made[20,21] of the unsteady loading on a single blade rather than the net unsteady loading on the propeller shaft. This method has the advantage of

being able to determine loading frequencies that would otherwise be canceled by the effect of the other blades. Huse[20] applied this technique to measuring fluctuating thrust, torque, and bending moment on one four-bladed propeller behind a model tanker hull and drew conclusions regarding the optimum axial propeller position. Rousetsky et al.[21] have not yet reported experimental results.

Expanded area ratio (EAR) is the propeller parameter most extensively studied experimentally. However, the available data are so inconsistent that the trends with blade width cannot be determined. Wereldsma[17] concluded that thrust and torque decreased with increasing EAR whereas side forces and bending moments increased with EAR. But his study was limited to relatively high values of EAR ($0.60 \leq EAR \leq 1.0$). Krohn,[7,8] on the other hand, concluded that all six loading components increased with increasing EAR. But his study was limited to relatively low values of EAR ($0.35 \leq EAR \leq 0.75$). Shuster[22] (as cited by Krohn) concluded from a collection of various measurements that thrust and torque decreased with increasing blade width. Recent results obtained by Wereldsma[18] for three-bladed propellers in a 3-cycle wake indicated that thrust monotonically decreased as EAR increased from 0.4 to 1.2. However, the corresponding torque increased as EAR increased from 0.4 to 0.6 and decreased for further increase in EAR. This difference in tendency between thrust and torque is inconsistent and causes some doubt concerning the validity of the Wereldsma results. Apparently Wereldsma doubted the torque measurement at $EAR = 0.4$. He stated, "Generally it can be concluded that for increasing blade-area ratio, the fluctuations reduce considerably, although the disturbed inflow remains the same for the various propellers."

From this brief review of previous work it can be concluded that there is a need for reliable experimental data with which to evaluate the various theoretical techniques. Further, there is a need for reliable information on the variation of unsteady loading with the important propeller parameters.

REVIEW OF THEORETICAL METHODS

Figure 1 shows a schematic representation of the flow field geometry considered in this study. The vector field represents the circumferential variation of the incoming velocity at one radius. The velocity field is the steady-state wake of the upstream body.* As the propeller blade advances along a helicoidal path, this velocity variation has a component normal to the resultant inflow velocity; hence, the blade section experiences a time-dependent angle of attack variation. The wake also has a component parallel to the resultant inflow velocity, producing a time-dependent surge velocity. However, the effect of this surge velocity

*Turbulen velocity fluctuations are not considered in this report. The response of a propulsor to turbulence was considered by Sevik.[23]

is generally very small. The time-dependent angle of attack at each radius produces a time-dependent circulation and hence time-dependent vorticity in both the radial and stream directions, both on the blades and in the downstream wake. In this report the vorticity in the wake in the radial direction is designated the "shed vorticity" γ_s and the vorticity in the wake in the direction of the stream is designated the "trailing vorticity" γ_t.

The problem is complicated by the complex geometry

1. The blades are generally of low-aspect ratio with arbitrary outline.
2. There is generally a substantial interaction between the blades.
3. The blades and downstream vorticity lie on helicoidal surfaces.
4. The harmonics of the wake vary radially in both amplitude and phase.

Since the inflow velocity is considered to be a function of space only, it can be resolved into Fourier components with the propeller rotational frequency (shaft frequency) as the fundamental. In a like manner, the loading can be resolved into a Fourier series with the same fundamental. If linearity between the inflow velocity and the propeller loading is assumed, then the amplitude of each loading frequency is a function only of the corresponding frequency of the incoming velocity. Most of the theories assume such linearity.

As shown in the literature,[24] only those harmonics of loading which are integer multiples of blade frequency (kZ) contribute to the unsteady thrust and torque, and only those harmonics of loading adjacent to multiples of blade frequency ($kZ \pm 1$) contribute to the unsteady transverse forces and bending moments. All other harmonics of shaft frequency cancel when summed over the blades. This cancellation is a consequence of the symmetry of the propeller (assuming that the blades are identical and equally spaced) and is independent of the type of theory used for determining the loading. Further, within the assumption of linearity, only the corresponding harmonics of the wake contribute to the respective components of loading. Thus, if linearity is accepted as being approximately true (and available information seems to confirm this), selection of the number of blades can be based on the relative strengths of the harmonics in the wake and the response characteristics of the vessel so that the probability of vibration within a specified speed range is minimized.

Basically four different methods have been applied to calculate the unsteady forces and moments on marine propellers caused by circumferentially nonuniform inflow. These are quasi-steady, two-dimensional unsteady along a strip, combination quasi-steady two-dimensional unsteady along a strip, and three-dimensional unsteady.

QUASI-STEADY METHOD

The quasi-steady theory completely neglects the influence of all time-dependent effects on the loading. The instantaneous loading at any time is taken to be the loading which would occur if the propeller were operating continually at the instantaneous inflow conditions. There are basically two techniques used for applying the quasi-steady method (1) uniform-flow propeller tests, and (2) steady-state propeller theory.

In using uniform-flow propeller tests (open water tests), the assumption is made that the average inflow conditions, from root to tip, may be determined at each angular position of a propeller blade in a wake. In the most general approach,[11] an effective line of encounter considering blade skew is assumed, and a weighted radial average (such as a volume or a thrust mean) of the longitudinal and tangential inflow velocity is taken along this line. Some less general techniques consider only the inflow conditions at a representative blade radius[25,26] and most proposed techniques neglect the effect of skew.[25-27] The effective inflow conditions thus determined at each angular position of the blade are then used in entering the open water performance curves of the propeller to determine the instantaneous thrust and torque coefficients of the propeller. An harmonic analysis is performed to determine the harmonic content of the thrust and torque variation. A slightly different approach entails performing an harmonic analysis on the effective inflow conditions and entering the open water characterization curves to determine the amplitude of the corresponding blade-frequency harmonic of thrust and torque.[25,26] The latter approach implicitly assumes that the loading varies linearly with the wake, whereas the former approach does not.

In using steady-state propeller theory, a propeller-design procedure is worked inversly so that the radial load distribution is determined for the local inflow conditions at each angular position of the propeller blade in the circumferentially nonuniform inflow field. Quasi-steady calculation procedures have been proposed by Ritger and Breslin[9] and by Yeh,[12] based upon the Burrill propeller design method;[28] by Lotveit,[29] based upon the Hill propeller design method;[30] and by Haskins at the Center, based upon the Eckhardt and Morgan propeller design method[31] together with the Lerbs induction factors.[32] These design procedures are all lifting-line techniques, the primary differences being the criterion used for optimum circulation distribution and the manner of applying corrections for both lifting-surface and viscous effects. They are intended to accurately assign pitch, camber, and thickness to the blades for a single operating condition. However, in calculating fluctuating loading, where local inflow conditions must be considered, there may be large deviations from the average inflow conditions assumed in the propeller design. Thus successful use of these techniques to calculate fluctuating forces in a quasi-steady manner depends upon the success with which mean thrust and torque over a wide range of inflow conditions can be predicted by using them.

All the previously mentioned design procedures employ the Goldstein factors[33] which are derived for the special case of optimum circulation distribution along a blade. For locally varying wake, the Lerbs induction factors which consider arbitrary circulation along a blade, should be used, rather than the Goldstein factors for calculating induced velocities. Only the Haskins method among the proposed quasi-steady calculation techniques uses the Lerbs induction factors. McCarthy[11] presents a thorough review of the quasi-steady technique.

The quasi-steady technique totally neglects all influence of the shed vorticity. At a given angular position of a blade the strength of the trailing vorticity is assumed to be independent of downstream angular position. Its strength is determined by the gradient of the

bound vorticity associated with the wake at the effective line of encounter of the blade

$$\gamma_s = \frac{d\Gamma^B}{d\rho}$$

Since the shed vorticity is neglected, its effect in mitigating the effective angle of attack variation is neglected. Thus, the variation of the bound vorticity and the radial gradient of the bound vorticity is overestimated. Therefore the magnitude of the variation of the trailing vorticity with blade angular position is overestimated, which results in an overestimation of the influence of the trailing vorticity.

TWO-DIMENSIONAL UNSTEADY METHOD

The two-dimensional unsteady technique considers the section at each radius as a two-dimensional airfoil, operating in the local resultant inflow velocity field. This method has been proposed by Lane,[34] Lewis,[13] Ryall,[35] and Sevik[36] and has been applied by Casellini.[37] All three-dimensional influences (such as finite aspect ratio, helicoidal geometry of the propeller blades and the downstream wake, and blade interaction) are totally ignored. In each radial strip, the component of the pertinent wake harmonic normal to the resultant inflow velocity is determined from the relationship; see Figure 2

$$V_N{}^n(r) = V_L{}^n(r) \cos \beta - V_T{}^n(r) \sin \beta$$

The effect of the harmonics of the wake component parallel to the resultant inflow velocity (sinusoidal surge velocity) is generally small and is thus neglected or considered in a quasi-steady manner. The response to the harmonics of the wake component normal to the resultant inflow is obtained from the Sears[14] two-dimensional sinusoidal gust theory. According to Sears, the lift on a blade element is

$$\tilde{L}(r) = Re\,[\pi\rho c(r)\, \bar{U}_r(r)\, V_N{}^n(r)\, e^{i\omega t} \phi(k)]$$

where $Re[\ ]$ is the real part of the expression,

$c(r)$ is the chord length,

$\bar{U}_r(r)$ is the resultant mean inflow velocity,

$V_N{}^n(r)$ is the harmonic amplitude of velocity normal to chord,

ω is the incidence frequency of gust,

k is the reduced frequency, and

$\phi(k)$ is the Sears function.

The Sears function $\phi(k)$ is defined by

$$\phi(k) = [J_0(k) - i J_1(k)] \frac{K_1(ik)}{K_1(ik) + K_0(ik)} + i J_1(k)$$

where the J's and K's are Bessel functions of the first kind and modified Bessel functions of the second kind, respectively. Figure 3 shows a plot of the Sears function. The reduced frequency is defined as

$$k = \frac{\omega c}{2\overline{U}_r}$$

This may alternately be expressed as the ratio of the two length scales of the flow field

$$k = \frac{\pi c}{\lambda}$$

where λ is the wavelength of the sinusoidal gust. For propellers, the reduced frequency is very closely approximated by

$$k = n\theta_b$$

where θ_b is the projected semichord expressed in radians. The magnitude of reduced frequency is a direct measure of the unsteadiness of the flow field. For low reduced frequency, or long wavelength relative to the chord, the effects of unsteadiness are small, and the unsteady lift approaches the quasi-steady lift in both amplitude and phase.

The quasi-steady two-dimensional fluctuating lift is

$$L_{QS}(r) = Re\left[\pi\rho c(r)\ \overline{U}_r(r)\ V_N{}^n(r)\ e^{\ \omega t}\right]$$

Thus the ratio of the unsteady to the quasi-steady amplitude is

$$\frac{\widetilde{L}}{L_{QS}} = \left|\phi(k)\right|$$

The two-dimensional unsteady technique completely neglects the effect of the trailing vorticity. The effect of the shed vorticity within a small radial segment is considered in a two-dimensional fashion, and the influence of the shed vorticity in other radial segments and from other blades is totally ignored. The shed vorticity is assumed to follow a linear path rather than a helical path. Since the trailing vorticity is neglected, its effect of mitigating the effective angle of attack variation is neglected. The magnitude of the shed vorticity is directly proportional to the angle of attack variation; therefore, the magnitude of the shed vorticity is overestimated. Thus this method overestimates the effect of the shed vorticity and neglects the trailing vorticity.

COMBINATION QUASI-STEADY TWO-DIMENSIONAL UNSTEADY METHOD

In the combination techniques, the unsteady effects are determined by two-dimensional methods similar to those discussed in the previous section. In addition, quasi-steady three-dimensional corrections are applied from steady-state propeller theory in a manner similar to that discussed in the section on quasi-steady methods.

Ritger and Breslin[9] extended their quasi-steady technique based on the Burrill propeller-design method by multiplying the component of quasi-steady lift due to the fluctuating normal velocity by the Sears function. Moreover, the much less significant effect of the surge velocity fluctuations was considered only in a quasi-steady manner.

Reed and Bradshaw[38] also developed a combination method based upon the Burrill propeller design procedure. The component of quasi-steady lift due to the fluctuating normal velocity is adjusted by multiplying by the Sears function. The component of quasi-steady lift due to the fluctuating surge velocity is adjusted by application on a strip of the technique developed by Greenberg[39] for calculating the unsteady lift of a two-dimensional airfoil due to a sinusoidal surge velocity.

Krohn[7,8] developed a combination technique whereby the lift in each radial strip was initially calculated by direct application of the Sears two-dimensional sinusoidal gust theory as discussed in the previous section. This two-dimensional unsteady lift was then modified by dividing by the camber correction coefficients as applied in the Eckhardt and Morgan procedure for propeller design. No three-dimensional corrections were applied to the incoming angle of attack variation.

The combination quasi-steady two-dimensional unsteady technique considers the trailing vorticity in the same manner as does the quasi-steady technique. However, the effect of the shed vorticity as considered by the two-dimensional approach is then superimposed. Hence this method overestimates the effect of both the trailing and the shed vorticities.

A three-dimensional unsteady theory is necessary to account for the time-dependent effects of both the trailing and shed vorticity in a consistent manner.

THREE-DIMENSIONAL UNSTEADY METHOD

Hanaoka[40] formulated a linearized unsteady lifting-surface theory for calculating the unsteady propeller loading in incompressible potential flow. He assumed that both the lifting-surface and trailing vorticity lay on a predetermined helicoidal surface of constant pitch and considered any deviation from this surface by either the flow or the lifting surface as a small perturbation. The Hanaoka theory is applicable to unsteady flow due to rigid body oscillation of the propeller, oscillation of the propeller blades, and circumferentially nonuniform inflow velocity. The problem under consideration in this report involved the special case of a rigid propeller operating at constant angular velocity and speed of advance in a circumferentially nonuniform inflow field. Hanoka derived the following higher order singular surface integral equation, relating the known unsteady downwash distribution on the blades to the unknown unsteady loading distribution[41]

$$V_N^n(r)\, e^{in(\Omega t - \phi_0)} = \sum_{m=1}^{Z} \frac{e^{in\Omega t}}{4\pi\rho V_A} \iint_S \Delta p(\xi, \rho, \theta_0)\, X$$

$$\frac{\partial}{\partial n'} \int_{-\infty}^{x} e^{in\,[a(\tau' - x) - \overline{\theta}_m]}\, \frac{\partial}{\partial n}\left(\frac{1}{R}\right) d\tau' dS \qquad [1]$$

where $V_N{}^n(r)$ is the known amplitude of relative velocity normal to helicoidal surface given by $x = \phi_0/a$,

Δp is the unknown pressure jump across lifting surface,

x, r, ϕ is the cylindrical coordinate system of control points,

ξ, ρ, θ is the cylindrical coordinate system of loading points,

$R = \{(\tau' - \xi)^2 + r^2 + \rho^2 - 2r\rho \cos\,[\theta_0 - \phi_0 + \overline{\theta}_m - a(\tau' - x)]\}^{1/2}$, the Descartes distance between load point and control point,

$\frac{\partial}{\partial n} = \frac{\rho}{\sqrt{1 + a^2\rho^2}}\left(a\,\frac{\partial}{\partial \xi} - \frac{1}{\rho^2}\,\frac{\partial}{\partial \theta_0}\right)$, directional derivative normal to helicoidal surface at loading point, and

$\frac{\partial}{\partial n'} = \frac{r}{\sqrt{1 + a^2 r^2}}\left(a\,\frac{\partial}{\partial x} - \frac{1}{r^2}\,\frac{\partial}{\partial \phi_0}\right)$ directional derivative normal to helicoidal surface at control point.

Hanoka mathematically investigated in detail the properties of the kernel function and the finite contributions of the singularities. However, he did not perform a numerical evaluation of this extremely complex integral equation.

Subsequently, several investigators have attempted to numerically evaluate Equation [1] for the case of a nonoscillating rigid propeller in circumferentially nonuniform inflow with the aid of various assumptions regarding the propeller geometry and loading.

Greenberg[42] simplified the unsteady lifting-surface equation to allow contributions from the various influences to be considered separately. He assumed that the blade self-induced downwash was that caused by a tangent flat plate of finite aspect ratio operating in rectilinear flow plus that due to a small helical correction, which was approximately accounted for. The induced downwash from the bound vorticity of the other blades was considered in a lifting-line sense and was thus zero. The shed and trailing vorticity of the other blades was represented as a cascade, and the induced downwash was calculated by two-dimensional strip theory. Greenberg concluded that the propeller could be represented by a plane wing and its wake, since the interactions and the helicoidal effects were small.

Brown[19] simplified the lifting-surface equation by expressing the induced velocity at a point on the blade as the sum of the induced velocity calculated by the two-dimensional sinusoidal gust theory and a three-dimensional two-dimensional "downwash difference." This correction of downwash difference to two-dimensional strip theory was approximated from a lifting-line model of the propeller. In this model, the downwash difference was calculated along a radial line which also served as the location of the concentrated bound vorticity, the line of encounter of the incoming flow, the locus along which the boundary

condition was satisfied, and the line from which the shed vorticity emanated. In addition to neglecting the chordwise boundary conditions for three-dimensional effects (implying narrow-bladed propellers), was the curvature of the leading and trailing edges neglected on this model, which meant that the important radial phase variation of the downstream vorticity was not properly taken into account.

Yamazaki[43] numerically evaluated the unsteady lifting-surface equation under the assumption that the chordwise loading distribution in the harmonic of interest was the same as that of an inclined flat plate ($\gamma_r^B = \cot \theta_\alpha/2$), where θ_α was an angular measure of the linear chordwise coordinate χ; θ_α was defined by $\chi = -c/2 \cos \theta_\alpha$, with $\chi = -c/2$, and $\theta_\alpha = 0$ at the leading edge, and $\chi = +c/2$, and $\theta_\alpha = \pi$ at the trailing edge. The chordwise boundary condition was then satisfied by a weighted average by application of the Glauert lift operator

$$\frac{1}{\pi}\int_0^\pi \{\ \}(1 - \cos \phi_\alpha)\, d\phi_\alpha$$

where ϕ_α was the control point coordinate defined by $\chi = -c/2 \cos \phi_\alpha$. This, in effect, reduced the surface integral equation to a radial line integral equation. The use of only one chordwise loading mode, implied that the interaction with the other blades and blade sections could affect only the magnitude of the chordwise load distribution. Interactions which affected the shape of the chordwise load distribution were neglected. For the limited example calculated by Yamazaki, this method yielded unsteady thrust and torque predictions which were approximately the same as the quasi-steady predictions.

From 1962 to 1967, the Davidson Laboratory, under NSRDC contract, conducted a series of investigations in which the unsteady lifting-surface equation was numerically evaluated under successively less restrictive assumptions regarding the propeller geometry and the chordwise loading distribution.

The following fundamental simplifications have been retained (except as noted) throughout the Davidson Laboratory evaluations of Equation [1].

1. The directional derivatives normal to the helicoidal surface are replaced by directional derivatives in the axial direction

$$\frac{\rho}{\sqrt{1 + a^2\rho^2}}\left(a\frac{\partial}{\partial \xi} - \frac{1}{\rho^2}\frac{\partial}{\partial \theta_0}\right) \rightarrow \frac{\partial}{\partial \xi}$$

$$\frac{r}{\sqrt{1 + a^2 r^2}}\left(a\frac{\partial}{\partial x} - \frac{1}{r^2}\frac{\partial}{\partial \phi_0}\right) \rightarrow \frac{\partial}{\partial x}$$

2. The helicoidal surface of integration both on the blades and in the downstream wake is approximated in a staircase manner. That is, integration over the helicoidal surface

$$x = \phi_0/a$$

is replaced by integration over the series of planar segments

$$x = \frac{1}{a}\left(\frac{2\pi}{Z}\right)m$$

where m is an integer whose value depends upon the interval of ϕ_0 as follows

$$\left(m - \frac{1}{2}\right)\frac{2\pi}{Z} < \phi_0 < \left(m + \frac{1}{2}\right)\frac{2\pi}{Z}$$

In the earliest evaluation, Shioiri and Tsakonas[44] applied the Weissinger approximation[45] in which the vorticity was concentrated at the 1/4-chord position and the boundary condition was satisfied at the 3/4-chord position.

Rather than satisfy the actual boundary condition at the 3/4-chord position, Shioiri and Tsakonas applied the Glauert lift operator to satisfy the boundary condition by a weighted average over the chord. This means that if the chordwise normal induced velocity distribution is expressed as

$$V_0(r) - \sum_{m=1}^{\infty} V_m(r) \cos m\phi_\alpha \qquad [2]$$

then the boundary condition due to only the first two terms of Equation [2] (i.e., $V_0(r) - V_1(r) \cos \phi_\alpha$) is satisfied at the 3/4-chord position. Such a technique yields the same result as thin airfoil theory for the steady two-dimensional case.

To examine the suitability of the Weissinger model in the unsteady case, the authors compared its predictions with those of the Sears sinusoidal gust theory for two-dimensional flow. This comparison showed that even for two-dimensional flow, the error due to the Weissinger approximation increased with reduced frequency so that the Weissinger model was in error by 50 percent or more in the reduced frequency range of interest ($1 < k < 3$) in marine propellers. This was because the normal induced velocity distribution was not adequately approximated by $V_0(r) - V_1(r) \cos \phi_\alpha$ for high reduced frequencies.

The Weissinger approximation assumed that the downstream radial and stream directive vorticity started at the 1/4-chord position. This assumption neglected radial phase variation in the downstream vorticity due to the curvature of the leading and trailing edges. Because of the general chordwise distribution of the induced velocities in the unsteady case, satisfying the boundary condition only at the 3/4-chord position was not justified here.

Tsakonas and Jacobs[46] solved the unsteady lifting-surface equation under the assumption that the chordwise circulation distribution in the harmonic of interest was the same as that of an inclined flat plate. The chordwise boundary condition was then satisfied by a weighted average by using the Glauert lift operator. Fundamentally, this was the same approach used by Yamazaki.[43] Tsakonas and Jacobs further assumed that the propeller blades had a sector-type outline so that both the leading edge and the trailing edge would be

radial straight lines. This unrealistic blade outline exaggerated the effect of the blade sections toward the tip, implied that the reduced frequency was constant with radius, and neglected the curvature of the blade leading and trailing edges which eliminated important spanwise phase variation.

Tsakonas et al.[41] have recently numerically evaluated the unsteady lifting-surface integral equation considering a large number of chordwise loading modes. The chordwise load distribution is expressed by the Birnbaum series

$$S(\rho, \theta_\alpha) = \frac{1}{\pi}\left\{L^1(\rho)\cot\frac{\theta_\alpha}{2} + \sum_{n=2}^{N} L^n(\rho)\,\frac{\sin(n-1)\theta_\alpha}{n-1}\right\}$$

This series, which is commonly used in two-dimensional airfoil theory, produces a flat plate-type singularity at the leading edge and satisfies the Kutta condition at the trailing edge.

Retained in this model are the approximations replacing the directional derivatives normal to the helicoidal surface by directional derivatives in the axial direction and replacing the helicoidal surface of integration by a series of planar segments. These approximations are justified via a worked sample[47] for a blade with radial leading and trailing edges and one chordwise loading mode (as in Reference 46). Blade-frequency thrust as calculated with "exact" treatment of the normal derivatives and path of integration agrees within 15 percent of that calculated with both of the previously described approximations retained.

The inverse Descartes distance $1/R$ is expanded in a series whereby the ϕ_0 and θ_0 dependence in the kernel appears in separated form in terms of cos $(m\phi_\alpha)$ and cos $(n\theta_\alpha)$. Chordwise integration with respect to θ_α (the loading) then reduces the surface integral equation to a line integral equation. The chordwise boundary conditions are then satisfied for each of the chordwise loading modes by use of the following series of generalized lift operators

$$m = 1, \quad \frac{1}{\pi}\int_0^\pi \{\ \}(1-\cos\phi_\alpha)\,d\phi_\alpha \quad \text{(Glauert lift operator)}$$

$$m = 2, \quad \frac{1}{\pi}\int_0^\pi \{\ \}(1+2\cos\phi_\alpha)\,d\phi_\alpha$$

$$m > 2, \quad \frac{1}{\pi}\int_0^\pi \{\ \}\frac{\cos(m-1)\phi_\alpha}{m-1}\,d\phi_\alpha$$

The structure and application of these lift operators is dictated by the separable (or degenerate) form of the kernel function so that the orthogonality property of the set $\{\cos m\phi_\alpha$, $m = 1, 2, 3 \ldots\}$ is utilized. This orthogonality property eliminates the cross-coupling terms and thus allows each lift operator to act upon only one loading mode, which greatly reduces

computation time. Finally, the span is divided into I-strips, and the set of M-line integral equations is reduced by the collation method to a set of $M \times I$ algebraic equations in the unknown spanwise and chordwise loading distributions.

This method is superior to previous techniques in that it provides for flexibility of chordwise loading and analytic chordwise integrations. It is the only available numerical evaluation of the unsteady lifting-surface integral equation in which these essential lifting-surface features are retained.

This technique has been programmed for a high-speed digital computer and takes about 3 1/2 minutes for calculating one harmonic of thrust and torque on an IBM 7090. The computer program can consider arbitrary blade outline, including skew, and can take into account a large number of chordwise loading modes under the basic assumption that the helicoidal geometry can be approximated in a staircase fashion.

EXPERIMENTAL METHOD AND RESULTS

Accurate and reliable experimental results are required to evaluate the various methods of calculating the unsteady propeller loading in circumferentially nonuniform inflow. For valid comparison, the experimental conditions should simulate as closely as possible the important conditions assumed in the theories. These are primarily a known inflow velocity field and an absence of nearby boundaries.

A water tunnel with a velocity distribution control device provides an ideal facility for conducting these experiments. Devices used to date for producing nonuniform flow without introducing solid boundaries in the flow are wire grids of nonuniform properties[48] and arrays of valve-controlled nozzles.[19,49] In either case, the propeller must be located far enough from the device to insure that the pressure field due to the propeller loading has a negligible influence on the velocity distribution produced. In this investigation, wire-grid screens were used because of their relative simplicity. Screens produce only an axial velocity variation, which is sufficient for the purpose of this study.

Burstein[15] showed experimentally that the action of the propeller on the wake behind a slender body of revolution with fins very significantly affected the harmonic content of the wake. The mean pressure reduction generated by the propeller on the near afterbody surface reduced the adverse pressure gradient and thus altered the distribution of the velocity shed into the propeller plane. This wake alteration comprised both a potential part due to the effect of images of the propeller in the body and a viscous part due to changes in the boundary layer thickness and the point of separation. Thus the interaction effect was expected to become more important as the afterbody became fuller or nearer to the propulsor. Most previous attempts to measure unsteady propeller loadings were conducted in wakes behind bodies or struts. Hence the harmonic content of the wake in which the propeller operates is somewhat uncertain, which renders these results questionable for evaluating theoretical calculation techniques.

Brown[19] measured the blade-frequency thrust and torque on a single propeller operating in a nonuniform inflow field produced by an array of valve-controlled nozzles. However, the limited scope of this experimental study precluded extensive comparisons with theoretical predictions.

The present tests were conducted at the Naval Ship Research and Development Center in a water tunnel using a 27-inch-diameter, closed-jet test section. Figure 4 shows the experimental setup. The wire-mesh wake screens were constructed using a base screen having an 0.009-inch-diameter wire, 16 per inch, and a single overlay screen with an 0.015-inch-diameter wire, 18 per inch, so oriented that these wires intersected those of the base screen at 45 degrees. Hence the action of the propeller 30 inches (2 1/2 propeller diameters) downstream did not alter the flow over these wires. Also, there was negligible unsteady interaction between the walls of the 27-inch-diameter test section and the 12-inch-diameter propellers.

PROPELLERS AND WAKES

For this experimental investigation, four three-bladed propellers were tested in two different wake patterns. The four propellers (three unskewed propellers with expanded area ratios of 0.3, 0.6, and 1.2 and one propeller with 120 degrees of skew and an expanded-area ratio of 0.6) were designed for the same diameter, thrust, speed of advance, and rotational speed, using the Lerbs induction factors with the lifting-surface and thickness corrections of Kerwin and the Leopold.[50] The pitch of the skewed propeller, however, varied from that developed by the lifting-surface design theory. The geometric properties and open water characteristics of these propellers are presented in Appendix A. Figure 5 shows a photograph of the four propellers.

A propeller responds in unsteady thrust and torque to those wake harmonics which are multiples of the number of blades (kZ) and in side forces and bending moments to wake harmonics which are of multiples of the number of blades plus or minus one ($kZ \pm 1$). In fact, linearized theory predicts that the propeller responds only to these harmonics. Thus, in a practical propeller design, selection of the number of blades can be based on the known or estimated harmonic content of the inflow velocity so that the most critical type unsteady propeller forces and moments are minimized. In the present experiments, the number of blades and strong wake harmonics were selected to produce large signals in measuring the unsteady forces and moments of interest. This permitted accurate measurements for comparison with theory and study of the less understood effects of some other parameters on unsteady loading.

For fixed wake and number of blades, it is conjectured that skew (effect of radial phase variation) and blade width (effect of aspect ratio and reduced frequency) are the propeller parameters which most significantly affect unsteady bearing forces. Thus the series of propellers was designed to enable determining the effect on unsteady bearing forces of varying only blade width and only skew.

Three-bladed propellers were selected since they exhibited all the general features of propellers with an arbitrary number of blades while minimizing the frequency of the propeller loading and providing ease of manufacture of propeller and wake screen. The skewed propeller had a constant skew rate so that the section at the tip lagged behind the section at the root by 120 degrees; this placed the root of each blade at the same angular position as the tip of the preceding blade. Thus at any instant, one and only one blade section was entering the wake at a given angular position.

For the propellers tested, the blade width varied by a factor of four. This allowed the unsteady loading response to a given wake harmonic to be studied over a factor of four in reduced frequency.

The wake-producing grids were constructed by arranging screens of various mesh sizes in carefully fitted patterns on a single support screen of low resistance coefficient.[48] Although it might have been desirable to produce a truly sinusoidal wake, this required several overlays of screens and was rather difficult to accomplish. Therefore, simple segmental overlays were used in the screens (see Figures 6 and 7) which produced a more nearly rectangular wave with rounded corners.

One screen produced a nonuniform inflow having a dominant third harmonic so that large blade-frequency thrust and torque was developed by the propellers. The other screen produced a nonuniform inflow having a dominant fourth harmonic so that large blade-frequency side forces and bending moments were produced by the propellers. The resultant wakes exhibited the desired dominant harmonics plus much weaker multiples of these harmonics; all other wake harmonics were small. The amplitude and phase of the most significant harmonics are shown in Figures 8 and 9. More details concerning the wake and its measurement are presented in Appendix B.

INSTRUMENTATION AND DATA ANALYSIS

The six components of unsteady loading were measured by a six-component dynamometer[51,52] utilizing a sting-mounted balance with semiconductor strain gages as the sensing elements. More details of this instrument are given in Appendix C.

The convention adopted in this report for the six components of unsteady force and moment is defined in Figure 10. Note that what is called horizontal bending moment is not a horizontal moment vector but a moment produced by a horizontal force. The balance is designed so that the transverse-force and bending-moment sensors, which measure force and moment along a pair of orthogonal axes, rotate with the propeller. Hence transverse-force and bending-moment vectors rotating with the propeller are measured. A propeller position ($\theta_p = 0$) is defined at which the rotating axis coincide with the (fixed) horizontal and vertical axes; then

$$M_1 = M_V, \quad M_2 = M_H, \quad F_1 = F_V, \quad F_2 = F_H$$

where M_1, M_2, F_1, and F_2 are forces and moments with respect to the rotating axes. At any propeller angle θ_p, the forces and moments with respect to the fixed axes are:

$$M_V = M_1 \cos \theta_p + M_2 \sin \theta_p$$

$$M_H = -M_1 \sin \theta_p + M_2 \cos \theta_p$$

$$F_V = F_1 \cos \theta_p - F_2 \sin \theta_p$$

$$F_H = F_1 \sin \theta_p + F_2 \cos \theta_p$$

Figure 11 shows a block diagram of the instrumentation used with the dynamometer. This setup provided for on-the-spot observation and analysis of the signals as well as for recording on magnetic tape for computer analysis. The thrust, torque, transverse-force, and moment gages were excited by separate adjustable d-c power supplies. The a-c output signals were separated from the steady signals and were amplified before leaving the rotating shaft through the sliprings and brushes. The d-c signals were read on a d-c electronic voltmeter. The a-c components went to amplifiers and attenuators where they were adjusted to the proper levels for the tape recorder and analyzer. The signals were monitored on an oscilloscope, and photographic records were made of the waveforms. The six signals were recorded on magnetic tape along with pulses from pickups on the propeller shaft. The pulses consisted of 1 pulse per revolution for a phase reference and 60 pulses per revolution to control the analog-to-digital conversion.

For the computer analysis, the tape record was digitized at 60 points per revolution. These values were averaged for 200 revolutions and were scaled to obtain 60 points at 6-degree intervals of an average cycle. The values for the six channels were then multiplied by a 6×6 calibration matrix to obtain values of thrust, torque, side forces, and bending moments in pounds and pounds-feet.

Anotner computer operation resolved the rotating side force and bending moment vectors into vertical and horizontal components. The amplitudes of the first 18 sinusoidal harmonic components were then computed along with the phase angle relative to the propeller position at which the single-tooth pulse was generated.

For the on-the-spot analysis, one signal at a time was fed into one channel of a two-channel wave analyzer whose channels were matched for frequency and phase. The single-tooth pulse was fed into the other channel as a phase reference. Since this pulse was narrow and symmetrical, it had in-phase components at any harmonic of shaft frequency. The analyzer was manually tuned to any desired harmonic with the aid of an oscilloscope. The signal level was read on a meter connected to the output of the signal channel, and the phase was read from a phase meter connected to the two outputs. All six components were multiplied by the calibration matrix, and side forces and bending moments were resolved into vertical and horizontal components by hand calculation. A more detailed description of this instrumentation is given in Reference 52.

TEST PROCEDURE

Each of the four propellers was run in both the 3- and 4-cycle wake patterns. The same values of mean thrust were set for each propeller (see Table 1) resulting in different advance coefficients for the different propellers. The highest loading condition was omitted for the narrow propeller in the 3-cycle wake and for the skewed propeller in both wakes. All tests were run at 15 revolutions per second, and the design condition ($\overline{K}_T = 0.150$) was repeated at 18 revolutions per second. This resulted in Reynolds numbers ranging from 0.8×10^6 to 3.4×10^6.

There is no method of directly measuring the mean tunnel-water speed in the nonuniform inflow condition. Hence the thrust and revolutions per second were set, and the mean water speed was assumed to be the same as that measured for comparable conditions in uniform flow (i.e., from open water tests).

Figure 12 shows typical signals from the six-component balance in the 3-cycle wake, and Figure 13 shows typical signals in the 4-cycle wake. One propeller revolution constituted the distance between the pulses in the upper trace as generated by the single-tooth gear. These signals were recorded on magnetic tape for digital computer analysis. The major harmonic components of each signal were also read from the on-the-spot analysis system. All thrust and torque data presented in this report (except as noted) were obtained from the on-the-spot analysis, and all side-force and bending-moment data presented were obtained from the digital analysis. The experimentally determined amplitudes of the blade-frequency harmonic of all six loading components are considered accurate within ± 5 percent.

EXPERIMENTAL RESULTS

In the 3-cycle wake, the thrust and torque signals clearly displayed the expected dominant blade-frequency harmonic as shown in Figure 12. The large shaft-frequency harmonic observed in the side-force and bending-moment signals was due to the weight of the propeller. This appeared at shaft frequency since the gages were rotating with the propeller. As expected, the propellers produced very weak hydrodynamic side forces and bending moments in the 3-cycle wake. (The amplification of the side-force and bending-moment signals shown in Figure 12 was much greater than that of the corresponding thrust and torque signals.) Figure 12 corresponds to the propeller with $EAR = 1.2$ at $J = 0.585$.

In the 4-cycle wake, the thrust and torque signals were very weak (as expected) and had no dominant harmonic (see Figure 13). (The amplification of the thrust and torque signals shown in Figure 13 was much greater than that of the corresponding side-force and bending-moment signals.) Here the side forces and bending moments displayed the expected dominant fourth harmonic. These signals appeared at the dominant wake harmonic because the gages rotated with the propeller. When transformed into nonrotating components of force and moment, the dominant fourth harmonic became a dominant third or blade-frequency harmonic. Figure 13 corresponds to the propeller with $EAR = 0.6$ at $J = 0.609$.

Figures 14 through 18 show the harmonic content of the thrust and torque in the 3-cycle wake and of the side forces and bending moments in the 4-cycle wake. These data are typical of the harmonic content of the dominant signals at all test conditions. The harmonics other than blade frequency arise primarily from the presence of harmonics other than the desired third or fourth harmonic in the flow field and are presented here for the purpose of completeness. These other harmonics are much weaker than the blade-frequency harmonic and, therefore, are considerably less accurate.

Figure 14 shows the harmonic content of the thrust and torque in the 3-cycle wake as determined by both the analog (on-the-spot) and the digital techniques. The digital system determined the first 18 harmonics of shaft frequency, whereas the analog system was tuned in to only the first four harmonics of blade frequency. The agreement between the two systems is very good. The blade-frequency harmonic is an order of magnitude larger than the multiples of blade frequency. Only harmonics of blade frequency appear above the noise level.

Figures 15 and 16 show the harmonic content of the side-force and bending-moment signals in the 4-cycle wake (as determined by the digital technique) relative to the rotating-coordinate system. In the rotating-coordinate system the side-force and bending-moment signals due to hydrodynamic loading should contain only harmonics adjacent to multiples of the number of blades ($kZ \pm 1$). Only these harmonics appear above the noise level in Figures 15 and 16. As expected, the fourth harmonic ($Z + 1$) is an order of magnitude larger than the others. The weight of the propeller produces the strong shaft harmonic in the side-force signals and the weaker shaft harmonic in the bending-moment signals. The mean value of the side-force and bending-moment signals is apparently due to an unbalance of the propeller.

Figures 17 and 18 show the harmonic content of the side-force and bending-moment data resolved into vertical and horizontal components. In this fixed-coordinate system the signals due to hydrodynamic loading should contain only harmonics equal to multiples of the number of blades (kZ). Some other harmonics appear in Figures 17 and 18. These apparently result from inaccuracies in the phase angles of the weak harmonics in the rotating-coordinate system. The weight of the propeller produces the substantial mean value of the vertical side force. The shaft-frequency harmonic in the side-force and bending-moment signals results primarily from the mean value in the rotating system.

The variations of blade-frequency thrust and torque with mean propeller loading in the 3-cycle wake are shown in Figures 19 and 20, and the variations of blade-frequency side forces and bending moments with mean propeller loading in the 4-cycle wake are shown in Figures 21 and 22. In these plots each curve is nondimensionalized on a single constant; the fluctuating thrust and side forces are nondimensionalized on design thrust, and the fluctuating torque and bending moments are nondimensionalized on the torque required to develop the design thrust in uniform flow. (Since all conditions were run at the same rpm, $\widetilde{K}_T$/design $\bar{K}_T = \widetilde{T}$/design $\bar{T}$, $\widetilde{K}_F$/design $\bar{K}_T = \widetilde{F}$/design $\bar{T}$, etc.).

The increase of all six components of blade-frequency loading with mean velocity for the three unskewed propellers is apparently due to the increase in the circumferential velocity variation proportional to the mean velocity. This same trend is shown in the experimental results of Brown;[19] however, Brown measured only unsteady thrust and torque.

The data generally indicate that for side force, the horizontal component is greater than the vertical component whereas for bending moment the vertical component is greater than the horizontal component. These measured differences are attributable to the influence of the weak second harmonic in the 4-cycle wake. As shown in the literature,[24] the horizontal side force and vertical bending moment are functions of the vector sum of the second and fourth loading harmonics which (within linearized theory) correspond to the same harmonics of the wake. The vertical side force and horizontal bending moment, however, are functions of the vector difference of the second and fourth loading harmonics. Thus, the data presented are consistent.

The measured values of the transverse forces at $J = 0.672$ for $EAR = 1.2$ and at either $J = 0.500$ or $J = 0.609$ for $EAR = 0.6$ are inconsistent with the other data. The corresponding bending-moment data are consistent. Careful examination of the data provided no explanation for this inconsistency. These transverse-force measurements are apparently in error.

For the skewed propeller, the indicated decrease of all six components of blade-frequency loading with increasing velocity (or advance coefficient) at greater than $J = 0.876$ is not understood. The experimental values for this propeller at $J = 1.040$ and $J = 1.175$ display some additional unexpected characteristics. For these conditions, the blade-frequency thrust and torque signals in the 3-cycle wake displayed a twice-bladed frequency harmonic of the same order as the blade-frequency harmonic. However, for $J = 0.657$ and $J = 0.876$ for this propeller and for all conditions for the unskewed propellers, the blade-frequency harmonic was an order of magnitude larger than the twice-blade frequency harmonic. In the 4-cycle wake, the side-force and bending-moment signals displayed some stronger higher harmonics for the skewed propeller at $J = 1.040$ and 1.175 than for the other conditions tested.

The possibility was considered that deflections or vibrations of the less rigid skewed blades might have contributed to the measured trends. Static deflection tests indicated that for the magnitude of the unsteady loading involved (about 20 pounds), the deflection of the blades would have been insufficient to produce the measured trends. The frequency of the force variations was 45 hertz in the 3-cycle wake and 60 hertz in the 4-cycle wake, almost an order of magnitude below the fundamental frequency of blade vibration for the skewed propeller. Thus, blade-vibration amplitudes would not be likely to significantly exceed static deflections for the same magnitude of force. Propeller singing could be heard at $J = 1.040$ and $J = 1.175$, but this is associated with blade vibrations at frequencies several times the fundamental frequency of blade vibration. The blade vibrations due to singing should therefore not affect the loading at blade frequencies.

Although no explanation is provided, it is considered very possible that the measured trends with advance coefficient for the skewed propeller are true. The cavitation characteristics of this propeller also displayed unexpected trends with the advanced coefficient.[53] It appears that the skew influences the flow over the blades in a manner which is not fully understood.

At the design advance coefficient the extreme skew reduced the blade-frequency thrust and torque by a factor of 10 and the side forces and bending moments by a factor of 2 from the respective values on the corresponding unskewed propeller. The greater reduction in thrust and torque is largely attributable to the blades being skewed by 120 degrees. For the 3-cycle wake (120 geometric degrees per cycle) this results in one and only one blade section entering the high-velocity region at any instant, resulting in a maximum radial cancellation of blade-frequency loading. However, in the 4-cycle wake (90 geometric degrees per cycle) sections at the outer radii are entering the high-velocity region at the same time as sections at the inner radii, resulting in less radial cancellation of blade-frequency loading. Wereldsma[18] found experimentally that the fluctuating thrust and torque was reduced approximately by a factor of two by skewing the blades of a five-bladed propeller (EAR = 1.0) by approximately half-blade spacing.

Figure 23 shows the blade-frequency harmonic of all six loading components for the three unskewed propellers at advanced design coefficient. The thrust and torque loading is that measured in the 3-cycle wake whereas the side forces and bending moments are those measured in the 4-cycle wake. The blade frequency harmonic of all six loading components indicates parallel trends, increasing with expanded area ratio to some maximum value and then decreasing for further increase in blade-area ratio. Of course the shapes of these curves are not uniquely defined by the three blade widths tested.

The apparent parallel variation of the six components of loading with EAR may be a little misleading. Although one might generally expect a maximum at some blade width for the fluctuating thrust and torque, the shape of these curves is expected to be sensitive to the details of propeller and wake geometry. The side-force and bending-moment data presented here represent predominantly the response to the fourth harmonic of the wake. This means that the associated lift is at a higher reduced frequency; hence the maximum value may be expected to occur at a lower EAR than the associated maximum in thrust and torque (because unsteady effects are expected to become important at about the same reduced frequency in the two cases). Similarly, the side-force and bending-moment response to the weak second harmonic in the wake should occur at a higher value of EAR. In a general wake, the blade-frequency side force and bending moment is a function of the vector sum, or difference, of the lift responses to the $(Z + 1)$ and $(Z - 1)$ harmonics of the wake. The phase lag of these responses is different for the different frequencies and both vary with EAR in amplitude and phase. Hence, it is difficult to generalize on the variation of side force and bending moment with blade width.

The experimental trends of blade-frequency thrust and torque with EAR obtained for this paper are in qualitative agreement with the majority of previous experimental results. Wereldsma[17] concluded that blade-frequency thrust and torque decreased with blade width, but his study was limited to relatively high values of EAR ($0.6 \leq EAR \leq 1.0$). Krohn[7] concluded that blade-frequency thrust and torque increased with blade width, but his study was limited to relatively low values of EAR ($0.35 \leq EAR \leq 0.75$). Hence both of these results were in qualitative agreement with the results of this report in the respective range of EAR. In the recent study by Wereldsma[18] over a wide range of EAR ($0.4 \leq EAR \leq 1.2$), he obtained inconsistent results for fluctuating thrust and torque for the narrow-bladed propeller. If the thrust value of the narrow-bladed propeller conceived by Wereldsma is accepted, then his data show thrust montonically decreasing with EAR in contrast to the results of this report. However, if one accepts the torque value for this propeller (which Wereldsma evidently doubted) then his results for torque display an increase with EAR to some maximum value and then a decrease for further increase in EAR. This is in agreement with the trend of the data of the present report.

Previous studies to show the variation of blade-frequency side forces and bending moments with blade width were conducted in complex wakes that exhibited substantial amplitude of both the $(Z + 1)$ and $(Z - 1)$ harmonics. Hence, as indicated earlier, these data cannot be expected to collapse into a clear pattern. However, the data for a given wake should indicate a smooth trend. From measurements on three-bladed propellers ($0.6 \leq EAR \leq 1.0$) in the wake of a flat plate, Wereldsma[17] concluded that side forces and bending moments increased with EAR. This was contrary to the trends obtained for this report in this range of EAR. From measurements on five-bladed propellers ($0.35 \leq EAR \leq 0.75$) in the wake of a single-screw commercial ship, Krohn[8] concluded that transverse forces and bending moments increased with increasing EAR. This is the same trend obtained for this report in this range of EAR.

Phase angles of the principal components of the unsteady forces and moments are shown in Figures 24 through 26. These are blade-frequency thrust and torque in the 3-cycle wake and blade-frequency vertical and horizontal side forces and moments in the 4-cycle wake. The angles given are those by which these sinusoidal components lead to the same frequency components of the longitudinal velocity at the blade-reference line (radial line through midchord of root section). Figure 24 shows the phase angles of thrust and torque in the 3-cycle wake. For these results the thrust was assumed to be positive in the normal direction for forward propulsion, i.e., opposite the direction shown on Figure 10. The experimental values have not been plotted for some of the higher J values for the unskewed propeller with $EAR = 0.60$ and the skewed propeller. The phase angles for the unskewed propeller indicated a gross error in reading. The skewed propeller had peculiar values probably due to the large second harmonic component mentioned previously. Since thrust and torque decrease as the velocity increases, quasi-steady theory indicates that the phase angles should be near 180 degrees for a narrow-bladed propeller. This is approximated by the values for the

EAR = 0.30 propeller. As the blades become wider or are skewed, the effective line of encounter (the locus of the 1/4-chord points) is shifted forward or aft. This could explain the phase shifts shown for the wider and the skewed propellers. The phase angles for the the side forces and bending moments are shown in Figures 25 and 26. Blade width and skew have an effect similar to their effect on thrust and torque phase angles. The vertical components lead the horizontal by approximately 270 degrees, which is correct for the right-hand rotation of the propeller.

COMPARISON WITH THEORETICAL CALCULATIONS

Experimental blade-frequency thrust and torque were compared with theoretically obtained values to determine the range of validity of the various calculation techniques.

CALCULATION TECHNIQUES

One typical procedure for each of the following basic techniques was used: quasi-steady, using results from uniform flow tests (open water); quasi-steady, using steady-state lifting-line theory; two-dimensional unsteady; combination quasi-steady and two-dimensional unsteady; and three-dimensional unsteady.

For the quasi-steady technique, using uniform flow tests, a procedure somewhat similar to that outlined by McCarthy[11] was used. However, in the present technique, linearity is assumed. Since the blade-frequency harmonic of the wake is radially in phase, a radial thrust mean amplitude is easily calculated. The effective line of encounter was assumed to be the locus of the midchords of the blade sections. For a given mean advance coefficient, the open water test is then entered at

$$J_{max} = \frac{V_A + \bar{V}_L^{(3)}}{nD} \qquad J_{min} = \frac{V_A - \bar{V}_L^{(3)}}{nD}$$

where

$$\bar{V}_L^{(3)}(r) = \frac{1}{\bar{T}} \int_{r_h}^{R} V_L^{(3)}(r) \frac{d\bar{T}}{dr} dr$$

The amplitude of the corresponding harmonics of thrust and torque fluctuations are then

$$\tilde{K}_T = \frac{1}{2} [(\bar{K}_T \text{ at } J_{min}) - (\bar{K}_T \text{ at } J_{max})]$$

$$\tilde{K}_Q = \frac{1}{2} [(\bar{K}_Q \text{ at } J_{min}) - (\bar{K}_Q \text{ at } J_{max})]$$

For the quasi-steady technique using uniform flow propeller theory, the Haskins method was used. This is an inverse lifting-line method, utilizing the Lerbs induction factors and the Eckhardt and Morgan correction factors. The effective line of encounter was assumed to

be the locus of the midchords of the blade sections. For the calculations performed, the steady component of thrust and torque very nearly reproduced the slopes of the $\overline{K}_T$ and $\overline{K}_Q$ curves of the open water tests. However, the magnitudes were off by about 5 percent at design advance coefficient.

The two-dimensional unsteady technique was a direct application of the Sears two-dimensional sinusoidal gust theory as outlined by Lewis.[13]

For the combination quasi-steady, two-dimensional unsteady method, the blade-frequency lift calculated by the Haskins method at each radial section was multiplied by the Sears function based on the local reduced frequency. In principle, this was the procedure proposed by Ritger and Breslin;[9] however, they applied the correction to a quasi-steady lift as calculated from the Burrill propeller-design procedure.

The three-dimensional unsteady calculations were performed by the method of Tsakonas et al.[41] These calculations were performed on an IBM-7090 computer, utilizing a program developed at Davidson Laboratory. In these calculations, both the "normal" component of wake and the section lift were taken to be normal to the section nose-tail line. All calculations were performed using eight radial strips and five chordwise loading modes.

COMPARISONS

Figure 27 shows the experimental blade-frequency thrust over a range of expanded area ratios together with predictions according to the various aforementioned techniques. Also shown is the reduced frequency at the 0.75 radius. Figure 28 reveals similar information for blade-frequency torque. The blade-frequency thrust curves are nondimensionalized on the design thrust and the blade-frequency torque curves are nondimensionalized on the torque required to develop the design thrust in uniform flow. These values of the mean thrust and torque are determined from the open water tests.

The quasi-steady techniques have been observed to yield reasonable predictions for the two relatively narrow-bladed propellers but unreasonable predictions for the wide-bladed propeller (no calculation was performed by the quasi-steady lifting-line technique for the wide-bladed propeller because this computer program would not run for this condition). The fairly good agreement for the narrow-bladed propellers indicates that the effect of the unsteadiness is small for these relatively low reduced frequencies. However, quasi-steady predictions become increasingly in error for reduced frequencies greater than 1.6, indicating that the effects of unsteadiness become important in this region. It is also significant that the quasi-steady predictions are conservative over the entire range, even for the narrow-bladed propellers. This increasingly conservative prediction with increasing reduced frequency would be expected from a two-dimensional analogy. However, this may not hold true for propellers in general because, depending on the relative phase, the unsteady effects of the other blades and their wakes may either add to or subtract from the unsteady propeller loading. Additional calculations

with the quasi-steady lifting-line technique indicate that if the locus of the quarter chords is used as the effective line of encounter rather than the locus of the midchords, the predictions are approximately 3 percent lower for $EAR = 0.3$ and 5 percent lower for $EAR = 0.6$.

The two-dimensional unsteady technique displays the proper general trend with expanded-area ratio but overpredicts the blade-frequency thrust by roughly a factor of two. In essence, two counteracting simplifications are made in this approach: (1) the effect of the shed vorticity on reducing the unsteady lift is overestimated, and (2) the effect of the trailing vorticity on reducing the unsteady lift is totally ignored. This technique can be expected to yield better predictions for conditions in which chordwise unsteady effects dominate variations in the spanwise direction, i.e., where the shed vorticity is much greater than the trailing vorticity. Such conditions would exist for narrow blades at moderate reduced frequencies or for moderately wide blades at high reduced frequencies. For the propellers tested, reduced frequency varied inversely with aspect ratio so that neither of these conditions was met. However, the more realistic condition of a larger number of blades at a given EAR implies a higher aspect ratio at a given reduced frequency and, hence, a closer prediction by the two-dimensional unsteady theory.

The calculations using this technique assumed a lift-curve slope of 2π. However, steady data indicate that this slope should be closer to $(0.95)(2\pi)$. If this lift curve slope were used, the two-dimensional predictions would be closer than indicated in Figures 27 and 28.

From the Sears two-dimensional sinusoidal gust theory, the lift is proportional to $c \cdot \phi(k)$. When the reduced frequency is increased by increasing c for a fixed inflow, the product $c \cdot \phi(k)$ is a monotonically increasing function of k ($c \sim k$, $\phi(k) \simeq 1/\sqrt{1 + 2\pi k}$).[54] However, at high reduced frequency, the phase of $\phi(k)$ varies rapidly with reduced frequency; see Figure 3. For a marine propeller, it is the reduced frequency variation with radius and the subsequent radial phase variation of the lift response which produce the reduction in thrust with increasing blade width for the high reduced frequencies.

The combination quasi-steady, two-dimensional unsteady theory underestimates the blade-frequency thrust by a factor of two or more. Application of a two-dimensional unsteady correction to the quasi-steady loading results in an overestimate of the reduction in lift due to the shed vorticity. The quasi-steady approach overestimates the effect of the trailing vorticity and neglects the effect of the shed vorticity (two counteracting simplifications). The two-dimensional unsteady approach neglects the effect of the trailing vorticity but overestimates the effect of the shed vorticity (again two counteracting simplifications). However, when both the quasi-steady and the two-dimensional unsteady approaches are used, the effect of both the trailing and the shed vorticities is overestimated (two additive simplifications), resulting in a substantial underprediction of the section lift and hence of the propeller thrust and torque.

The substantial underprediction of the unsteady loading by use of such a combination technique would be expected from solutions for plane wings of finite aspect ratio. For plane wings, it has been shown[55] that the ratio of the unsteady lift to the quasi-steady lift substantially increases with decreasing aspect ratio. Since the combination method is inherently more complicated than either the quasi-steady or the two-dimensional unsteady techniques and gives nonconservative estimates, it is not recommended for any application.

The unsteady lifting-surface theory gives better agreement with the experimental results in the region shown than do any of the simpler techniques. Later it will be shown that the approximate numerical techniques employed in this theory break down for propellers with overlapping blades and for a propeller with very narrow blades. For this reason, no comparison is shown for the wide-bladed propeller.

Within the usable range of the numerical technique, the theory and experiment deviate by as much as 15 percent. As stated earlier, it is felt that the experimental measurements are accurate to within ± 5 percent. The staircase approximation to the helicoidal geometry in the numerical evaluation of the theory certainly contributes some inaccuracy. Also, the Hanaoka basic lifting-surface model assumes a potential downstream vortex wake lying on a helicoidal surface of constant pitch. However, Magnuson[56] has recently experimentally demonstrated on a two-dimensional oscillating foil that the shed vorticity rolls up into discreet vortices very near the trailing edge in the reduced frequency range above unity. This tendency of the vorticity to roll up becomes more pronounced with increased reduced frequency. Such a rolling up of the shed vorticity may contribute to the deviation between theory and experiment shown in Figures 27 and 28.

Figures 29 and 30 show that the superiority of the unsteady lifting-surface theory is maintained over the range of mean propeller loading.* Since the two-dimensional unsteady theory displays the proper trend, this increase in fluctuating thrust with mean velocity is produced primarily by the increase in fluctuating velocity with the mean velocity.

Figure 31 shows that the lifting-surface theory takes skew into account rather well.

Figure 32 presents the experimental blade-frequency transverse forces over a range of expanded area ratio together with predictions according to the unsteady lifting-surface technique[41] and the quasi-steady lifting line technique. Figure 33 presents similar information for bending moments. Over the range shown (the computer program does not work for larger values of expanded area ratio) the quasi-steady technique shows the proper general trend with expanded area ratio but overpredicts the magnitude by approximately 50 percent. This is consistent with the predictions for thrust and torque in this range of expanded area ratio. The quasi-steady predictions are also in agreement with the experimental results in that the horizontal component of side force is slightly larger than the vertical component and the vertical component of bending moment is slightly larger than the horizontal component for all values of expanded area ratio calculated or tested.

*The same comparisons for the other unskewed propellers showed similar trends. Therefore the comparisons for only one propeller are presented.

The unsteady lifting-surface predictions of transverse forces and bending moments shown in Figures 31 and 32 were made at Davidson Laboratory. The program for calculating transverse forces and bending moments has not yet been released by Davidson Laboratory. The calculated values available here are insufficient to establish any definite trends. These predictions are observed to agree with the experiment within 30 percent for all cases calculated. However, the apparent trend with expanded area rati is not in agreement with the experimental results. The theoretical differences in sensitivity of the two components of force to expanded area ratio look questionable, especially since the difference between these two components arises solely from the phase relationship between the second and fourth harmonics of the wake, and the second harmonic is very weak. It appears that some refinement in the numerical technique is necessary for better prediction of transverse forces and bending moments.

PARAMETRIC STUDY

PARAMETERS AND CONDITIONS

The foregoing comparisons have shown that the unsteady lifting-surface theory as numerically evaluated by Tsakonas et al.[41] is the best method available for predicting unsteady thrust and torque. Accordingly, this theory was utilized in a parametric investigation to obtain an understanding of the effect of various propeller parameters upon unsteady loading.

It is well known that selection of the number of blades should be based on the harmonic content of the wake and the response characteristics of the vessel. However, once the number of blades is selected, additional propeller parameters may be chosen to further reduce unsteady loading. Very little information is available on the effect of these other parameters.

Under assumed, somewhat idealized conditions, calculations were performed to establish the variation of unsteady thrust and torque with blade-area ratio, pitch-diameter ratio, and blade skew, and the relative thrust and torque response with number of blades and blade harmonics.

For the velocity field, it was assumed that the amplitude of all harmonics of the axial velocity was 0.1 V_A at all radii and that each harmonic was radially in phase. The tangential component of the inflow velocity field was taken to be zero. This neglect of the tangential velocity did not significantly limit the generality of these results for the following reasons:

1. At the outer radii which produce most of the loading, the pitch angle is small, thus producing much greater sensitivity to the axial wake;

2. In most realistic wakes, the amplitudes of the harmonics of tangential wake which produce unsteady loading are small;

3. It is the component of wake normal to blade section which produces the loading (the small effect of surge is neglected in this theory);

hence the trends with all parameters studied, except pitch, would be unchanged by the inclusion of a nonzero tangential wake.

The propeller-blade outline was the same as that of the propellers tested and was held invariant through this parametric study. The geometric pitch was independent of radius.

As in the previous section, the "normal" component of the wake and the section lift were taken to be normal to the section nose-tail line. All calculations were performed using eight radial strips and five chordwise loading modes.

DISCUSSION OF RESULTS

Figure 34 shows the effect of number of blades and blade harmonic on the fluctuating thrust response. The expanded area ratio and thus reduced frequency for a given blade harmonic is held constant. This plot shows that (for a fixed expanded area ratio) the thrust response to a unit-wake blade-frequency harmonic increases with number of blades. The effective aspect ratio increases in direct proportion to the number of blades. Therefore, the reduction in unsteady loading due to aspect ratio is smaller for the greater number of blades, hence the greater unsteady loading. Predictions of a constant response with number of blades are obtained from using the two-dimensional unsteady technique. Hence this technique would yield better predictions for propellers with larger numbers of blades than for the three-bladed propellers discussed in the previous section.

This plot also shows that the response of multiples of blade-frequency thrust decreases with increasing blade harmonic. This is analogous to the two-dimensional result that lift decreases with increasing reduced frequency.

Figure 35 shows the variation of blade-frequency thrust with expanded area ratio and the approximate limits of EAR to which the numerical techniques outlined in Reference 41 may be applied. The upper limit of EAR is a consequence of the manner in which the staircase approximation of the helical geometry is considered. This breakdown occurs when the blade-overlap condition is approached (when a portion of each blade is situated directly behind a portion of an adjacent blade). The failure of the numerical technique for very narrow blades depends on the individual blade width, hence the EAR at which this occurs is directly proportional to the number of blades. At the time of this writing (September 1967), modifications to the computer program were understood to be underway so that propellers with blade overlap could be considered.[57]

Figure 36 shows blade-frequency thrust as a function of pitch, and Figure 37 shows the corresponding data for blade-frequency torque. The charts assume that the speed of advance is constant and that the rpm varies inversely with pitch. Projected area ratio is held constant; hence in these plots reduced frequency and safety from cavitation are insensitive to

pitch ratio and number of blades. The difference in trends with pitch is attributable to the changing direction of the lift vector as a function of pitch. The thrust component of the lift vector is a decreasing function of pitch, whereas the torque component of the lift vector is an increasing function of pitch.

The charts assume a constant ratio between pitch and advance coefficient. However, for the most efficient propeller design, this ratio varies with pitch. Additional calculations have shown that for a fixed speed of advance, blade frequencies $\widetilde{K}_T$ and $\widetilde{K}_Q$ are insensitive to J in the range from $J = 0.6\ P/D$ to $J = 1.0\ P/D$. Therefore, Figures 36 and 37 may be applied for any advance coefficient in this range by multiplying the ordinate $\widetilde{K}_T \times 10^2/J^2 = \widetilde{K}_T \times 10^2/(0.8P/D)^2$ by $(0.8P/D)^2/\text{actual } J^2$:

$$\left[\frac{\widetilde{K}_T \times 10^2}{(0.8\,P/D)^2}\right] \times \left[\frac{0.8\,P/D}{\text{actual } J}\right]^2 = \frac{\widetilde{K}_T \times 10^2}{\text{actual } J^2}$$

The variation of blade-frequency thrust and torque with pitch will be somewhat different for cases in which the tangential wake contributes significantly. As the pitch increases, the component of the tangential wake normal to the blade increases, whereas the component of the axial wake normal to the blade decreases. Hence, in a wake with significant amounts of both components, the reduction in thrust with increasing pitch would be less pronounced than that indicated in Figure 36 and the maxima in the torque curves would be shifted to higher values of P/D. Further computations should be performed to establish the extent of the influence of the tangential wake on the variation with pitch.

Figure 38 gives an indication of the reduction in blade-frequency thrust attainable by introducing skew to the blades. The plot shows blade-frequency thrust as a fraction of its unskewed value versus projected skew at the tip as a fraction of blade angular spacing. These curves are for a linear rate of angular skew, $d\sigma/d\rho$ = constant.

The plots show that maximum reduction in blade-frequency thrust is obtained for skew equal to blade spacing. For this condition, there is always one and only one blade section entering the high velocity region in the assumed flow field. Hence, there is a maximum radial cancellation of unsteady thrust and torque (for the assumed radial distribution of skew). Note that the shapes of these curves are essentially independent of the number of blades. In each case, the blade-frequency thrust is reduced to about one-tenth of the unskewed value.

Unfortunately, the computer program for calculating side forces and bending moments is not yet available. Some indication of the variation of these components with the various propeller parameters may be inferred from the foregoing calculations with thrust and torque. It must be remembered that side forces and bending moments depend on two different harmonics of the wake so that the amplitude of any particular component is acutely dependent on the phase relationship between the two harmonics. However, for a fixed wake, the trends with propeller parameters (except A_E/A_R) should not be greatly affected by this phase relationship.

For the ideal wake assumed in the parametric study, the variation of side forces and bending moments with number of blades and blade harmonics should be qualitatively the same as those shown for thrust. Calculations have shown that the variation of torque with these parameters is essentially the same as that shown for thrust (hence only thrust is shown). The variation of bending moments with pitch should be qualitatively the same as that shown for thrust since both bending moment and thrust arise from the axial component of fluctuating loading. Similarly, the variation of side forces with pitch should be qualitatively the same as that shown for torque.

The great reduction in blade-frequency thrust and torque with skew arises from the radial phase cancellation of unsteady lift. However, blade-frequency side forces and bending moments arise from both the $(Z + 1)$ and $(Z - 1)$ harmonics of the loading and (within linearized theory) the same harmonics of the wake. The amount of skew which produces a maximum cancellation of the $(Z + 1)$ harmonic of the loading will not, in general, produce a maximum cancellation of the $(Z - 1)$ harmonic of the loading. Therefore a compromise amount of skew is necessary to produce the maximum reduction in side forces and bending moments. If only the $(Z + 1)$ or the $(Z - 1)$ harmonic is present in the assumed flow field (both amplitude and phase of the pertinent harmonic being independent of radius) the maximum reduction for the assumed radial distribution of skew would be expected for the blades skewed by the number of geometric degrees of this harmonic.

APPLICATION TO DESIGN

The plots presented in the previous section should be interpreted as qualitative data indicating trends with particular parameters. These charts are useful for comparing competitive designs for the same vessel and can give a very good indication of which will be superior from a vibration standpoint.

By selecting a higher pitch (lower rpm) the designer can substantially reduce the expected blade-frequency thrust. For the idealized wake used in the parametric study, for example, the blade-frequency thrust is reduced by more than a factor of two by selecting $P/D = 1.2$ rather than $P/D = 0.6$.

When designing a propeller considering vibratory loading, the number of blades is generally selected on the basis of the relative strengths of the various harmonics in the wake and the response characteristics of the vessel to the various modes and frequencies of excitation. The relative response with number of blades (as shown in Figure 34) would be a factor only if the relative strengths of the wake harmonics (weighted by the corresponding hull responses) associated with two alternative choices of the number of blades are nearly equal. The reduced response to multiples of blade frequency is favorable, but the amplitudes of the wake harmonics associated with these frequencies are generally small; so the associated

loading is usually of little concern to the designer. However, the response to multiples of blade frequency may be very significant for special applications in which a low number of blades is desirable.

These studies indicate that the introduction of skew is generally the most effective method of reducing unsteady propeller loading. Figure 38 gives an indication of the amount of reduction in blade-frequency thrust and torque that may be expected from skew. However, this figure represents the effect of one radial distribution of skew ($d\sigma/d\rho$ = constant) in one simple wake pattern (longitudinal velocity field with constant amplitude and phase of each harmonic). These data generally indicate the more skew that is applied (within practical limits) the greater is the reduction in blade-frequency thrust and torque. However, the amount of allowable skew may be limited by strength considerations.

If the radial distribution of skew is selected so that most of the radial phase cancellation of lift occurs at the outer radii where the loading is concentrated, even greater reduction in fluctuating thrust and torque can be expected than shown in Figure 38. In principle, by using an unsteady lifting-surface theory, the radial distribution of skew can be selected (considering the amplitude and phase of the pertinent wake harmonics and the amplitude and phase of the local lift response) so that the net blade-frequency harmonic of any loading component is zero.

SUMMARY AND CONCLUSIONS

STATEMENT OF PROBLEM

The present study had three objectives:

1. To obtain a fundamental set of accurate experimental measurements of the unsteady forces and moments produced on marine propellers by circumferentially nonuniform inflow.
2. To correlate the measured unsteady thrust and torque with calculated values based on the various proposed theories.
3. To investigate the unsteady thrust and torque variation over a range of pertinent parameters, using the method determined as the best available for calculating unsteady loading.

EXPERIMENTAL PROCEDURE AND RESULTS

All six components of unsteady loading were measured on a series of four three-bladed propellers in two different wake patterns. The propellers consist of three unskewed propellers with expanded area ratios of 0.3, 0.6, and 1.2 and one propeller with 120 degrees of skew and an expanded area ratio of 0.6. The tests were conducted in a water tunnel with a closed-jet test section. The nonuniform flow field was produced by upstream screens. Thus the important assumptions of the mathematical models, i.e., a known inflow velocity field and an

absence of nearby boundaries, were duplicated in the experimental setup. One screen produced a nonuniform inflow with a dominant third harmonic so that a substantial blade-frequency harmonic of thrust and torque was developed by the propellers. The other screen produced a nonuniform inflow with a dominant fourth harmonic so that a substantial blade-frequency harmonic of transverse forces and bending moments was produced by the propellers.

The tests were run at a constant speed of 15 revolutions per second, and a few check tests were run at 18 revolutions per second. The water speed in the tunnel was varied to change the mean propeller loading from zero thrust to approximately twice design thrust. The resulting Reynolds number ranged from 0.8×10^6 to 3.4×10^6. The signals were monitored with an oscilloscope, and photographic records were made of each test condition. These output signals were analyzed for harmonic content by two techniques: (1) an analog system with a two-channel wave analyzer that was used for on-the-spot analysis (this system permitted any desired harmonic to be tuned in and its amplitude and phase determined) and (2) the output signals were recorded on magnetic tape and later digitized and analyzed by a high-speed digital computer.

The experimental results indicated that all components of the blade-frequency loading increased with increasing *EAR* to some maximum value and then decreased for further increase in *EAR*. For the three blade widths tested, the largest value occurred for *EAR* = 0.6; however, data were insufficient to define the *EAR* at which maximum loading occurred. Extreme skew resulted in reduction of blade-frequency thrust and torque to about 10 percent of the unskewed values and reduction of blade-frequency side forces and bending moments to about 50 percent of the unskewed values.

COMPARISON WITH THEORIES

Numerous schemes have appeared in the literature for calculating the unsteady loading on a propeller caused by circumferentially nonuniform inflow. These schemes may be categorized as follows: quasi-steady, using uniform flow tests; quasi-steady, using steady-state lifting-line theory; two-dimensional unsteady along a strip; combination quasi-steady and two-dimensional unsteady; and three-dimensional unsteady. The ranges of validity of the various calculation techniques were determined by correlating the calculated blade-frequency thrust and torque with the experimental results obtained in the present study. One typical calculation procedure from each of the previously mentioned categories was used for these comparisons over a range of blade width and mean propeller loading.

The three-dimensional unsteady technique (unsteady lifting-surface theory as numerically evaluated by Tsakonas et al.[41]) gives the best prediction of unsteady thrust and torque; however, the numerical technique breaks down for very narrow-bladed propellers and for propellers having blade overlap. Within its range of validity, this theory agrees with experiment within approximately 15 percent. The quasi-steady techniques overpredict blade-frequency thrust and torque by about 25 percent for effective reduced frequency less than

about 1.6 (EAR = 0.6). However, for higher reduced frequency (or wider blades), the quasi-steady predictions are excessively high. The two-dimensional unsteady theory yields the proper general trend with blade width but overpredicts the blade-frequency thrust and torque by roughly a factor of two. The combination quasi-steady, two-dimensional unsteady technique underpredicts the blade-frequency thrust and torque by a factor of two or more.

Since the foregoing comparisons revealed that the unsteady lifting-surface technique was the best method available, predictions from using it were used for further comparisons considering skew and transverse forces and bending moments. Comparison of blade-frequency thrust and torque for the propeller with extreme skew revealed very good agreement. Preliminary results indicated that within its range of validity, the lifting surface theory predicts transverse forces and bending moments within approximately 30 percent. However, the apparent variations with blade width were not in agreement with the experimental results. It appears that some refinement in the numerical technique is necessary for better prediction of transverse forces and bending moments.

PARAMETRIC STUDY

The foregoing comparisons reveal that the unsteady lifting-surface theory considers the effects of blade width over a limited range, mean propeller loading, and skew rather well. To obtain a more complete understanding of the effect of the various parameters on unsteady loading, a parametric study employing this method was undertaken. The variation of unsteady thrust and torque with pitch, blade width, and skew and the relative thrust and torque response with the number of blades and blade harmonics was investigated for propellers operating in a longitudinal flow field in which the amplitude and phase of all harmonics were independent of radius.

The results of this study indicate that blade-frequency thrust and torque can be reduced most effectively by introducing blade skew. For a propeller in the assumed longitudinal flow field, skewing the blade tip by a projected angle equal to blade spacing reduced blade-frequency thrust and torque by a factor of 10 from the unskewed value. Skewing the tip by only half-blade spacing reduced blade-frequency thrust and torque by approximately a factor of two. A smaller reduction in blade-frequency thrust is attainable by designing for a higher pitch (lower rpm); however, for P/D less than about 0.7 (in the assumed flow field) this is accompanied by an increase in blade-frequency torque. Blade-frequency thrust and torque generally increase with blade width to approximately EAR = 0.7; at more than this, the numerical evaluation of the theory is invalid. The fluctuating thrust and torque response to blade-frequency harmonic in the wake increases with increasing number of blades (EAR held fixed); however, the response rapidly decreases with increasing blade harmonic.

CONCLUSIONS

The experimental variation of the six components of blade-frequency force and moment with EAR indicates a maximum at some EAR. This trend is the result of blade width (for a fixed number of blades) entering the fluctuating loading in two conflicting manners: (1) fluctuating forces increase with blade width because the quasi-steady loading increases with blade width, and (2) fluctuating forces decrease with blade width because unsteady effects become increasingly important (reduced frequency is directly proportional to blade width).

For thrust and torque, this trend indicating a maximum at some EAR is expected to hold for any realistic propeller and wake geometry. However, the variation of side forces and bending moments with EAR is expected to be critically dependent on the wake because these components are functions of the vector sum and difference of the lift response to the $(Z+1)$ and $(Z-1)$ harmonic in the wake. These two lift responses vary differently with EAR in both amplitude and phase.

The superiority of the unsteady lifting-surface theory shows that the effect of the variation of both the trailing and the shed vorticity is important in the range of practical interest. However, the breakdown of the numerical technique for very narrow blades and propellers with blade overlap and the relatively poor agreement between theory and experiment for the side forces and bending moments indicate that considerable numerical refinements may still be necessary.

The reasonably close predictions by the quasi-steady techniques for reduced frequency of less than 1.6 show that the effect of unsteadiness is relatively unimportant in this region. However, the effect of unsteadiness becomes increasingly important for higher reduced frequencies; thus the quasi-steady predictions become increasingly too high.

The overprediction of the two-dimensional theory along a strip over the range of blade widths tested indicates that the trailing vorticity does not dominate the shed vorticity in this region. Plane wing data indicate that the two-dimensional unsteady theory should yield good predictions for high aspect ratio blades at moderate reduced frequencies or for moderately low aspect ratio blades at very high reduced frequencies. Reduced frequency for the propellers tested varied inversely with aspect ratio so that neither of these conditions was met. For a larger number of blades at a given expanded area ratio (a more realistic condition), the aspect ratio is larger at a given reduced frequency; hence this method would yield a closer prediction. This conclusion is substantiated by the parametric study which shows that the unsteady thrust response of a propeller increases with number of blades for a fixed EAR (i.e., increasing aspect ratio at fixed reduced frequency).

The substantial underprediction of the blade-frequency loading by the combination quasi-steady two-dimensional unsteady technique is a consequence of the overestimation of the effect of both the shed and the trailing vorticities by this method. This model is inconsistent and thus cannot be expected to yield reasonable predictions under any conditions.

Skewing the blades is generally the most effective method of reducing the fluctuating forces and moments on a propeller. This produces a radial phasewise variation of harmonics of lift and thus usually a reduction in all components of fluctuating force and moment. In selecting the distribution of skew the amplitude and phase variation of all pertinent harmonics of the wake should be considered.

RECOMMENDATIONS

Either the quasi-steady or the two-dimensional unsteady technique may be used to obtain conservative estimates of fluctuating thrust and torque, but if close predictions are required, it is recommended that the unsteady lifting-surface technique be used. Combination techniques employing both quasi-steady and two-dimensional unsteady corrections are not recommended for any application since by their use the unsteady loading is underestimated by a factor of two or more.

In designing a propeller from a vibratory loading consideration, it is recommended that the blades be skewed by as much as strength considerations will allow, to an amount equal to blade spacing.

The calculation procedure used for evaluating the unsteady lifting-surface theory should be modified to permit treating propellers both with very narrow blades and with blade overlap. If such modification is made, the computed blade-frequency thrust and torque should be compared with the experimental measurements presented in this report for the propeller with $EAR = 1.2$. If satisfactory agreement is obtained, the parametric study presented in this report should be extended to include a wider range of blade widths so that the EAR at which maximum fluctuating loading occurs is clearly defined for a varying number of blades.

Once a satisfactory computer program is available for calculating side forces and bending moments, a more detailed correlation with the experimental results should be undertaken. If satisfactory correlation is attained, the parametric study presented in this report should be extended to include these other components of fluctuating loading.

The results of the present study have shown that blade skew is an extremely powerful technique for reducing the fluctuating forces and moments acting on a propeller. The availability of a usable unsteady lifting-surface theory which determines both amplitude and phase of the radial lift distribution provides a powerful tool for defining an "optimum skew distribution." The criterion for such an optimum skew would be to obtain the maximum radial cancellation of the critical component of unsteady loading for an allowable blade-stress level. Such information would be of great value to the designer; therefore, it is recommended that such a study be undertaken.

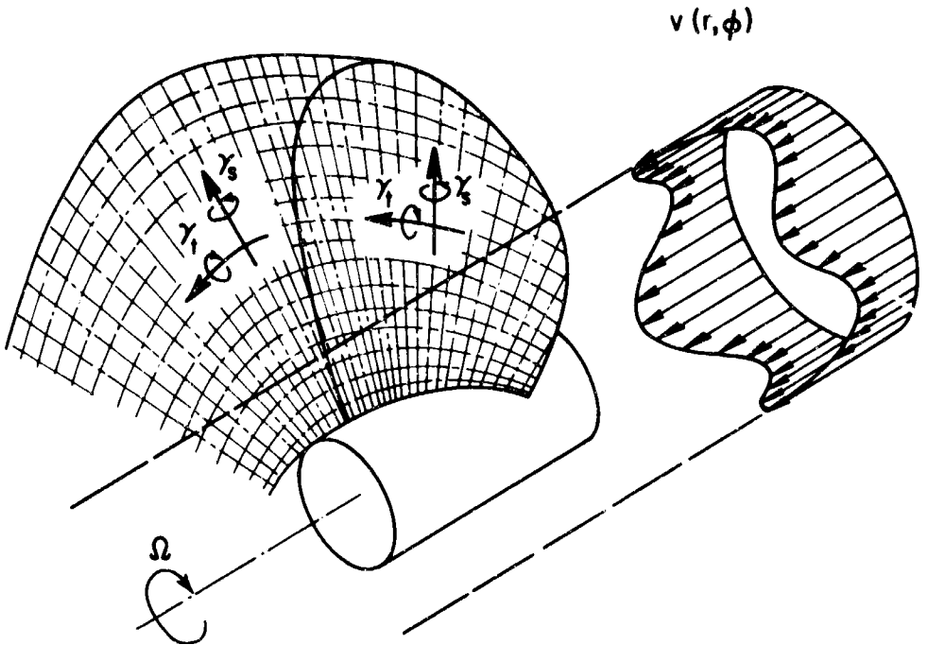

Figure 1 – Schematic of Problem

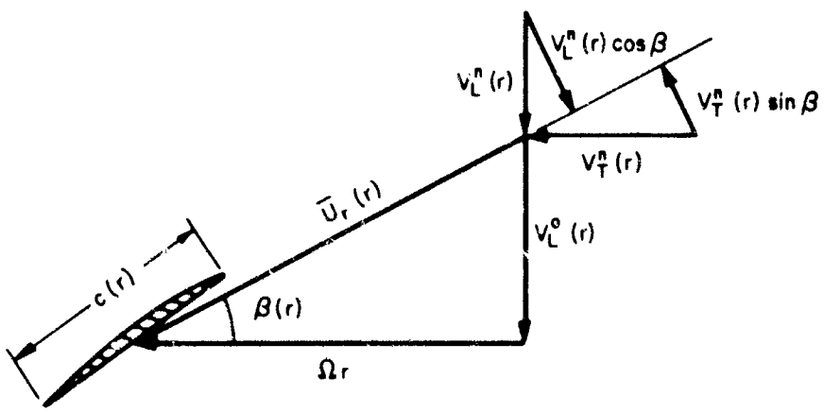

Figure 2 – Velocity Diagram

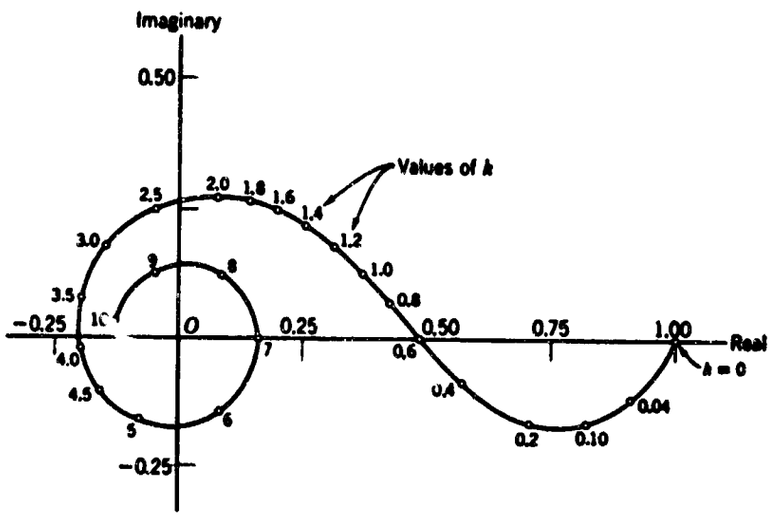

Figure 3 – Sears Function for Airfoil in Sinusoidal Gust

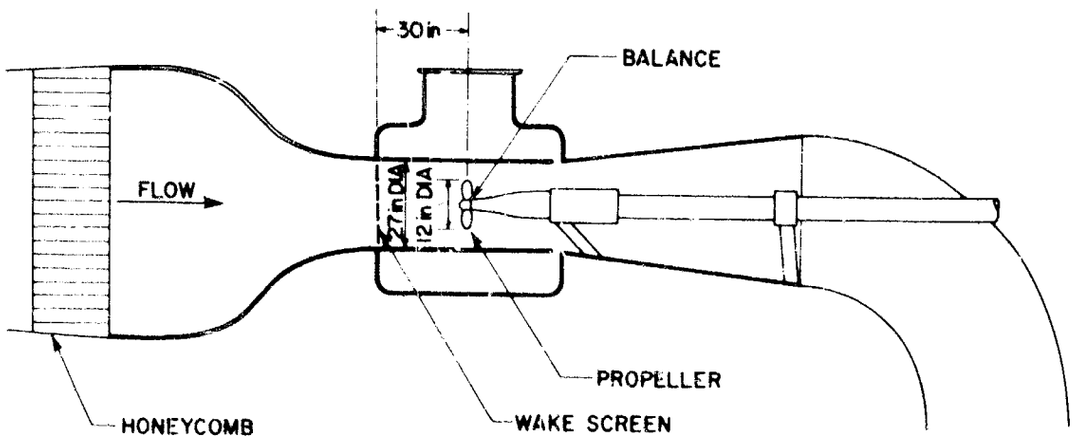

Figure 4 – Test Setup

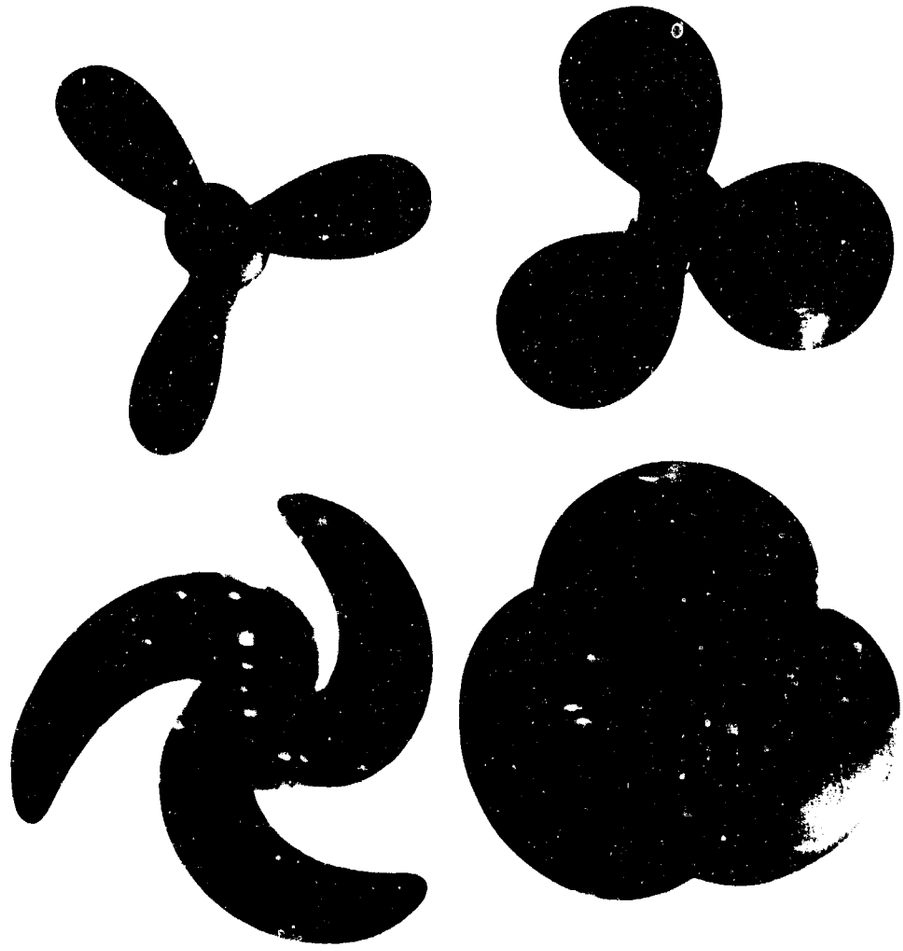

PSD 322802

Figure 5 - Three-Bladed Propeller Series

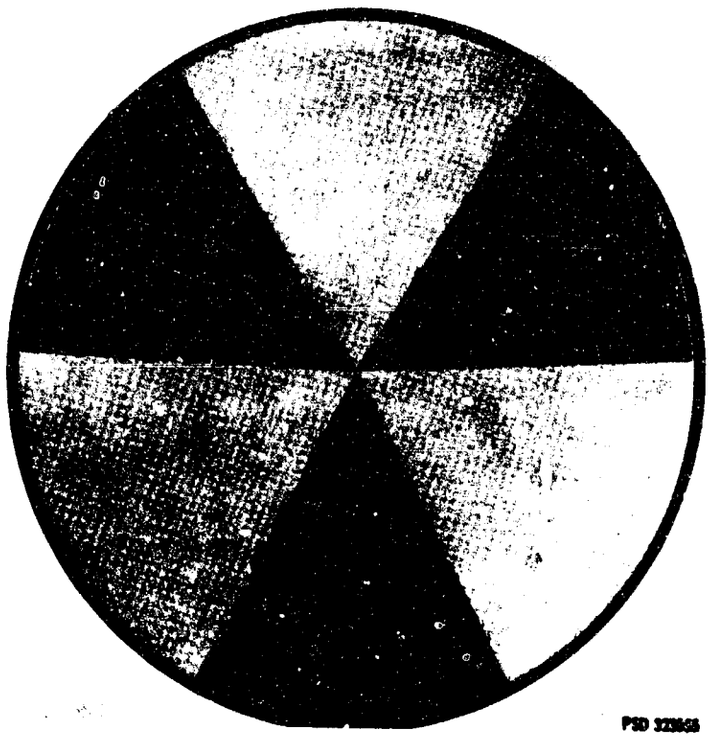

Figure 6 – Three-Cycle Wake Screen

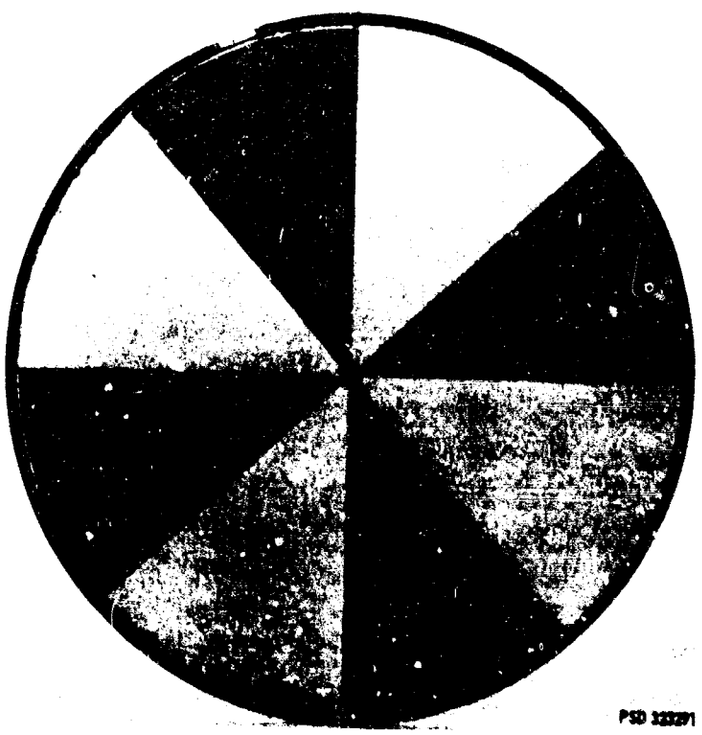

Figure 7 – Four-Cycle Wake Screen

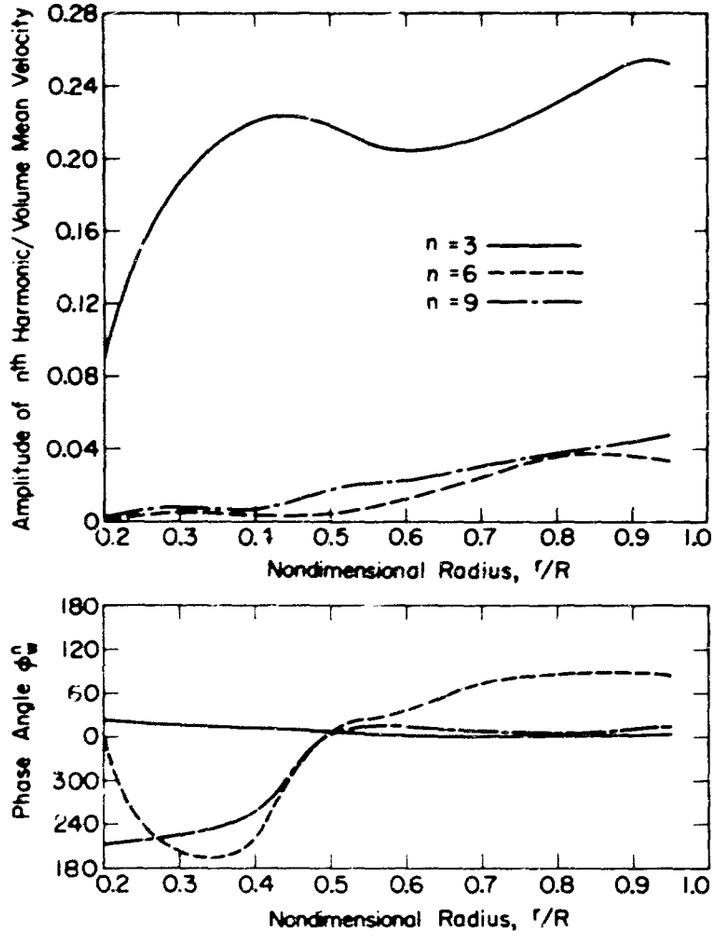

Figure 8 – Harmonic Content of 3-Cycle Wake

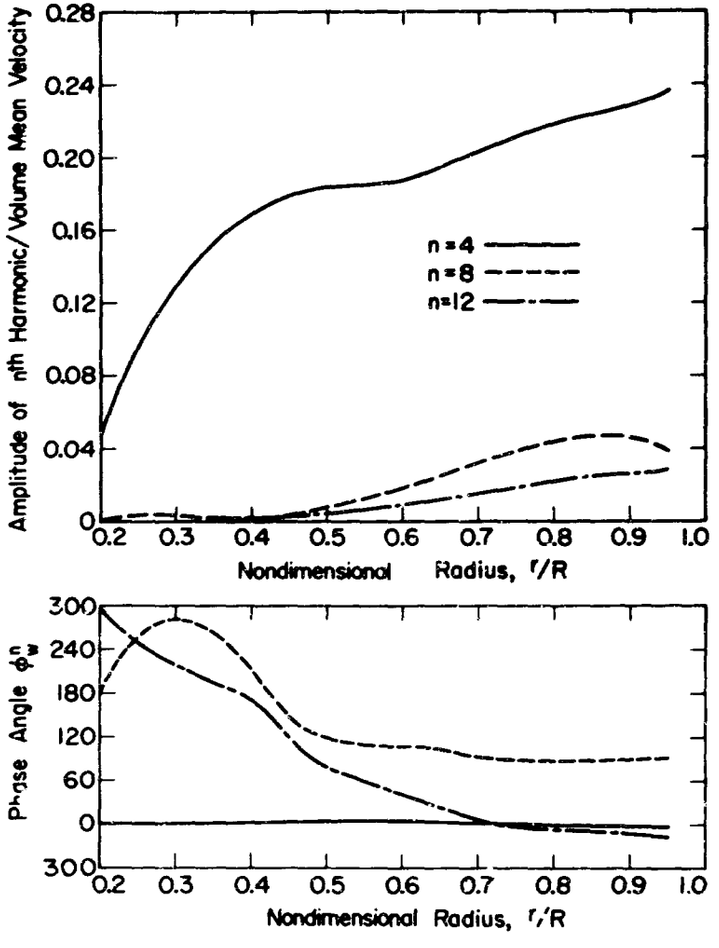

Figure 9 – Harmonic Content of 4-Cycle Wake

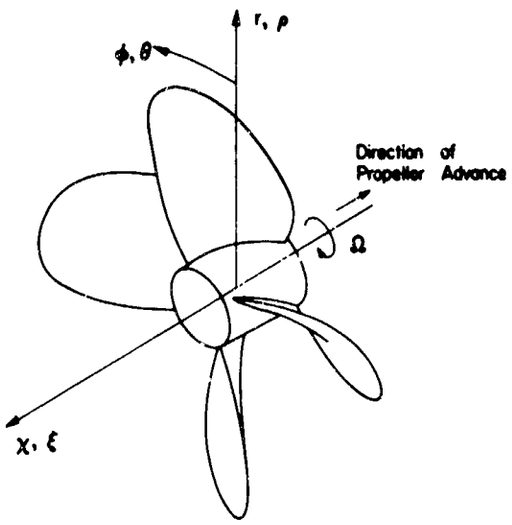

Figure 10 – Forces and Moments Acting on Propeller

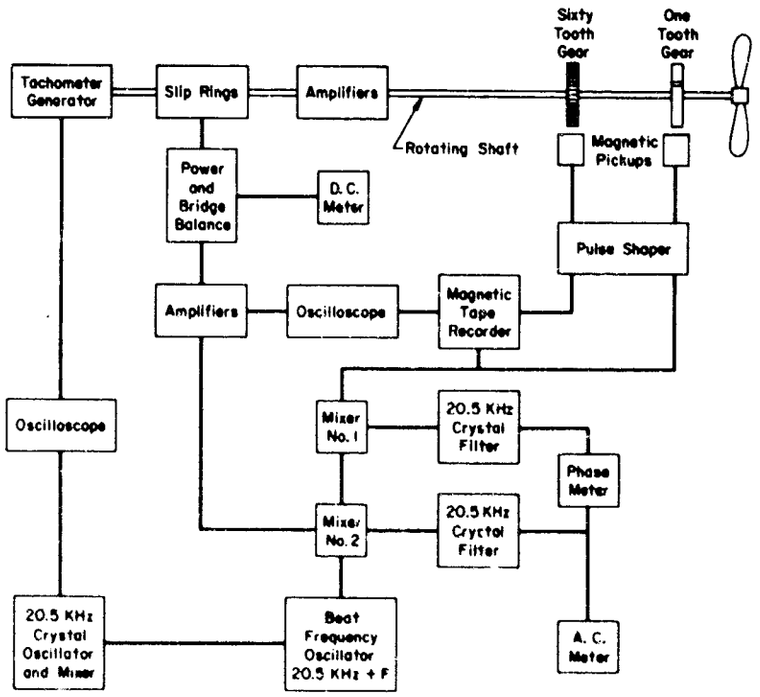

SCHEMATIC DIAGRAM OF INSTRUMENTATION

Figure 11 – Diagram of Instrumentation

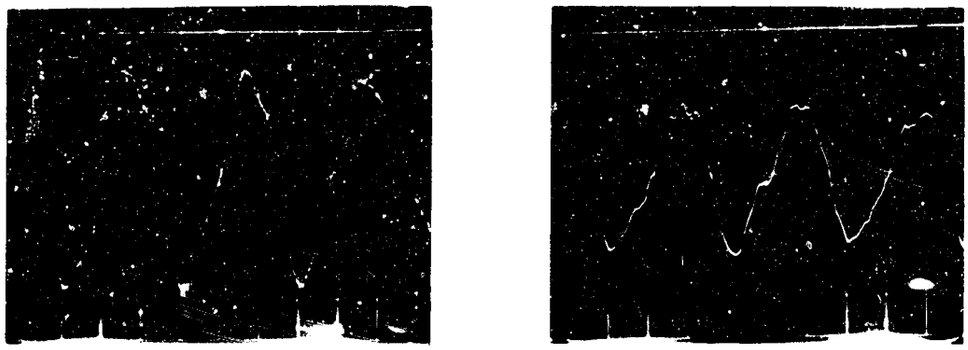

THRUST TORQUE

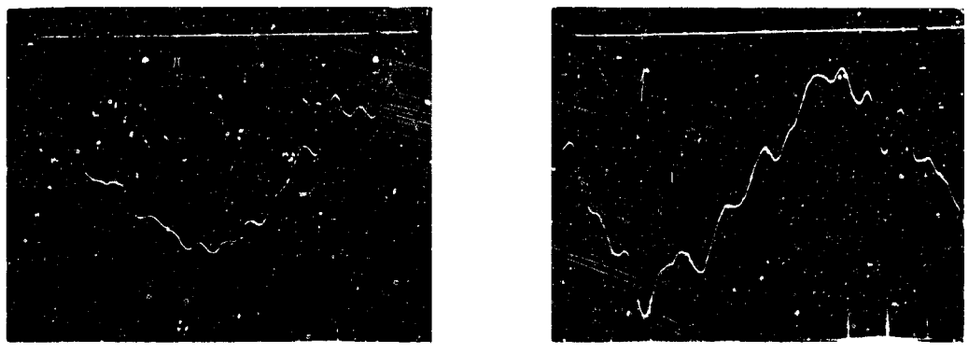

BENDING MOMENT 1 BENDING MOMENT 2

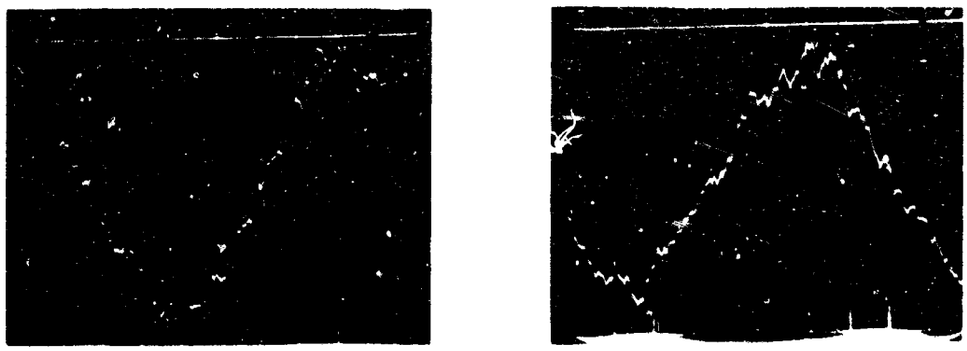

SIDE FORCE 1 SIDE FORCE 2

Figure 12 – Typical Signals in 3-Cycle Wake

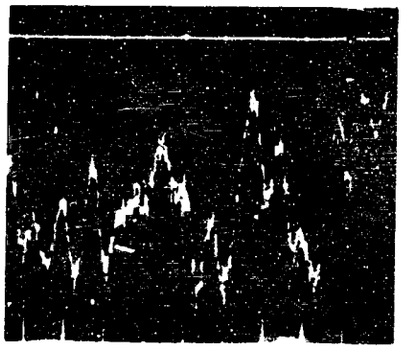

THRUST

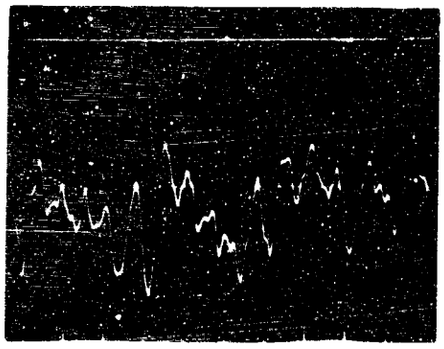

TORQUE

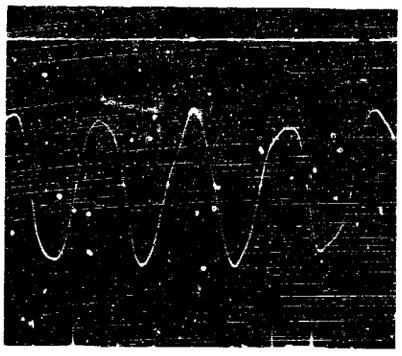

BENDING MOMENT 1

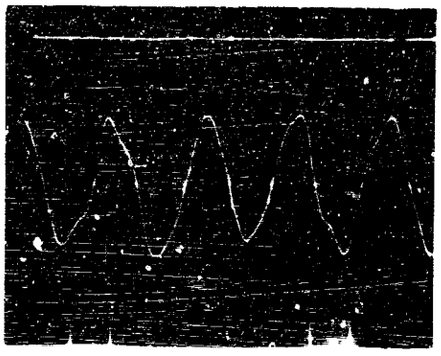

BENDING MOMENT 2

SIDE FORCE 1

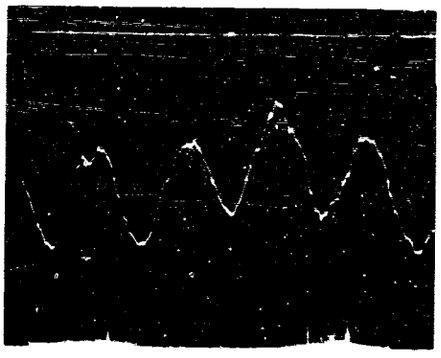

SIDE FORCE 2

Figure 13 – Typical Signals in 4-Cycle Wake

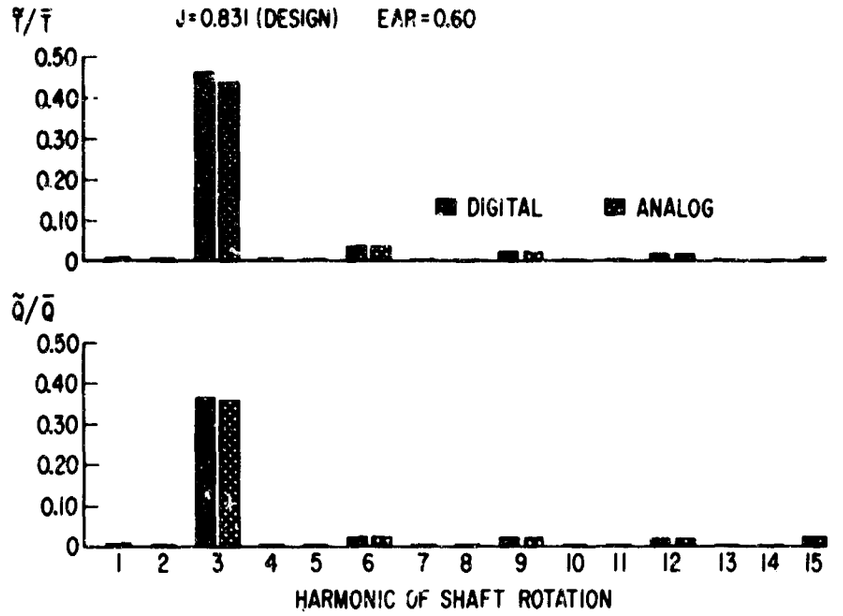

Figure 14 – Harmonic Content of Thrust and Torque in 3-Cycle Wake

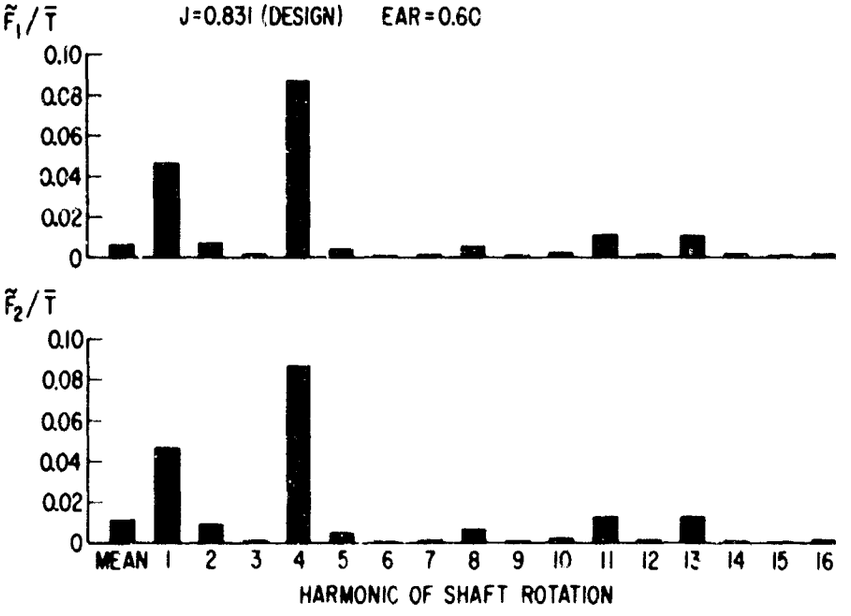

Figure 15 – Harmonic Content of Side Forces Relative to Rotating Coordinate System in 4-Cycle Wake

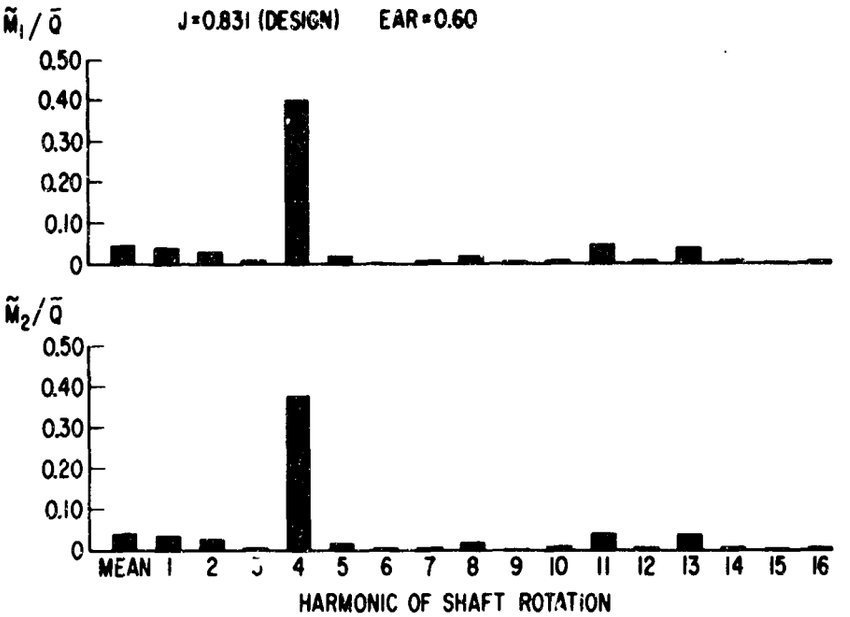

Figure 16 – Harmonic Content of Bending Moments Relative to Rotating Coordinate System in 4-Cycle Wake

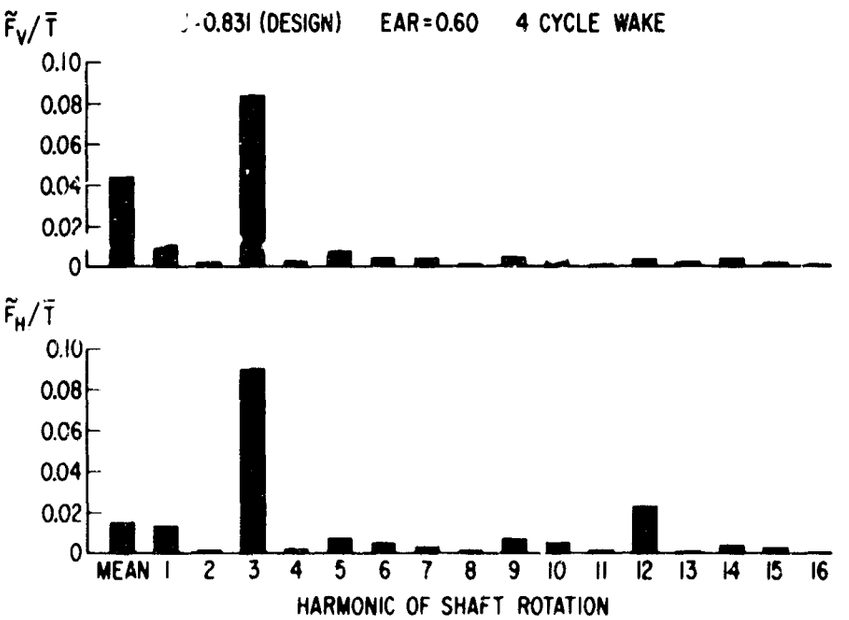

Figure 17 – Harmonic Content of Side Forces Relative to Fixed Coordinate System in 4-Cycle Wake

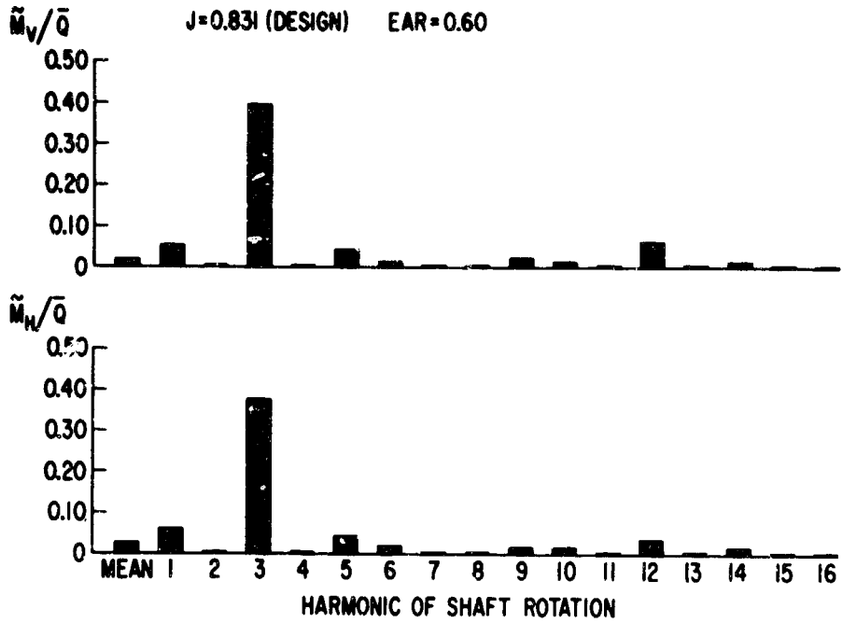

Figure 18 – Harmonic Content of Bending Moments Relative to Fixed Coordinate System in 4-Cycle Wake

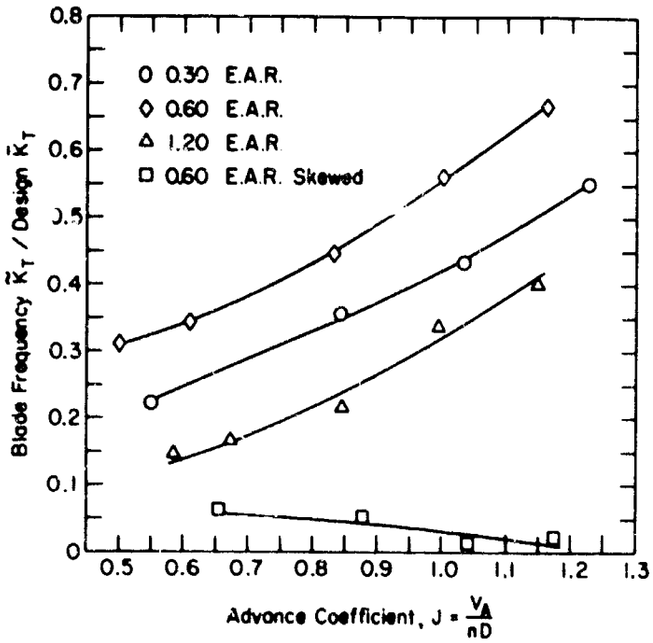

Figure 19 – Experimental Blade-Frequency Thrust in 3-Cycle Wake

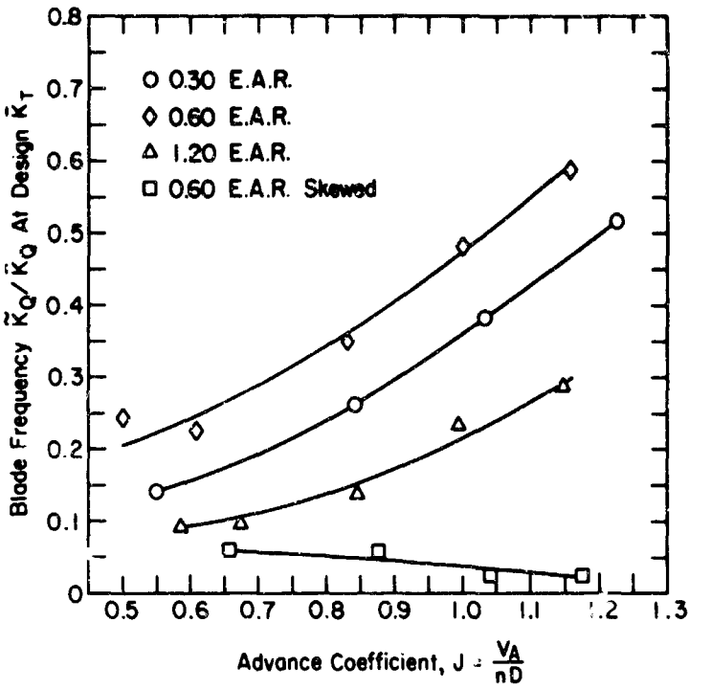

Figure 20 – Experimental Blade-Frequency Torque in 3-Cycle Wake

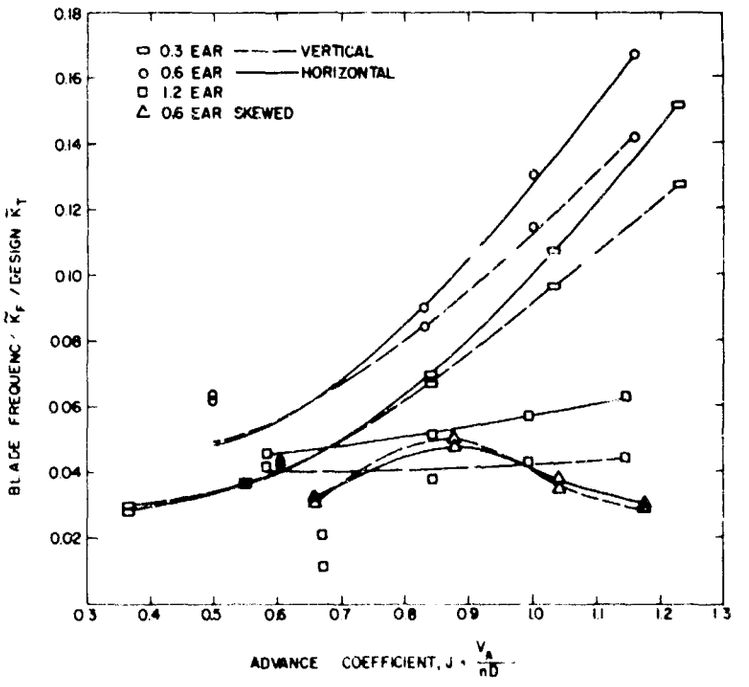

Figure 21 – Experimental Blade-Frequency Side Forces in 4-Cycle Wake

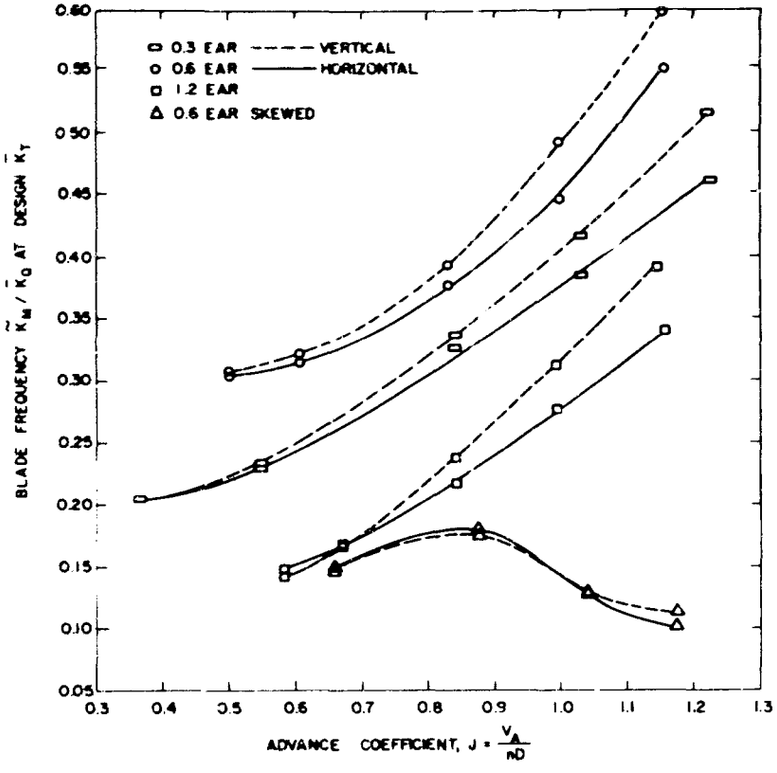

Figure 22 – Experimental Blade-Frequency Bending Moments in 4-Cycle Wake

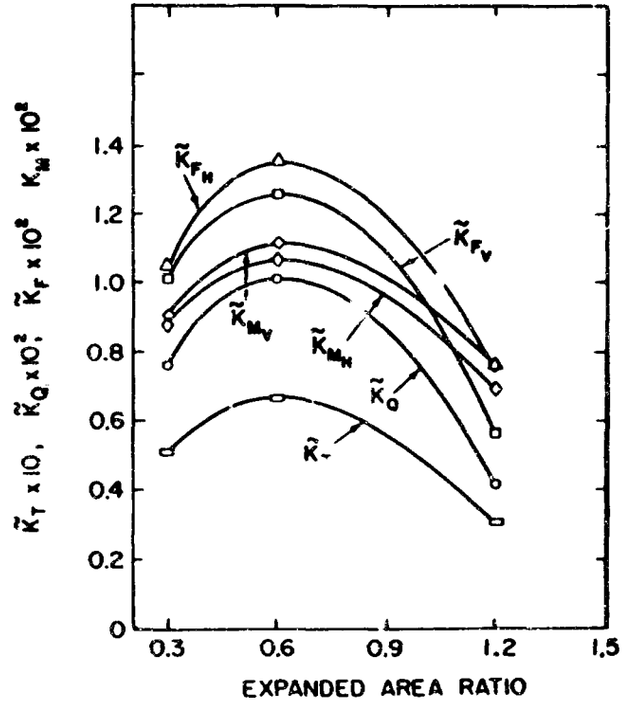

Figure 23 – Experimental Blade-Frequency Forces and Moments at Design $\bar{K}_T$

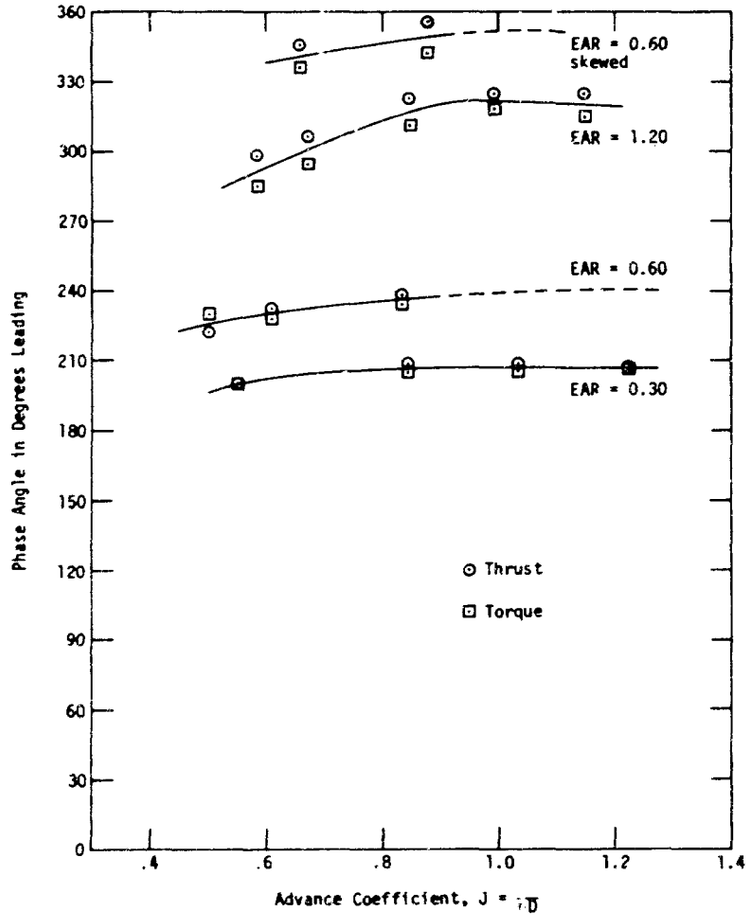

Figure 24 – Experimental Phase Angles of Thrust and Torque

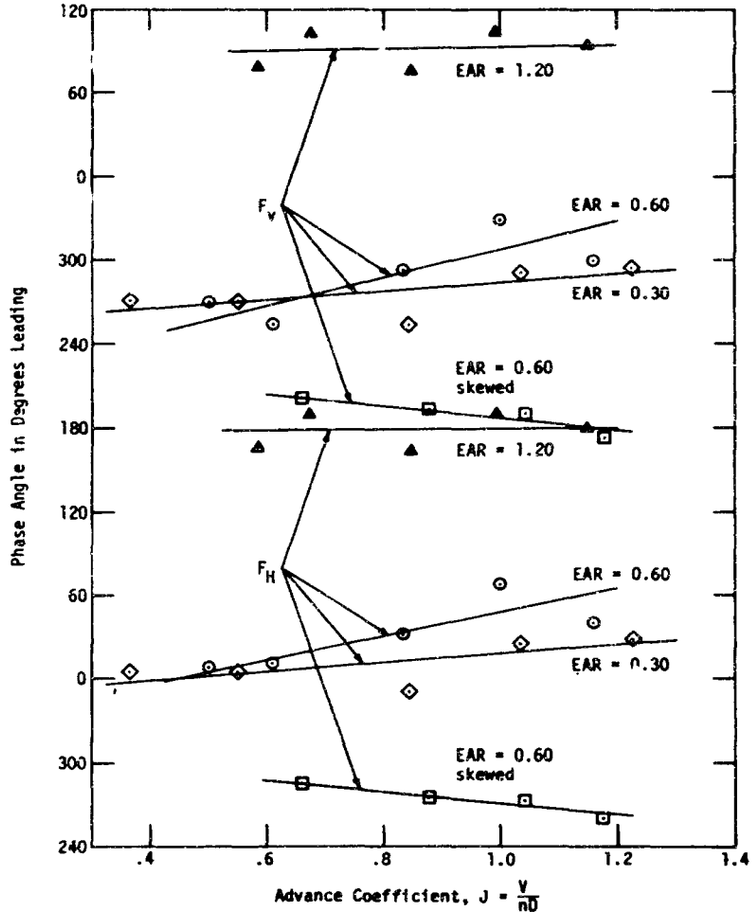

Figure 25 – Experimental Phase Angles of Vertical and Horizontal Side Forces

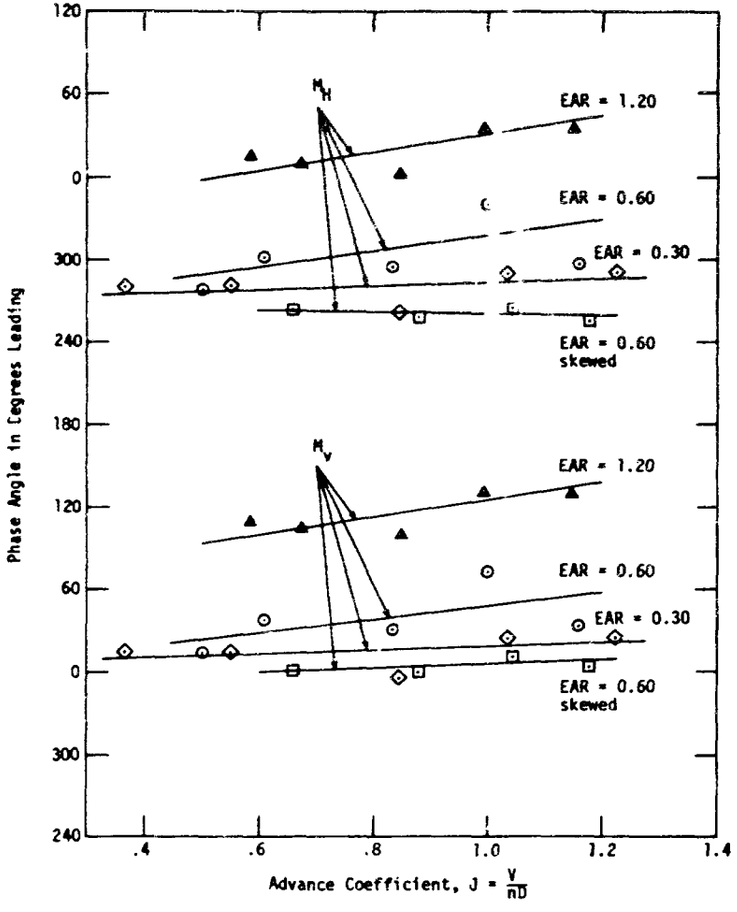

Figure 26 –Experimental Phase Angles of Vertical and Horizontal Bending Moments

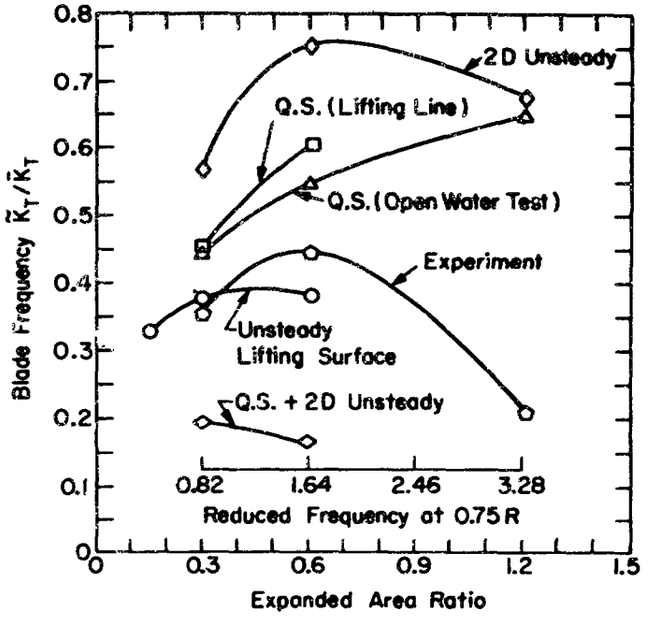

Figure 27 – Correlation of Blade-Frequency Thrust over Range of Expanded Area Ratio at Design $\bar{K}_T$

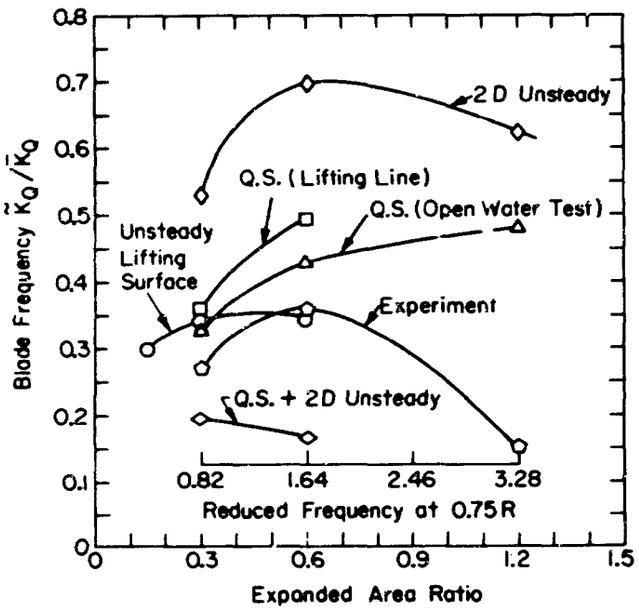

Figure 28 – Correlation of Blade-Frequency Torque over Range of Expanded Area Ratio at Design $\bar{K}_T$

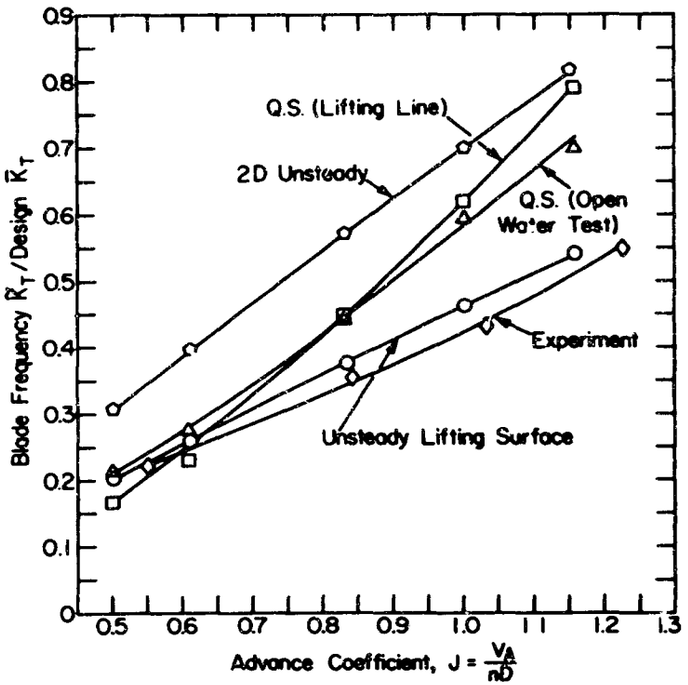

Figure 29 – Correlation of Blade-Frequency Thrust over Range of Advance Coefficient ($EAR = 0.3$)

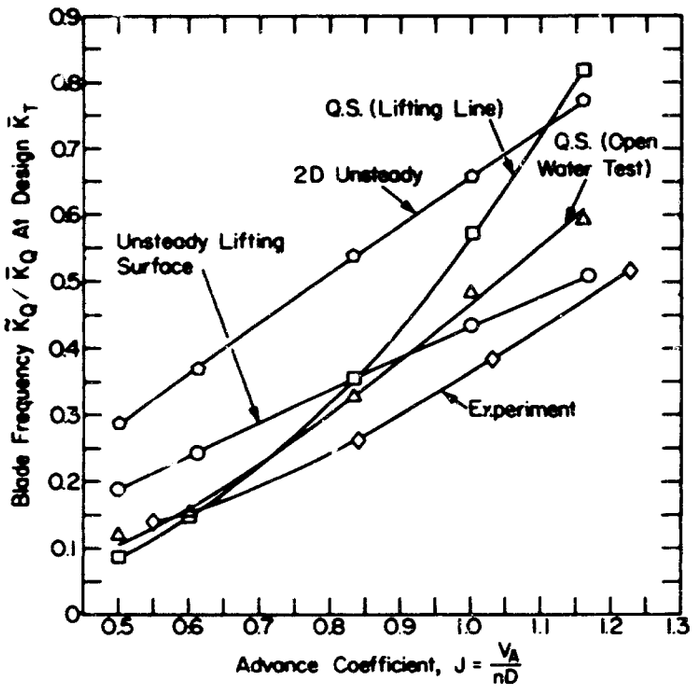

Figure 30 – Correlation of Blade-Frequency Torque over Range of Advance Coefficient (EAR = 0.3)

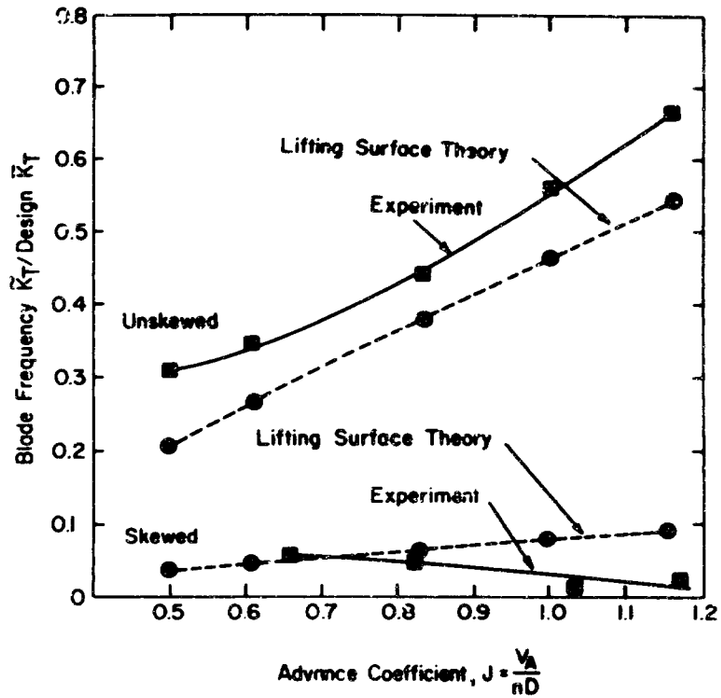

Figure 31 – Correlation of Experimental Blade-Frequency Thrust with Lifting-Surface Theory, Considering Skew (EAR = 0.6)

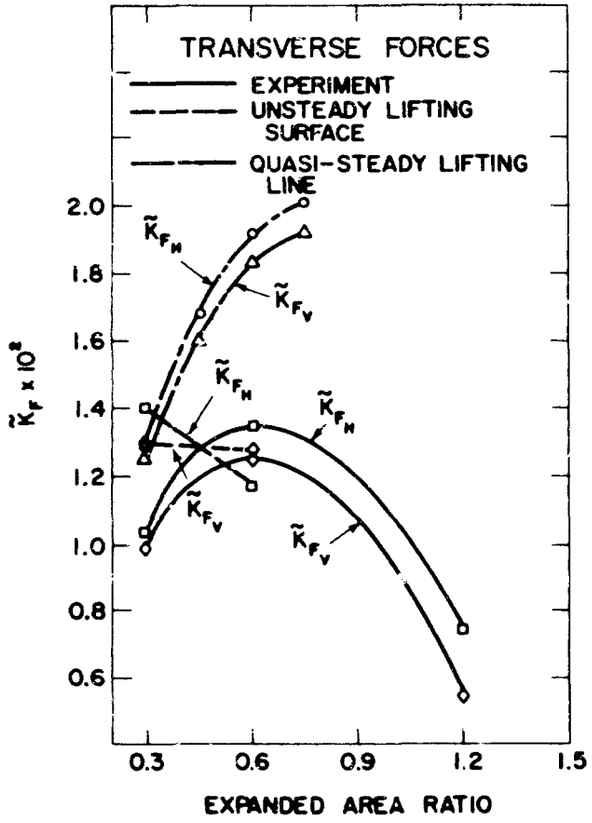

Figure 32 – Correlation of Blade-Frequency Transverse Forces over Range of Expanded-Area Ratio at Design $\overline{K}_T$

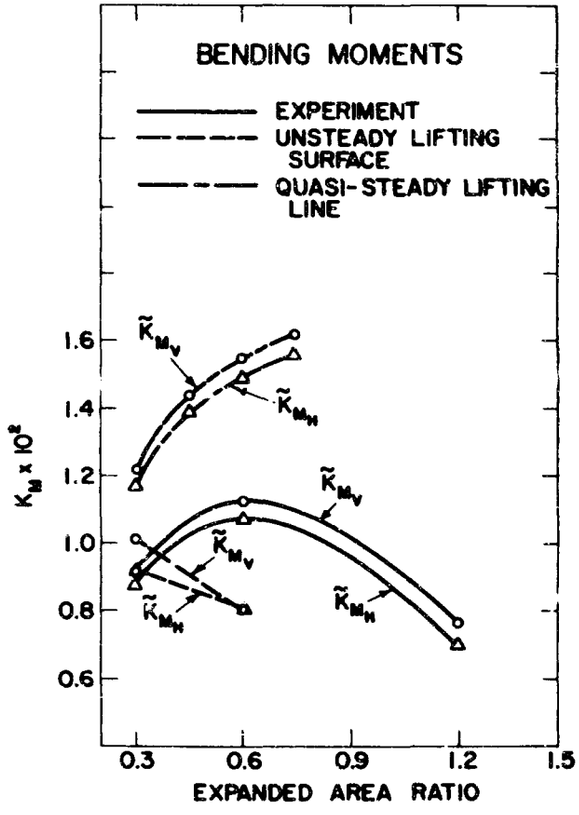

Figure 33 – Correlation of Blade-Frequency Bending Moments over Range of Expanded-Area Ratio at Design $\overline{K}_T$

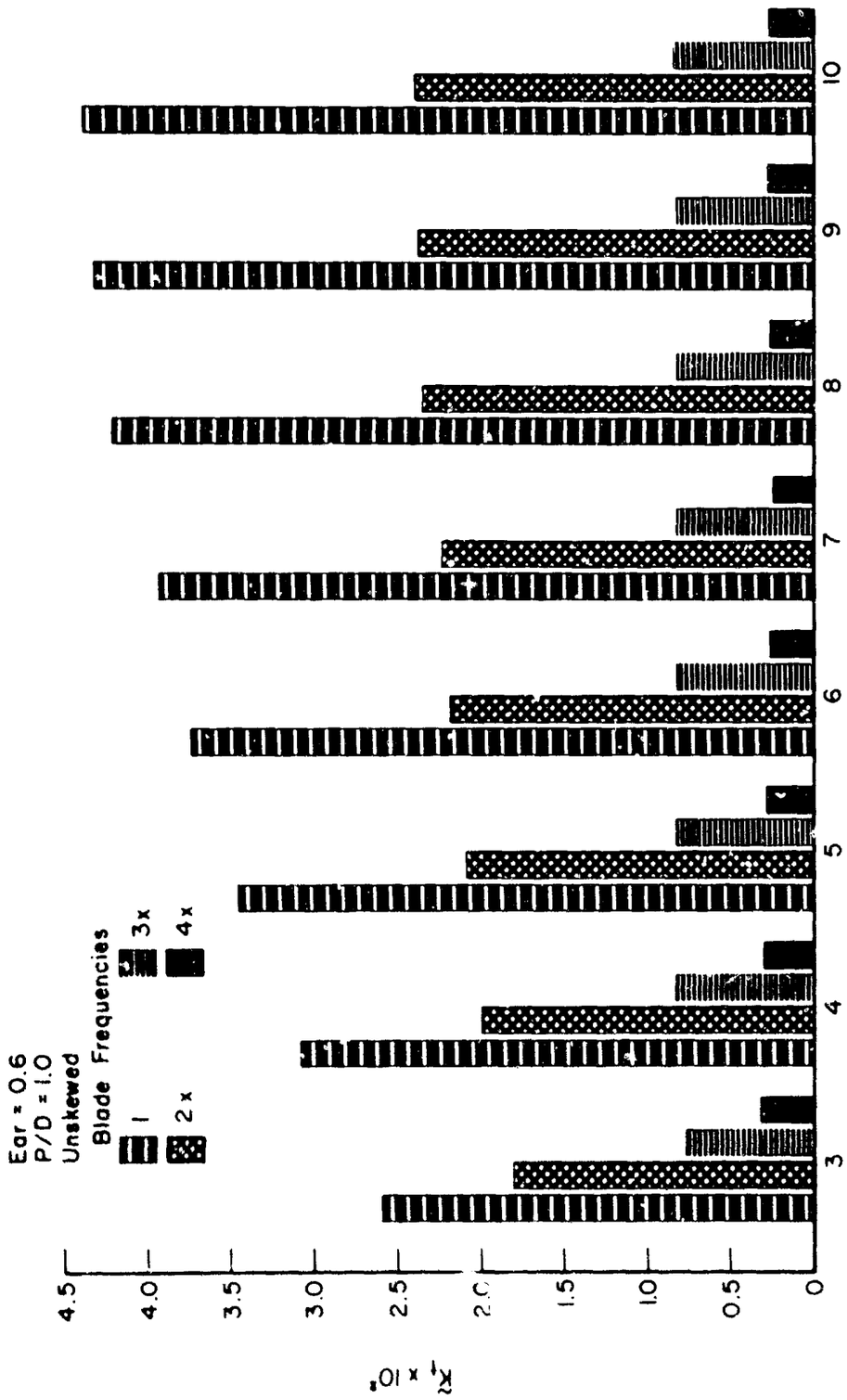

Figure 34 – Effect of Number of Blades and Blade Harmonic on Fluctuating-Thrust Response

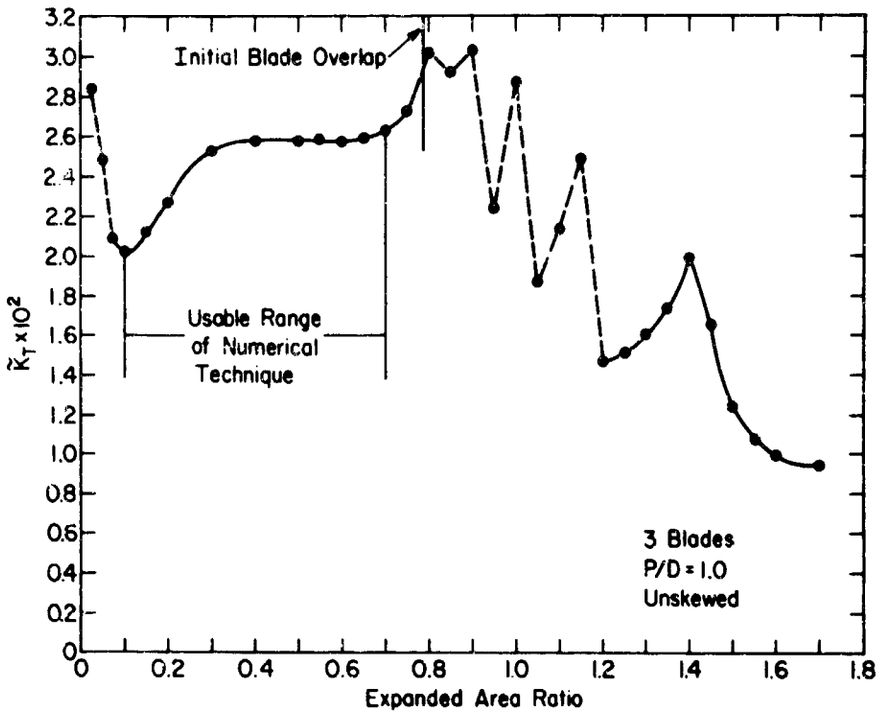

Figure 35 – Effect of Expanded Area Ratio on Blade-Frequency Thrust

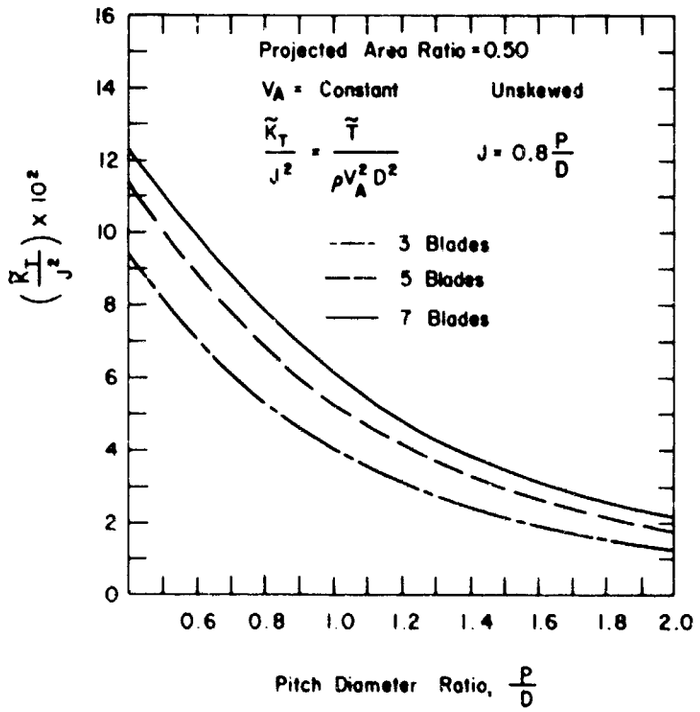

Figure 36 – Effect of Pitch on Blade-Frequency Thrust

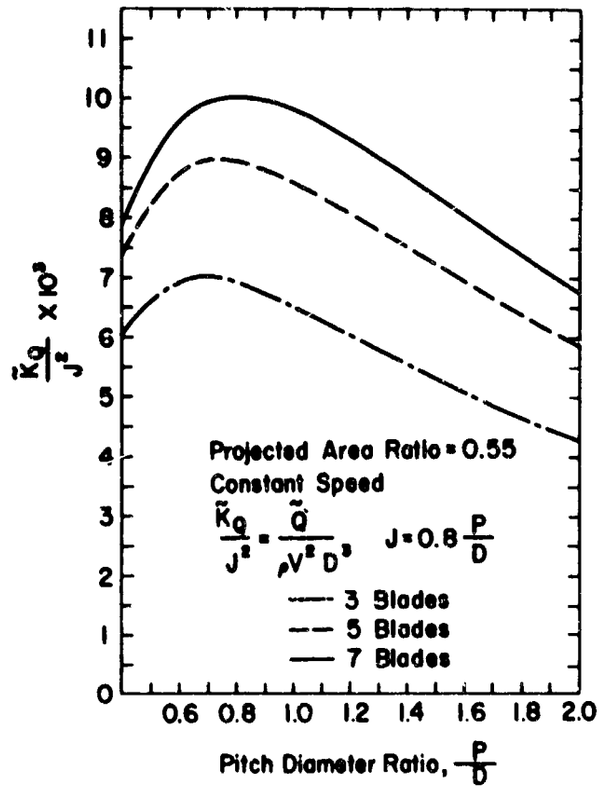

Figure 37 – Effect of Pitch on Blade-Frequency Torque

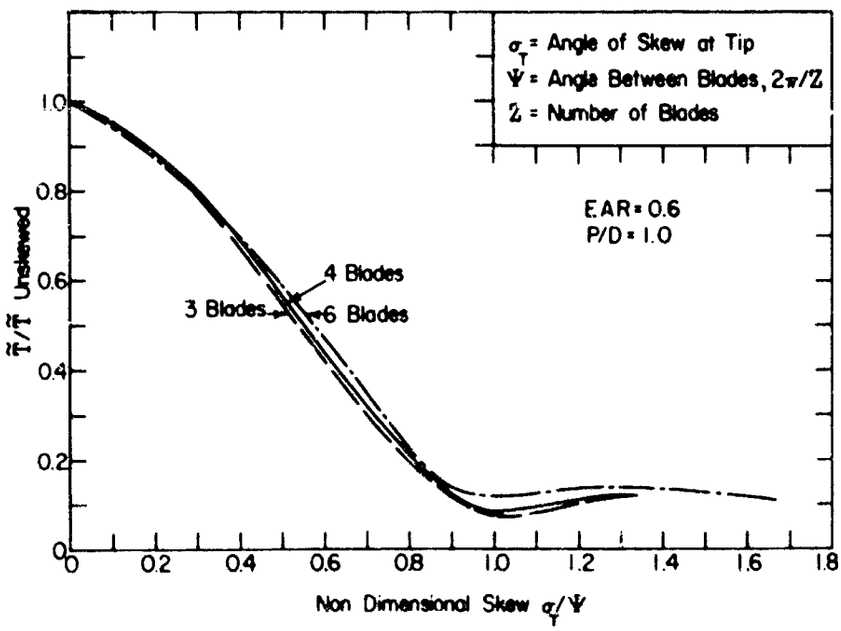

Figure 38 – Effect of Skew on Blade-Frequency Thrust

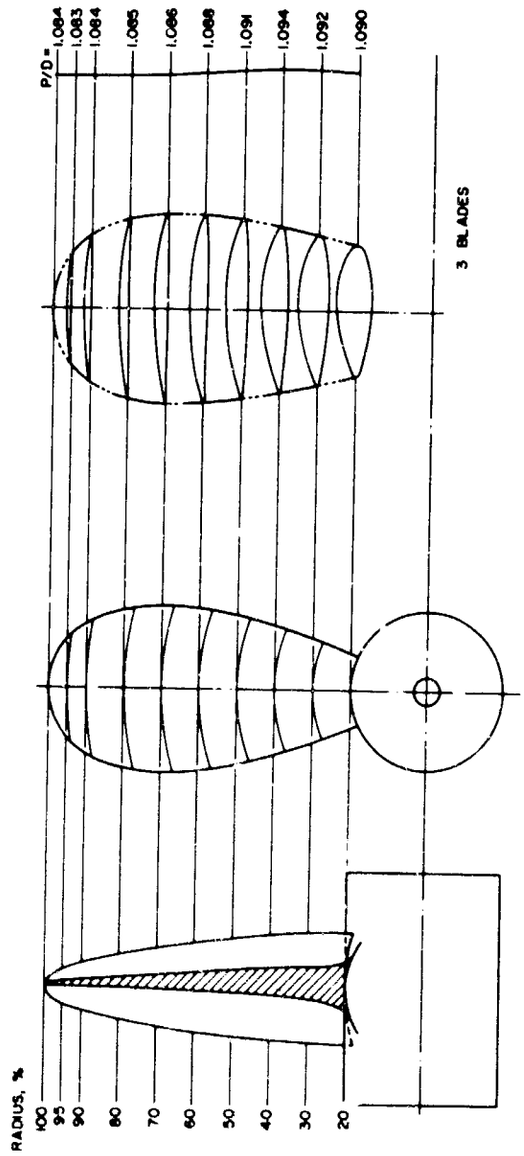

Figure 39 – Propeller with EAR = 0.3 (NSRDC 4132)

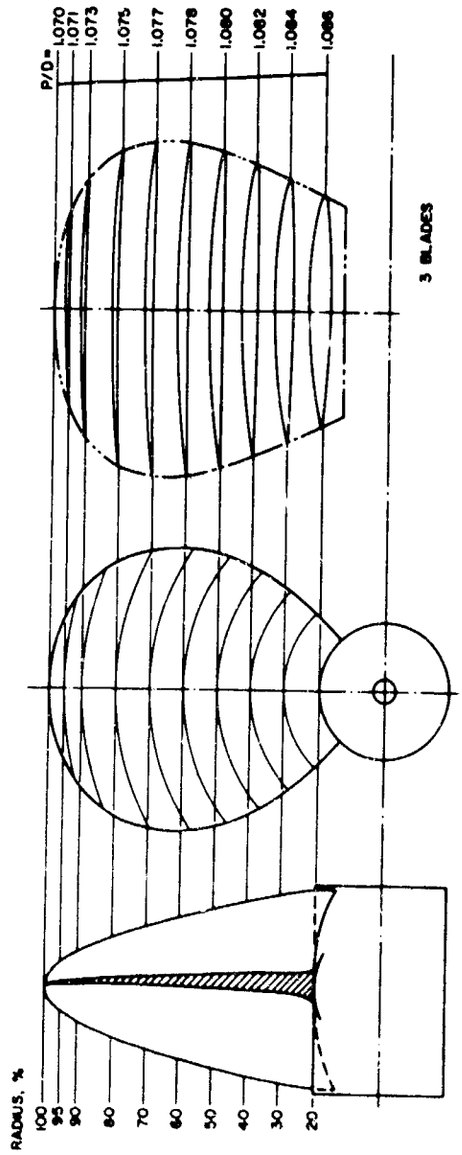

Figure 40 – Unskewed Propeller with EAR = 0.6 (NSRDC 4118)

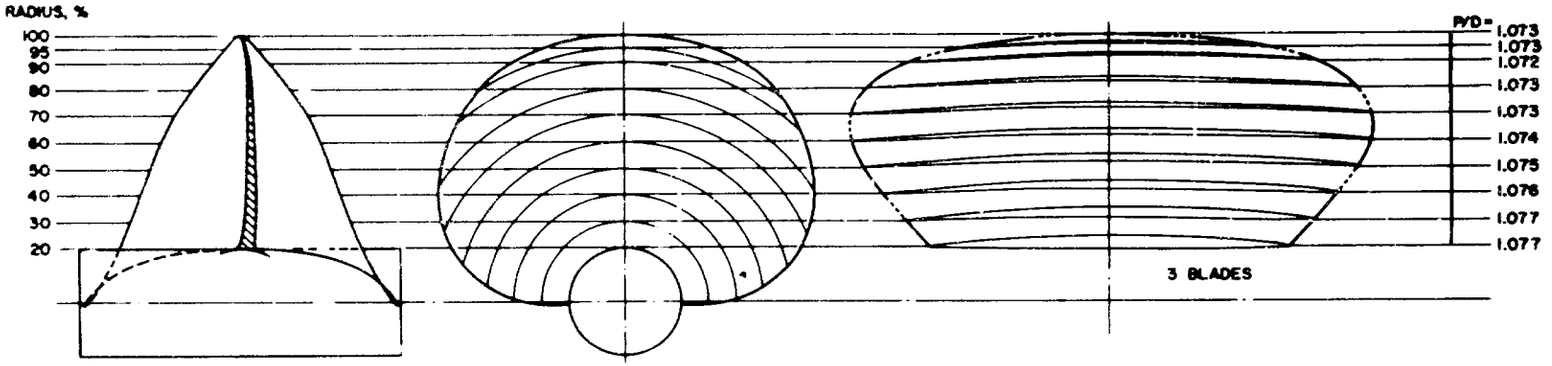

Figure 41 – Propeller with EAR = 1.2 (NSRDC 4133)

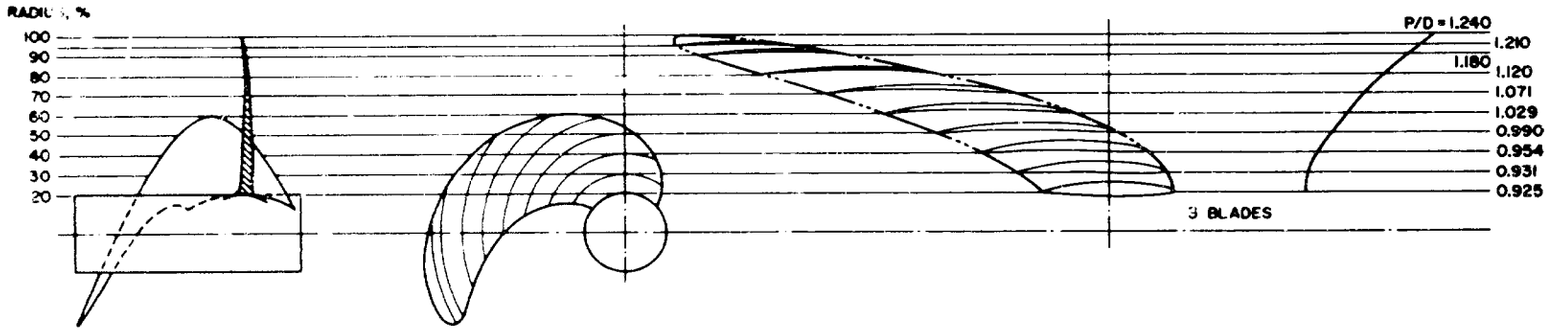

Figure 42 – Skewed Propeller (NSRDC 4143)

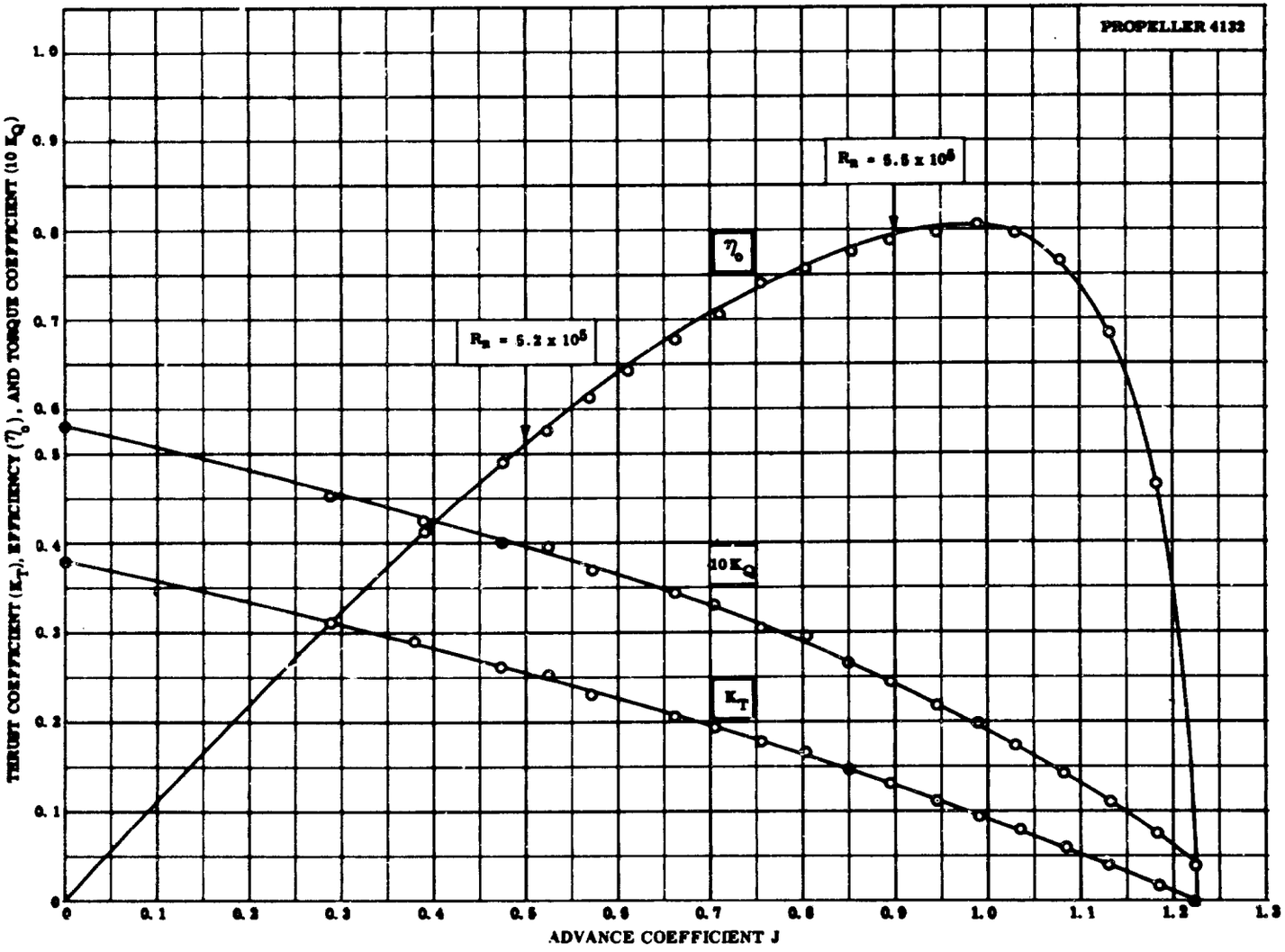

Figure 43.– Oper Water Characteristics of Propeller with *EAR* = 0.3 (NSRDC 4132)

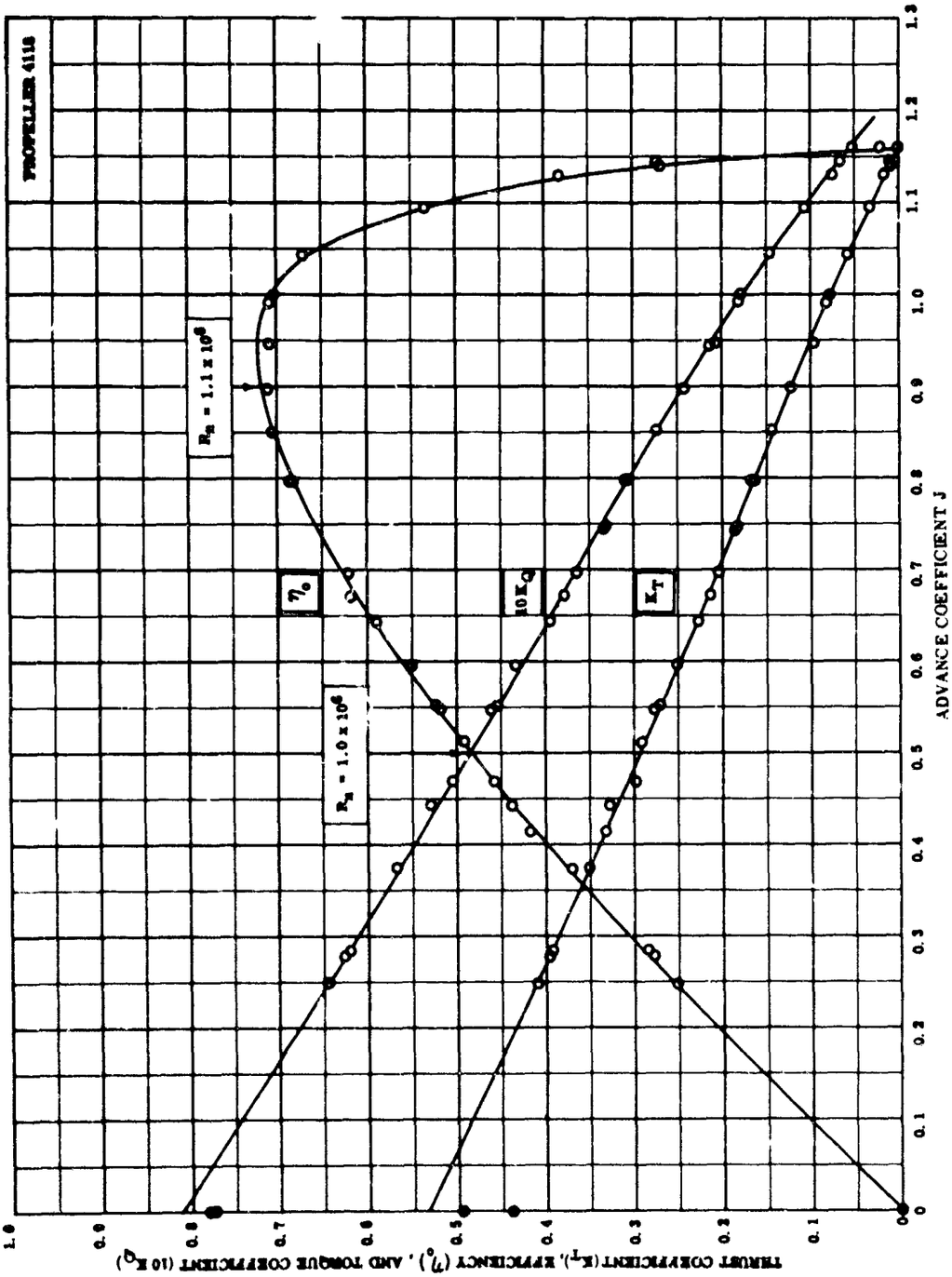

Figure 44 – Open Water Characteristics of Unskewed Propeller with EAR = 0.6 (NSRDC 4118)

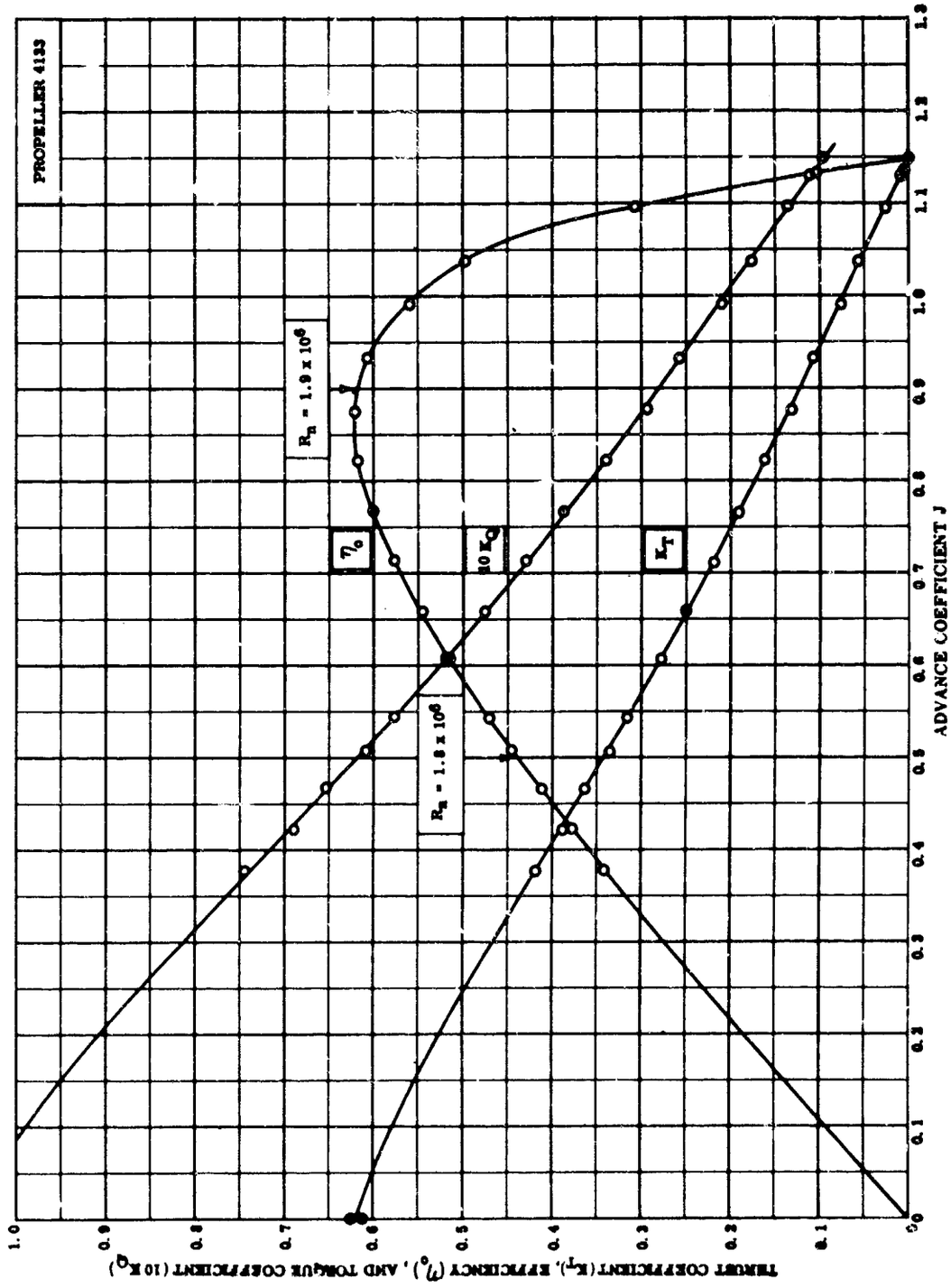

Figure 45 – Open Water Characteristics of Propeller with *EAR* = 1.2 (NSRDC 4133)

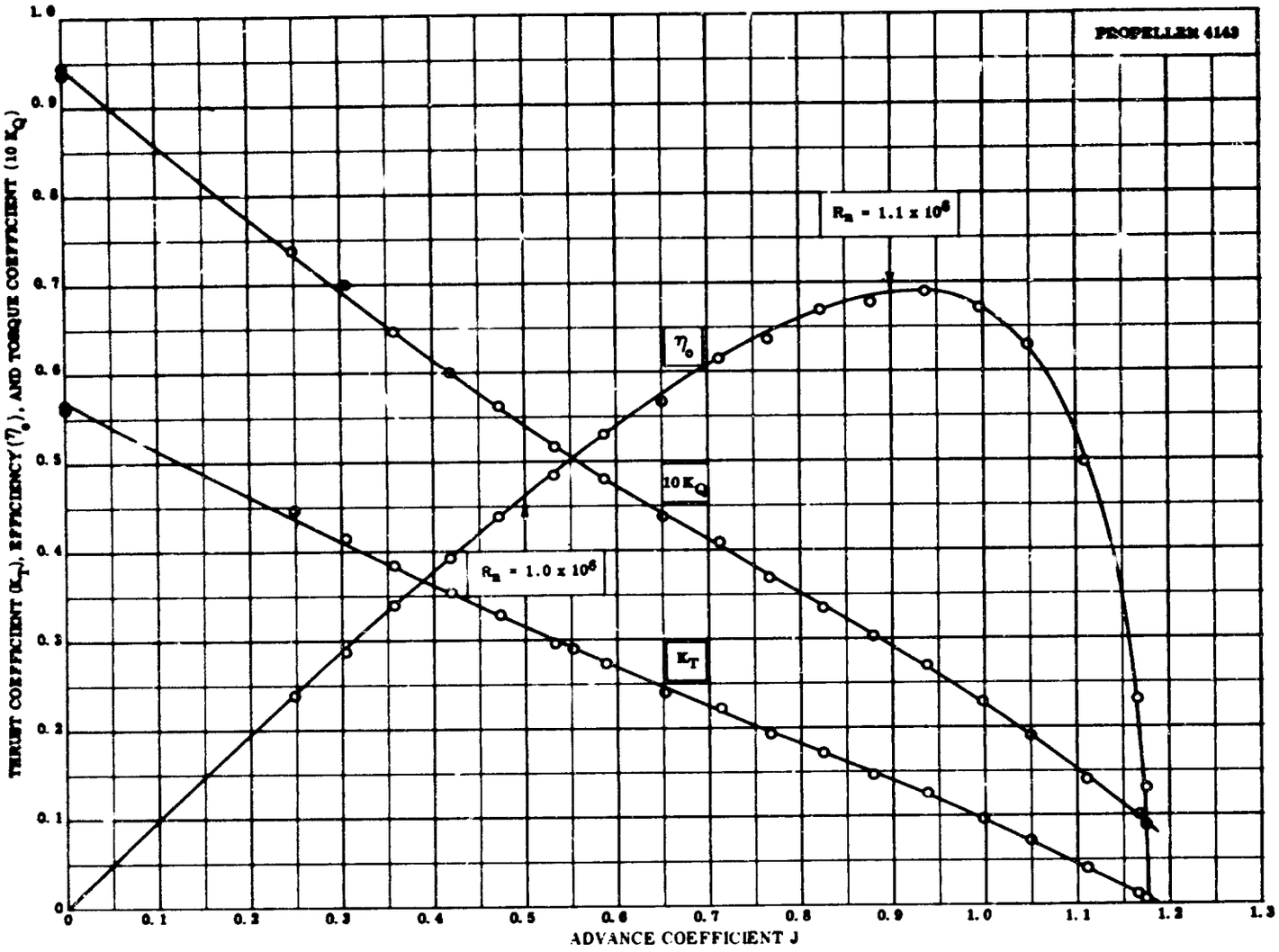

Figure 46 – Open Water Characteristics of Skewed Propeller (NSRDC 4143)

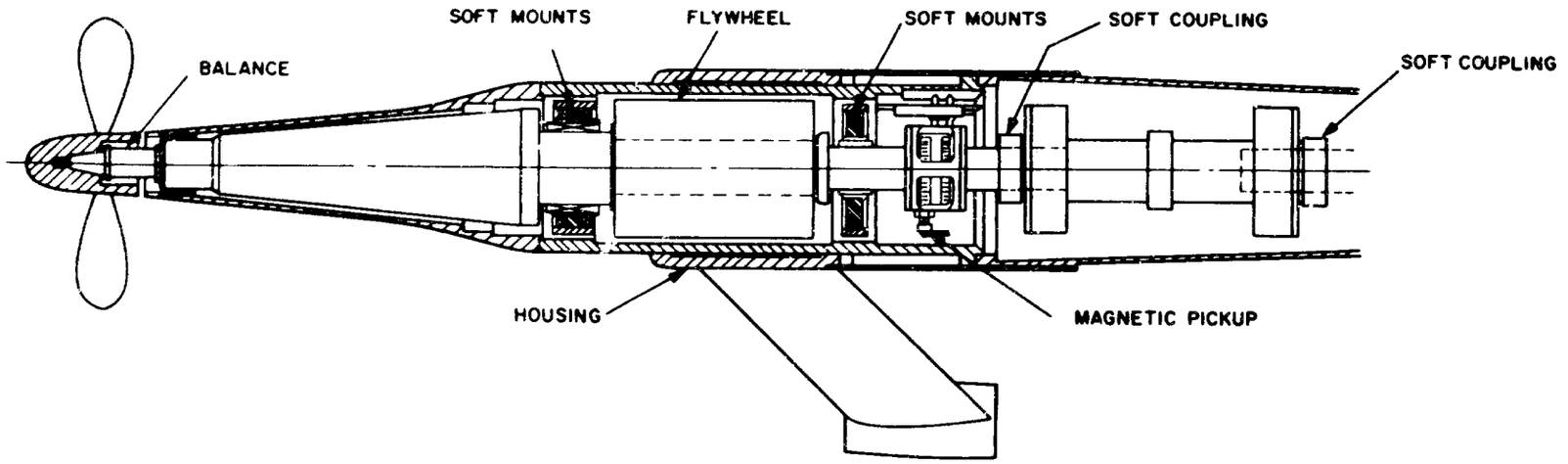

Figure 47 – Six-Component Propeller Dynamometer Assembly

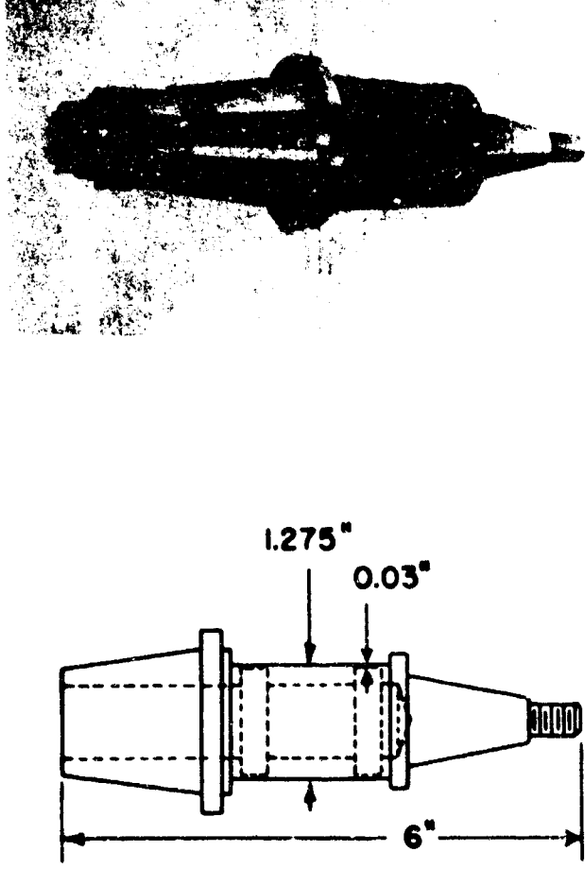

Figure 48 – Six-Component Balance

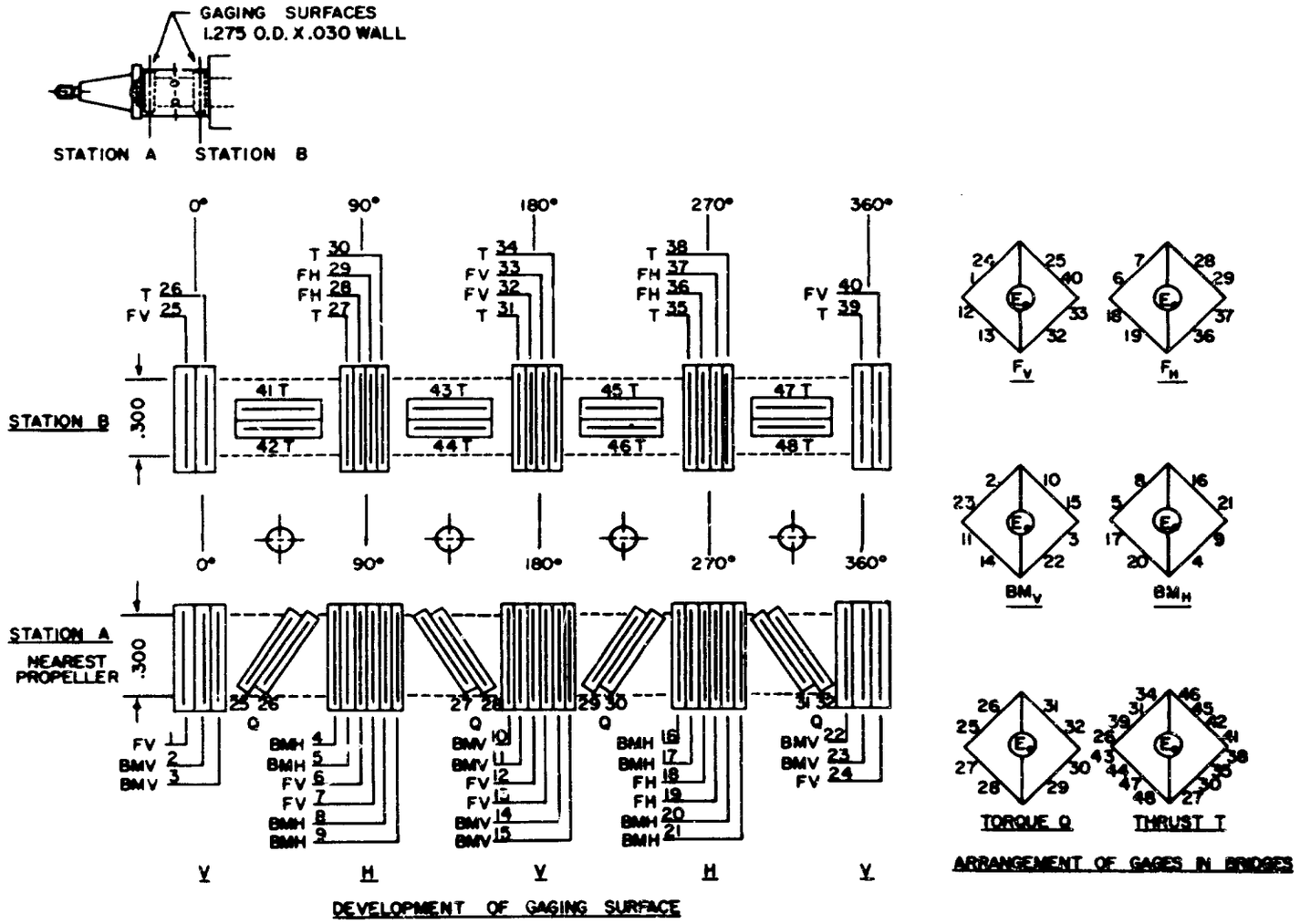

Figure 49 - Arrangement of Strain Gages on Balance

TABLE 1

Test Conditions

$\bar{K}_T$	Advance Coefficients			
All Propellers	EAR = 0.3	EAR = 0.6	EAR = 1.2	EAR = 0.6 (Skew)
0.292	--------	0.500	0.585	-------
0.242	0.550	0.509	0.672	0.657
0.150 (Design)	0.841	0.831	0.844	0.876
0.077	1.032	1.000	0.993	1.040
0.0	1.224	1.158	1.147	1.175

TABLE 2

Harmonic Content of 3-Cycle Wake

n	$\frac{V_L^n (.25R)}{V_{VM}}$	$\phi_w^n (.25R)$	$\frac{V_L^n (.35R)}{V_{VM}}$	$\phi_w^n (.35R)$	$\frac{V_L^n (.45R)}{V_{VM}}$	$\phi_w^n (.45R)$	$\frac{V_L^n (.55R)}{V_{VM}}$	$\phi_w^n (.55R)$
1	0.015	242.0	0.025	200.1	0.023	194.2	0.014	201.8
2	0.009	334.3	0.012	97.8	0.021	96.7	0.023	86.5
3	0.147	19.4	0.210	14.6	0.222	10.0	0.211	4.6
4	0.007	111.4	0.018	92.2	0.024	79.4	0.028	67.2
5	0.006	345.1	0.014	3.3	0.011	6.5	0.003	340.8
6	0.003	200.8	0.005	208.7	0.001	286.5	0.008	24.3
7	0.001	304.3	0.002	249.8	0.004	225.3	0.005	226.1
8	0.003	320.0	0.004	320.1	0.003	338.9	0.002	54.6
9	0.007	222.7	0.007	234.4	0.004	326.2	0.015	12.0
10	0.002	307.2	0.000	188.3	0.006	111.7	0.013	103.4
11	0.000	348.9	0.001	100.7	0.002	121.0	0.003	139.2
12	0.001	348.9	0.003	321.3	0.002	321.1	0.002	89.8
13	0.002	131.3	0.002	111.6	0.001	96.3	0.000	10.9
14	0.000	68.1	0.001	307.2	0.002	246.6	0.003	228.2
15	0.001	171.2	0.001	145.6	0.002	162.9	0.002	165.2

n	$\frac{V_L^n (.65R)}{V_{VM}}$	$\phi_w^n (.65R)$	$\frac{V_L^n (.75R)}{V_{VM}}$	$\phi_w^n (.75R)$	$\frac{V_L^n (.85R)}{V_{VM}}$	$\phi_w^n (.85R)$	$\frac{V_L^n (.95R)}{V_{VM}}$	$\phi_w^n (.95R)$
1	0.011	235.3	0.016	253.1	0.023	257.4	0.021	264.9
2	0.019	82.7	0.012	86.7	0.010	66.1	0.014	19.9
3	0.207	0.7	0.220	0.4	0.244	1.9	0.252	2.1
4	0.025	53.6	0.019	33.7	0.014	12.9	0.009	324.0
5	0.010	231.1	0.021	235.1	0.026	237.4	0.019	227.7
6	0.017	59.6	0.030	81.0	0.036	88.7	0.033	83.7
7	0.009	256.0	0.015	277.2	0.013	297.6	0.015	302.9
8	0.004	38.8	0.009	8.8	0.015	2.6	0.010	355.4
9	0.026	10.4	0.033	4.9	0.041	7.6	0.048	13.7
10	0.015	79.5	0.016	50.3	0.008	63.1	0.003	179.2
11	0.005	195.6	0.009	221.2	0.007	217.7	0.010	266.9
12	0.008	82.5	0.015	74.0	0.016	71.9	0.013	73.6
13	0.002	223.1	0.004	230.3	0.008	281.4	0.014	310.5
14	0.001	250.8	0.003	24.5	0.005	63.4	0.011	36.9
15	0.003	116.5	0.006	79.3	0.011	61.5	0.019	46.8

TABLE 3

Harmonic Content of 4-Cycle Wake

n	$\frac{V_L^n (.25R)}{V_{VM}}$	$\phi_w^n (.25R)$	$\frac{V_L^n (.35R)}{V_{VM}}$	$\phi_w^n (.35R)$	$\frac{V_L^n (.45R)}{V_{VM}}$	$\phi_w^n (.45R)$	$\frac{V_L^n (.55R)}{V_{VM}}$	$\phi_w^n (.55R)$
1	0.041	151.4	0.035	156.9	0.025	171.5	0.018	199.7
2	0.029	170.6	0.035	166.2	0.026	183.2	0.024	244.6
3	0.019	110.8	0.038	89.3	0.030	80.5	0.011	47.9
4	0.095	1.4	0.154	2.5	0.180	4.0	0.186	5.2
5	0.023	114.2	0.040	115.1	0.034	113.3	0.017	107.7
6	0.006	66.9	0.008	325.4	0.006	323.8	0.009	335.8
7	0.001	167.7	0.002	17.7	0.007	90.1	0.012	3.4
8	0.002	274.3	0.002	272.8	0.003	208.9	0.012	112.3
9	0.001	6.9	0.001	291.1	0.003	249.3	0.005	241.7
10	0.002	61.2	0.002	368.4	0.007	215.9	0.015	278.4
11	0.001	71.7	0.000	6.1	0.002	77.2	0.003	253.3
12	0.003	236.1	0.003	201.0	0.002	232.8	0.006	56.5
13	0.001	221.2	0.001	252.4	0.002	128.3	0.002	283.8
14	0.002	128.6	0.003	148.2	0.001	214.2	0.002	312.9
15	0.001	211.3	0.003	231.2	0.003	239.5	0.004	274.2

n	$\frac{V_L^n (.65R)}{V_{VM}}$	$\phi_w^n (.65R)$	$\frac{V_L^n (.75R)}{V_{VM}}$	$\phi_w^n (.75R)$	$\frac{V_L^n (.85R)}{V_{VM}}$	$\phi_w^n (.85R)$	$\frac{V_L^n (.95R)}{V_{VM}}$	$\phi_w^n (.95R)$
1	0.017	220.5	0.014	218.5	0.010	195.4	0.007	152.9
2	0.030	265.4	0.023	260.0	0.011	215.7	0.008	165.1
3	0.010	12.8	0.016	46.0	0.015	36.5	0.014	4.6
4	0.195	4.1	0.211	1.3	0.223	359.2	0.236	356.9
5	0.009	103.2	0.011	118.9	0.010	145.4	0.013	143.4
6	0.014	321.2	0.014	327.3	0.013	15.2	0.019	43.4
7	0.009	6.0	0.002	78.6	0.006	79.3	0.008	83.7
8	0.025	98.0	0.039	89.0	0.047	87.3	0.040	91.1
9	0.009	230.8	0.012	223.0	0.008	220.6	0.006	128.0
10	0.016	273.2	0.010	261.7	0.007	190.2	0.007	147.0
11	0.002	325.4	0.007	30.9	0.007	40.7	0.006	306.1
12	0.011	20.6	0.019	357.7	0.024	350.7	0.028	342.5
13	0.002	289.7	0.000	319.1	0.001	118.7	0.004	93.6
14	0.004	324.3	0.005	340.4	0.008	9.4	0.010	16.6
15	0.001	287.0	0.004	102.7	0.007	107.6	0.007	115.0

APPENDIX A

CHARACTERISTICS OF PROPELLERS

A series of four three-bladed propellers was designed to study the effect of expanded area ratio and skew upon the unsteady forces and moments when operating in circumferentially nonuniform inflow. There were three unskewed propellers with EAR = 0.3, 0.6, and 1.2 and one propeller with EAR = 0.6 and 120 degrees of skew.

These propellers were designed using the Lerbs induction factors with lifting-surface and thickness corrections by Kerwin and Leopold.[50] NACA 66 sections with an NSRDC modified tail and an NACA a = 0.8 mean line were used. The propellers were designed for a constant radial distribution of circumferential mean velocity (i.e., for the zeroth harmonic of wake independent of radius) and an optimum radial distribution of circulation so that $K_T \approx 0.15$ at J = 0.83. Thickness was assigned so that the stress level was invariant among the three unskewed propellers. The skewed propeller had the same thickness distribution as the unskewed propeller with EAR = 0.6, but an oversight in the design procedure produced incorrect lifting surface angle-of-attack corrections. The geometry of the propellers is presented in Figures 39 through 42, and the open water characteristics are presented in Figures 43 through 46. More design details and cavitation performances in uniform flow are presented in Reference 53.

APPENDIX B

CHARACTERISTICS OF WAKES

Detailed axial velocity surveys were conducted in the plane of the propeller with the propeller removed in order to determine the harmonic content of each inflow velocity field. Since the screens were incapable of producing tangential or radial components of velocity, these components were assumed to be zero. A pitot rake was connected to the propeller shaft axis such that several pitot tubes lay along a radial line (i.e., at the same angular position). The pitot tube leads passed from the tunnel through a hollow shaft, and the angular position of the pitot tubes was accurately set from outside the tunnel by rotating the shaft. For each wake-screen, velocity measurements were made in the propeller plane at six different radii and at every 10 degrees of shaft rotation at a volume mean velocity of approximately 18 feet per second. The screen resistance coefficients, and hence the harmonic content of the resulting wakes, are insensitive to Reynolds number based on the wire diameter over the velocity range of interest in the present experiments.

The volume mean velocity over the propeller plane is calculated from the measured wake velocities

$$V_{VM} = \frac{\int_0^{2\pi} \int_{r_h}^{R} V_L(r, \phi)\, r dr d\phi}{2\pi (R^2 - r_h^2)}$$

A detailed harmonic analysis[58] of each measured longitudinal velocity field is performed on a high-speed digital computer such that the velocity field is expressed as:

$$V_L(r, \phi) = V_L{}^0(r) + \sum_{n=1}^{N} [A_L{}^n(r) \cos(n\phi) + B_L{}^n(r) \sin(n\phi)]$$

or

$$V_L(r, \phi) = V_L{}^0(r) + \sum_{n=1}^{N} V_L{}^n(r) \sin(n\phi + \phi_v{}^n)$$

The harmonic contents of the velocity fields nondimensionalized on the corresponding volume mean velocity are shown in Tables 2 and 3.

APPENDIX C

CHARACTERISTICS OF DYNAMOMETER

The six components of unsteady loading were measured by a sting-mounted balance,[51,52] using semiconductor strain gages as the sensing elements. The assembly of the dynamometer is shown in Figure 47, balance details are presented in Figure 48; and the strain gage bridge layouts are given in Figure 49. The strain-gaged balance is mounted on a stiff sting attached to a heavy flywheel. This assembly runs in soft-mounted bearing and is driven through a soft coupling. The system has two principal resonances for each component. The first, determined by the mass of the assembly and the spring constant of the bearing mounts and coupling, is at a frequency between 5 and 10 hertz. The second, due to the mass of the propeller and the spring of the measuring elements, is between 450 and 1500 hertz. The dynamometer was designed to have these resonances below and above the desired working range.

The totally submerged dynamometer is driven by a 10-horsepower d-c motor through a slipring shaft and amplifier housing, all exterior to the tunnel walls. The connecting shaft is hollow to carry the signal cables and passes through a stuffing tube as it enters the tunnel. Before being taken from the shafting, the a-c signals are amplified with solid-state pre-amplifiers to improve the signal-to-noise ratio.

The balance was calibrated both statically and dynamically. Static calibration (which determines the sensitivity of each transducer to the forces applied in axial, torsional, transverse, and bending modes) was performed in increments over the input force range before assembly in the tunnel. Dynamic calibration was performed after assembly in the tunnel and consisted of exciting the measuring system with a known force in increments of driving frequency over a broad frequency range in order to establish the dynamic response of each transducer sensitivity over the desired range of measuring frequency.

This calibration technique has certain limitations. Dynamic calibrations are performed without the propeller rotating, and so no accounting is made for propeller entrained water mass and viscous damping coefficients. To check the effect of these factors, estimated mass and damping factors were introduced into the calculation of system response, using a two-degree of freedom, lumped mass-spring-dashpot representation of the system. These calculations indicate that propeller damping will significantly affect dynamic response only at frequencies corresponding to system resonances or antiresonances. The calibrations indicated that the maximum interactions between the loading components were about 3 percent and that the usable frequency range was:

	hertz
Thrust	12 to 1300
Torque	12 to 500
Transverse Forces	12 to 400
Bending Moments	12 to 400

REFERENCES

1. Lewis, F. M., "Propeller Vibration," Trans. SNAME, Vol. 43 (1935); Vol. 44 (1936).

2. Lewis, F. M. and Tachmindji, A. J., "Propeller Forces Exciting Hull Vibration," Trans. SNAME, Vol. 62 (1954).

3. Wereldsma, R., "Experimental Determination of Thrust Eccentricity and Transverse Forces, Generated by a Screw Propeller," International Shipbuilding Progress, Vol. 9, No. 95, (Jul 1962).

4. Van Manen, J. D. and Kamps, J., "The Effect of Shape of Afterbody on Propulsion," Trans. SNAME, Vol. 67 (1959).

5. Van Manen, J. D. and Wereldsma, R., "Propeller Excited Vibratory Forces in the Shaft of a Single Screw Tanker," International Shipbuilding Progress, Vol. 7, No. 73 (Sep 1960).

6. Kumai, T. et al., "Measurement of Propeller Forces Exciting Hull Vibration by Use of Self-Propelled Model," Reports of Research Institute for Applied Mechanics, Kyushu University, Japan, Vol. 9, No. 33 (1961).

7. Krohn, J. K., "Numerical and Experimental Investigations on the Dependence of the Fluctuations of Thrust and Torque on the Blade Area Ratio of Four-Bladed Ship Propellers," Hamburg Model Basin, Federal Republic of Germany, HSVA Report 1236 (May 1961).

8. Krohn, J. K., "Numerical and Experimental Investigations on the Dependence of Transverse Force and Bending Moment Fluctuations on the Blade Area Ratio of Five-Bladed Ship Propellers," Fourth Symposium on Naval Hydrodynamics, Office of Naval Research, ACR-92 (Aug 1962).

9. Ritger, P. D. and Breslin, J. P., "A Theory for the Quasi-Steady and Unsteady Thrust and Torque of a Propeller in a Ship Wake," Stevens Institute of Technology, Experimental Towing Tank Report 686 (Jul 1958).

10. Hadler, J. B. et al., "Correlation of Model and Full-Scale Propeller Alternating Thrust Forces on Submerged Bodies," Fourth Symposium on Naval Hydrodynamics, Office of Naval Research, ACR-92 (Aug 1962).

11. McCarthy, J. H., "On the Calculation of Thrust and Torque Fluctuations of Propellers in Nonuniform Wake Flow," David Taylor Model Basin Report 1533 (Oct 1961).

12. Yeh, Y. H., "Thrust and Torque Fluctuations for APA 249, TMB Model 4414," David Taylor Model Basin Report 1364 (Jan 1960).

13. Lewis, F. M., "Propeller Vibration Forces," Trans. SNAME Vol. 71 (1963).

14. Sears, W. R., "Some Aspects of Nonstationary Airfoil Theory and Its Practical Application," J. Aeronautical Sciences, Vol. 8, No. 3 (Jan 1941).

15. Burstein, N. M., "Boundary Layer Investigation on a Body of Revolution with Fins," Ordnance Research Laboratory TM 504.2461–07 (Sep 1965).

16. Tachmindji, A. J. and Dickerson, M. C., "The Measurement of Thrust Fluctuation and Free Space Oscillating Pressures for a Propeller," David Taylor Model Basin Report 1107 (Jan 1957).

17. Wereldsma, R., "Research on Propeller Vibratory Forces," Netherlands Ship Model Basin Report on Contract N62558–3303 (X) (FBM) Modification 2 (1964).

18. Wereldsma, R., "Further Research on Propeller Vibratory Forces," Netherlands Ship Model Basin Report 66–172AS (1966).

19. Brown, N. A., "Periodic Propeller Forces in Nonuniform Flow," Massachusetts Institute of Technology, Dept NAME Report 64-7, (Jun 1964).

20. Rousetsky, A. A. et al., "Investigation into Variable Screw Model Loadings in a Towing Tank and Cavitation Tunnel with Adjusted Velocity Field," 11th International Towing Tank Conference, Tokyo, Japan (1966).

21. Huse, E., "An Experimental Investigation of the Dynamic Forces and Moments on One Blade of a Ship Propeller," Symposium on Testing Techniques in Ship Cavitation Research, Trondheim, Norway (1967).

22. Schuster, S. et al., "Beispiele fur die Behandlung instationarer Probleme in Schiffmodellversuch," Jahrb. d. STG, Bund 42 (1958); cited by Krohn, J. K., "Numerical and Experimental Investigations on the Dependence of the Fluctuations of Thrust and Torque on the Blade Area Ratio of Four-Bladed Ship Propellers," Hamburg Model Basin, HSVA Report 1236 (May 1961).

23. Sevik, M., "The Response of Propulsors to Turbulence (U)," U. S. Navy J. Underwater Acoustics, Vol. 16, No. 1(Jan 1966) CONFIDENTIAL; Seventh Symposium on Naval Hydrodynamics, Office of Naval Research, Rome, August 25–30, 1968 UNCLASSIFIED.

24. Hadler, J. B. and Cheng, H. M., "Analysis of Experimental Wake Data in Way of Propeller Plane of Single and Twin-Screw Ship Models," Trans SNAME, Vol. 73 (1965).

25. Breslin, J. P., "Correlation of Existing Vibratory Thrust Data," 11th International Towing Tank Conference, Appendix 4 of the Report of the Propeller Committee (1966).

26. Kumai, T., "Some Aspects of Propeller Bearing Forces Exciting Hull Vibration of a Single Screw Ship," Schiffstechnik, Vol. 9, No. 45 (Jan 1962).

27. Schuster, S., "On the Hydrodynamically Determined Thrust and Torque Fluctuations in the Propelling Machinery of Ships," David Taylor Model Basin Translation 275 (Mar 1959); VDI-Zeitschrift, Vol. 98 No. 32 (Nov 1956).

28. Burrill, L. C., "Calculation of Marine Propeller Performance Characteristics," North-East Coast Institute of Engineers and Shipbuilders (Mar 1944).

29. Lotveit, M., "A Study of Propeller Action in the Behind Condition," European Shipbuilding 1 (1960).

30. Hill, J. G., "The Design of Propellers," Trans. SNAME, Vol. 57 (1949).

31. Eckhardt, M. K. and Morgan, W. B., "A Propeller Design Method," Trans. SNAME, Vol. 63 (1955).

32. Lerbs, H. W., "Moderately Loaded Propellers with a Finite Number of Blades and an Arbitrary Distribution of Circulation," Trans. SNAME, Vol. 60 (1952).

33. Goldstein, S., "The Vortex Theory of Screw Propellers," Proceedings of the Royal Society of London, Series A, Vol. 63 (1929).

34. Lane, F., "A Two-Dimensional Approximation to Propeller Oscillating Effects Behind Fins by the Method of Superposition of Fluctuating Wave Forms," Ordnance Research Laboratory TN 5.2400 (Oct 1949).

35. Ryall, D. L., "Loading Fluctuations of a Wake-Operating Propeller," Admiralty Research Laboratory Report ARL/G/R9 (Jun 1965).

36. Sevik, M., "Measurements of Unsteady Thrust in Turbomachinery," American Society of Mechanical Engineers Paper 64-FE-15 (Mar 1964).

37. Casellini, L. M., "Unsteady Propeller Forces," Ordnance Research Laboratory TM 504.2461-06 (Jun 1965).

38. Reed, F. E. and Bradshaw, R. T., "Ship Hull Vibrations – 2, The Distribution of Exciting Forces Generated by Propellers," CONESCO, Inc. Report F-101-2 (Jun 1960).

39. Greenberg, J. M., "Airfoil in Sinusoidal Motion in a Pulsating Stream," NACA TN 1326 (Jun 1947).

40. Hanaoka, T., "Hydrodynamics of an Oscillating Screw Propeller," Fourth Symposium on Naval Hydrodynamics, Office of Naval Research, ACR-92 (1962).

41. Tsakonas, S. et al., "Unsteady Propeller Lifting Surface Theory with Finite Number of Chordwise Modes," Stevens Institute of Technology, Davidson Laboratory Report 1133 (Dec 1966).

42. Greenberg, M. D., "The Unsteady Loading on a Propeller in Nonuniform Flow," J. Ship Research, Vol. 8, No. 3 (1964).

43. Yamazaki, R., "On the Theory of Screw Propellers in Nonuniform Flows," Memoirs of the Faculty of Engineering, Kyushu University, Japan, Vol. 25, No. 2 (1966).

44. Shioiri, J. and Tsakonas, S., "Three-Dimensional Approach to the Gust Problem for Screw Propeller," J. Ship Research, Vol. 7, No. 4 (1964).

45. Weissinger, J., "The Lift Distribution of Swept-Back Wings," NACA TM 1120 (Mar 1947); ZWB Forschungsbericht Nr. 1553, Berlin-Adlershaf (1942).

46. Tsakonas, S. and Jacobs, W. R., "Unsteady Lifting Surface Theory for a Marine Propeller of Low Pitch Angle with Chordwise Loading Distribution," J. Ship Research, Vol. 9, No. 2 (1965).

47. Tsakonas, S. et al., "Exact Treatment of the Helicoidal Wake in the Propeller Lifting Surface Theory," J. Ship Research, Vol. 11, No. 3 (Sep 1967).

48. McCarthy, J. H., "Steady Flow Past Nonuniform Wire Grids," J. of Fluid Mechanics, Vol. 19, Part 4 (1964).

49. Van Lammeren, W. P. A., "Testing Screw Propellers in a Cavitation Tunnel with Controllable Velocity Distribution over the Screw Disk," Trans SNAME, Vol. 63 (1955).

50. Kerwin, J. E. and Leopold, R., "A Design Theory for Subcavitating Propellers," Trans SNAME, Vol. 72 (1964).

51. Brandau, J. H., "Static and Dynamic Calibration of Propeller Model Fluctuating Force Balances," Naval Ship Research and Development Center Report 2350 (Mar 1967).

52. Miller, M. L., "Experimental Determination of Unsteady Propeller Forces," Seventh Symposium on Naval Hydrodynamics, Office of Naval Research, Rome (Aug 25–30, 1968).

53. Denny, S. B., "Cavitation Performance and Open Water Tests of a Series of Propellers Designed by Lifting Surface Methods," Naval Ship Research and Development Center Report 2878 (Sep 1968).

54. Fung, Y. C., "An Introduction to the Theory of Aeroelasticity," John Wiley and Sons, Inc., New York (1955).

55. Drischler, J. A., "Calculation and Compilation of the Unsteady Lift Functions for a Rigid Wing Subjected to Sinusoidal Gusts and to Sinusoidal Sinking Oscillations," NACA TN 3748 (Oct 1956).

56. Magnuson, A. H., "A Flow Visualization Study of the Wake Produced by an Oscillating Wing," M.S. Thesis, The Pennsylvania State University, Dept of Aerospace Engineering (Mar 1967).

57. Tsakonas, S. et al., "Correlation and Application of an Unsteady Flow Theory for Propeller Forces," Trans. SNAME, Vol. 75 (Nov 1967).

58. Cheng, H. M., "Analysis of Wake Survey of Ship Model Computer Program, AML Problem No. 840–219F," David Taylor Model Basin Report 1804 (Mar 1964).

UNCLASSIFIED

Security Classification

DOCUMENT CONTROL DATA - R & D

(Security classification of title, body of abstract and indexing annotation must be entered when the overall report is classified)

1 ORIGINATING ACTIVITY (Corporate author)	2a. REPORT SECURITY CLASSIFICATION
Naval Ship Research and Development Center Washington, D. C. 20007	UNCLASSIFIED
	2b. GROUP

3 REPORT TITLE

UNSTEADY PROPELLER LOADING–MEASUREMENT, CORRELATION WITH THEORY, AND PARAMETRIC STUDY

4. DESCRIPTIVE NOTES *(Type of report and inclusive dates)*

5 AUTHOR(S) *(First name, middle initial, last name)*

Robert J. Boswell and Marlin L. Miller

6 REPORT DATE	7a. TOTAL NO. OF PAGES	7b. NO. OF REFS
October 1968	91	58

8a. CONTRACT OR GRANT NO	9a. ORIGINATOR'S REPORT NUMBER(S)
b. PROJECT NO S-F113 11 09 Task 3801	2625
c. Problem Number 526-150	9b. OTHER REPORT NO(S) *(Any other numbers that may be assigned this report)*
d.	

10 DISTRIBUTION STATEMENT

This document is subject to special export controls and each transmittal to foreign governments or foreign nationals may be made only with prior approval of the Naval Ship Research and Development Center, Code 500.

11 SUPPLEMENTARY NOTES	12 SPONSORING MILITARY ACTIVITY
	Naval Ship Systems Command Washington, D. C.

13 ABSTRACT

Objectives of the present study are to measure the unsteady forces and moments on a series of marine propellers due to circumferentially nonuniform inflow; to correlate the measured unsteady thrust and torque with calculated values, based on various proposed theories; and to investigate variation of unsteady thrust and torque over a range of pertinent parameters, using the method determined from those described to be the best available for calculating unsteady loading.

All six components of unsteady loading were measured on a series of four three-bladed propellers, consisting of three unskewed propellers of varying blade widths and one with extreme skew in both 3- and 4-cycle flow fields. The experimental results indicate that all components of blade-frequency loading increase to some maximum value then decrease with increasing expanded area ratio. The extreme skew resulted in a reduction in blade-frequency thrust and torque to about 10 percent of the unskewed value and a reduction in side forces and bending moments to about 50 percent of the unskewed value.

Experimental blade-frequency thrust and torque were compared with values calculated by the following techniques: quasi-steady, two-dimensional unsteady, combination quasi-steady two-dimensional unsteady, and three-dimensional unsteady. The three-dimensional unsteady theory yields the best correlation with experiment; however, the numerical techniques employed breakdown for narrow-bladed propellers and for propellers with blade overlap.

The parametric study reveals that for a given number of blades, blade frequency thrust and torque can be reduced effectively by considerably skewing the blades.

DD FORM 1 NOV 68 1473 (PAGE 1)

S/N 0101-807-6801

UNCLASSIFIED

Security Classification

14 KEY WORDS	LINK A		LINK B		LINK C	
	ROLE	WT	ROLE	WT	ROLE	WT
Propellers						
Propeller parameters						
Vibration						
Theory						
Model tests						

GPO 862-971